IJCRT.ORG ISSN : 2320-2882

INTERNATIONAL JOURNAL OF CREATIVE RESEARCH THOUGHTS (IJCRT)

An International Open Access, Peer-reviewed, Refereed Journal

IMPACT OF LAND USE LAND COVER CHANGE ON SURFACE RUNOFF: THE CASE OF AMBO TOWN, ETHIOPIA

ADISU FIKIRE CHALCHISA, TAMENE ADUGNA DEMMISIE, ABEBA TAYE WORKU

ADISU FIKIRE CHALCHISA, TAMENE ADUGNA DEMMISIE, ABEBA TAYE WORKU

HYDRAULIC AND WATER RESOURCES ENGINEERING,
Dambi Dollo University, Dambi Dollo,Ethiopia

Abstract: The Impact of Land use Land cover change over the world currently develops direct and indirect impacts on surface runoff. Expansion of Ambo town urban areas causes the reduction of Huluka river watershed potential which is the main source of water supply and other miscellaneous use for the residents of Ambo town. Because of increasing of urbanization, floods are the main causes to affect the property, buildings, and infrastructures in case of Ethiopia. The main objective of this study was Impact of Land use Land cover change on surface runoff in the case of Ambo town on Huluka river watershed. Satellite image downloaded for 1997, 2005 and 2011 of the watershed area was taken based on the quality of data and the available resolution. Excel statistical software was used for filling missing value of precipitation data and data consistency was checked up using double mass curve. The surface runoff generated from the watershed was estimated based on the rainfall intensity and major characteristics of the watershed area which are the major factors for designing urban storm water drainage facilities and structures. Arc Geographical Information System and Geographical Information System extension tools were used to extract hydrological characteristics of the watershed; Hydrologic Engineering Center Hydrologic Modeling System to simulate rainfall - runoff process and Hydrologic Engineering Center River Analysis System for flood inundation assessment. The daily rainfall and stream flow data was used for Hydrologic Engineering Center Hydrologic Modeling System calibration and validation. To evaluate the accuracy of the model, calibration and validation was conducted. Nash Sutcliff efficiency during calibration and validation was 0.744 and 0.72 respectively whereas coefficient of determination during these two processes was 0.8556 and 0.8122 respectively. The hydrological and hydraulic modeling are accomplished by dividing the watershed in to different sub-basin. Hydrological modeling depending on land use/land cover of the peak discharge was generated 1997, 2005 and 2011 at the outlet was 36.5, 47.56 and 61.04 m^3/s respectively. The peak discharge simulated by frequency storm method for 10, 25, 50 and 100 return periods was 38.2, 47.2, 54.2 and 61.4m^3/s. The result found from Hydrologic Engineering Center Hydrologic Modeling System frequency storm method used for flood inundation map generation. Flood inundation maps produced using Arc Geographical Information System to

visualize flood depth and extent for each return period. Accordingly, maximum flood depth of 17.7632, 17.8779, 17.9548 and 18.0347m for 10, 25,50, and 100 year return periods respectively was found with flood extent of 97.58, 100.56, 103.34 and 105.54 ha for 10, 25, 50 and 100 year return periods at the middle of the final reach of the study area.

Index Terms DEM, Flood modeling; HEC-HMS/RAS; HEC- GeoHMS/RAS; Urbanization

I. INTRODUCTION

Nowadays there is a great need to detect spatial patterns of land use/land cover (LULC) change at local, regional and global scales. Understanding LULC change is a fundamental importance for environmental monitoring, urban planning and governmental decision making around the world. One particular consequence of LULC change is its considerable impacts on hydrological processes by affecting the nature of surface runoff and water quality, hence further impact on ecosystems, biotic systems, and even on human health (Chunhao, 2011).

Land-use and land-cover changes may have four major direct impacts on the hydrological cycle and water quality: they can cause floods, droughts, changes in river and groundwater regimes and they can affect water quality (McColl et al., 2017). Globally floods are most devastating natural disasters affecting human life than any other natural disasters. In 2010 alone, 178 million people were affected by floods and the total financial losses in the exceptional years such as 1998 and 2010 exceeded $40 billion (Shabir, 2013). It is also reported that one sixth of the global population (one billion people); the majority of them among the world's being low-income earners live in the potential path of a 1 in 100 year flood according to Department for International Development (DFID). Ethiopia is facing the same global challenges of climate change effects such as droughts and floods (Kotir, 2011).

The country experiences two types of floods: flash floods and river floods. Flash floods are the ones formed from excess rains falling on upstream watersheds and gush downstream with massive concentration, speed and force. Often, they are sudden and appear unnoticed. Therefore, damage caused by such kind of floods becomes pronounced and devastating when they pass across or along human settlements and infrastructures. For example, in the recent incident, that the Dire Dawa City experienced is typical of flash flood. On the other hand, much of the flood disasters in Ethiopia are attributed to rivers that overflow or burst their banks and inundate downstream plain lands. The flood that has been happened in Southern Omo Zone and Awash River is a typical manifestation of river floods (Gashaw & Dagnachew, 2011). On the other hand, population growth is increasing; runoff of rainwater's is expected to increase due to the decrease of the permeability of the urban environment. For the last one hundred seventeen years it has been noticed that there is an intensive conversion of rural land to urban development like buildings, transportation networks and facilities (airports and highways), recreation areas, reservoirs and other man made structures (Gantet al., 2011). Roads and bridges are destroyed, overtopped and washed away. Therefore, to reduce the impact of flood, during design of roads, bridges and culverts estimation of flood magnitudes using the appropriate parameters is very essential.

Generally, Ethiopia is one part of the developing country. Among that, Ambo town is one of the currently expanding and developing towns, as a result, rural residents are migrating to the town and are causing rapid urbanization.

Generally, floods are the causes of major destruction of property, buildings and infrastructures in Ethiopia and this problem is getting worse and worse in urban areas due to high rate of urbanization in the country (Jha, 2011). This has led to deforestation, use of high-quality corrugated roofs and paved surfaces or asphalts and its effect are high with the higher raindrop intensity on the city and also town. Urbanization has different stages and various effects can be noticed through those stages. At early, removal of vegetation and trees may decrease evapotranspiration and interception, which increase stream sedimentation (Davis, 2005). When construction of streets or roads, bridges, houses and culverts begins, infiltration will decrease and stream flow will increase. In addition to this when the development of residential and commercial buildings has been completed imperviousness increase consequently; the time needed for runoff will reduce; concentration will be peak with higher discharges and occur sooner after rainfall starts in basins. The volume of runoff and flood damage potential will greatly increase (Ching, 2014). As a result, the rainfall– runoff process in an urban area tends to be quite different from that in natural conditions (Barbero-Sierra, 2013).

The impacts of high rate of growth of Ambo town particularly in the study area reflected through street flooding and over topping as well as bridge, road, culvert materials are washed way. On the other hand, many river flood plains in the town have not yet been delineated considering the land use change and most of small tributary rivers in the town are ungauged. It is obvious, hydrological alterations and channel disturbances along streams because of changes in inputs like; slope, vegetation cover, geology, stream geomorphology and hydrologic processes from year to year. Therefore, its need to see carefully hydrologic responses to urbanization to improve the understanding of stream response to land use change for rivers found in towns. This study objectives to show the effects of urbanization on the amount surface runoff generated at Huluka River watershed in the case of Ambo town.

II. Data and Sources of Data

Secondary data was collected from the responsible organization. The data was collected annual, year and monthly report from the responsible organization (table 1).

Table 1 Type of data and its source

S.no	Type of data	Source	Period
1	DEM (30*30m)	GIS Department of MoWIE	-
2	Soil map	MoWIE	2011
3	LULC	Ethiopian Geospatial Information Agency	2011
4	Rainfall	NMAE	1987-2016
5	Stream flow	MoWIE	1997-2011

Table 2 Rainfall data and its geographical location

Stations names	Latitudes (in degrees)	Longitudes(in degrees)
Ambo	8.98	37.84
Guder	8.96	39.76
Dire Enchine	8.84	37.67
Waliso	8.55	37.98

Table 3 Stream gage data and its geographical location

Stream flow	Site	Latitudes (in degrees)	Longitudes (in degrees)
Huluka	Nr.Ambo	8.97	37.88

Filling missing data

The accuracy of the result was based on the quality of available data. Thus, before using collected data for analysis it has to be mandatory to check missing data, inconsistency and accuracy (Benchimol, 2015). The period of missing data has to be filled by different methods. For this study missing value was filled using linear Regression methods by XLSTAT 2018 software. XLSTAT is using for filling of missing rainfall and stream data (Taube, 2019).

XLSTAT is the richest tool for the data analysis and the statistical treatment with MS Excel. It can execute preparing, describing, visualizing, analyzing and modeling data, correlation tests, parametric and non-parametric tests, testing for outliers, homogeneity and trends. For quantitative data, XLSTAT allow to: Remove observations with missing values, use a mean imputation method, use a nearest neighbor approach and algorithm (Lloyd, 2019). This study uses a nearest neighbor approach to fill missing data.

Consistent check

Besides filling missing data, inconsistency problem should be checked, while data due to instrument malfunction, the records may be failed for continuity. Double mass curve is used for checking for data consistency. The plot line should be straight and the R-squared value is found between, 0.6 - 1 (Datoo, 2019). As seen (figure1) the R-squared is found about 0.99 which is close to 1. So, the data is a consistent, it can be used for analysis.

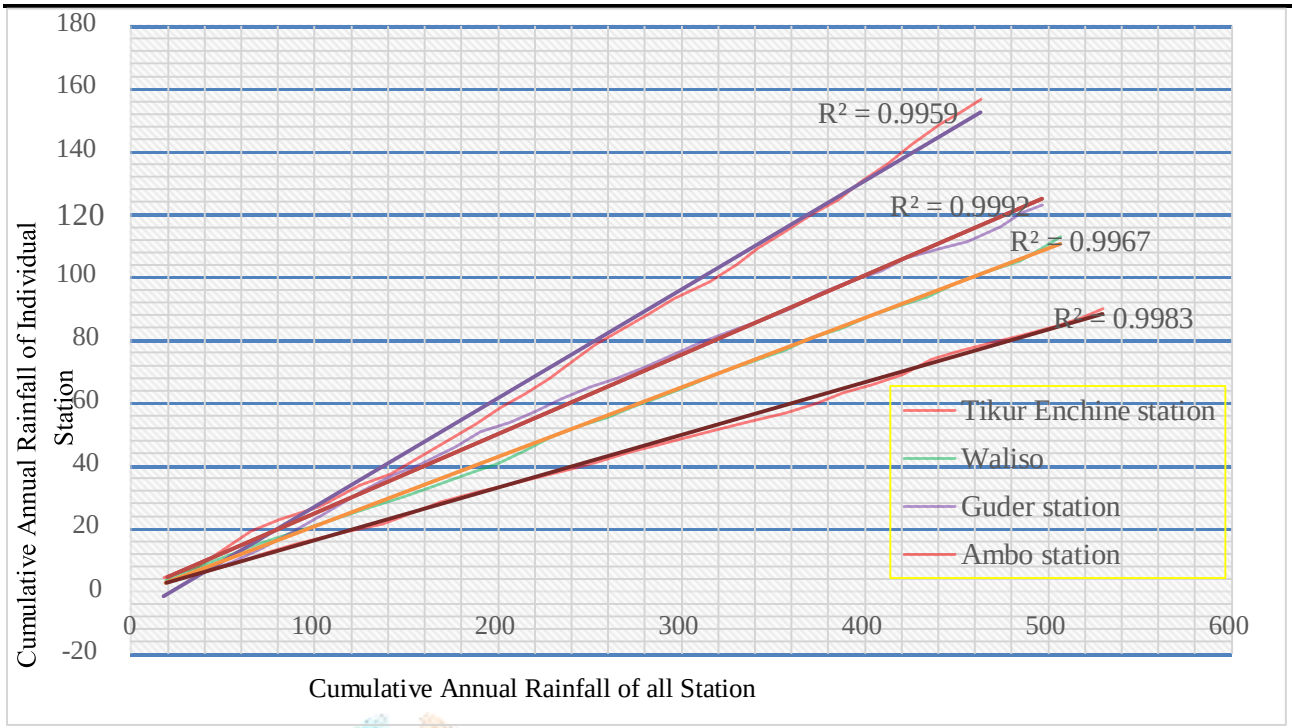

Figure 1Double mass curve

Homogeneity and stationarity test

The homogeneity and stationarity tests were analyzed using RAINBOW software. If the observed data falls below 90% significance level the data was well homogeneous and stationary (Raes, 2006). During homogeneity and stationarity tests, the probability values below (90%, 95% and 99%) shows well homogeneous and stationary (Jameson, 2019). In this study, the p-values for the stations, ambo, guder, dire enchine and waliso rainfall data test were below 90% significance level. Therefore the data's were well homogeneous and stationary(figure2).

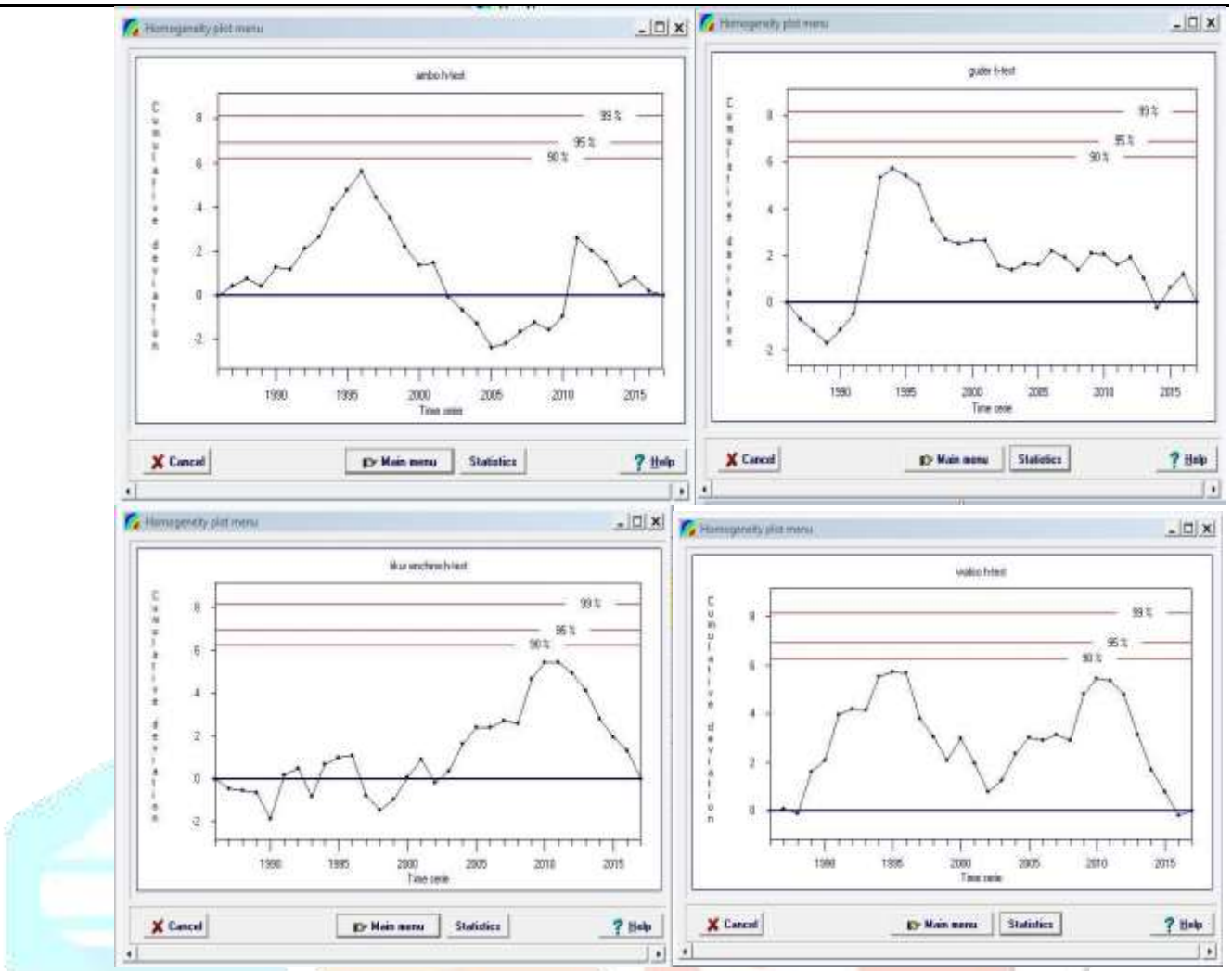

Figure 2 Homogeneity test

III. RESEARCH METHODOLOGY

Ambo town is one of the developing towns in West Shoa zone of Oromia region in Ethiopia. It is located at a distance of 114 km to the West of Addis Ababa, capital city of Ethiopia. It is endowed with rivers, one of which separates the town into two major parts known as Huluka River which starts from Dendi Lake near Wonchi town, 39 km from Ambo town, and flows from the southern part of Ambo towards the northern part of the town. In rural areas, these river waters are used for drinking, sanitation, livestock and agricultural purposes. Sewage from residential areas near these rivers is allowed to enter directly and dense weeds have occupied the sides of rivers, thus affecting the flow and photosynthesis process. Huluka River watershed has a watershed area of 206.05 km^2 and located in Abay River basin. It is located between latitude of $8^0$45’34.74”N to $9^0$00’00“N, longitude of $37^0$30’00’’E to $39^0$00’00’’E .

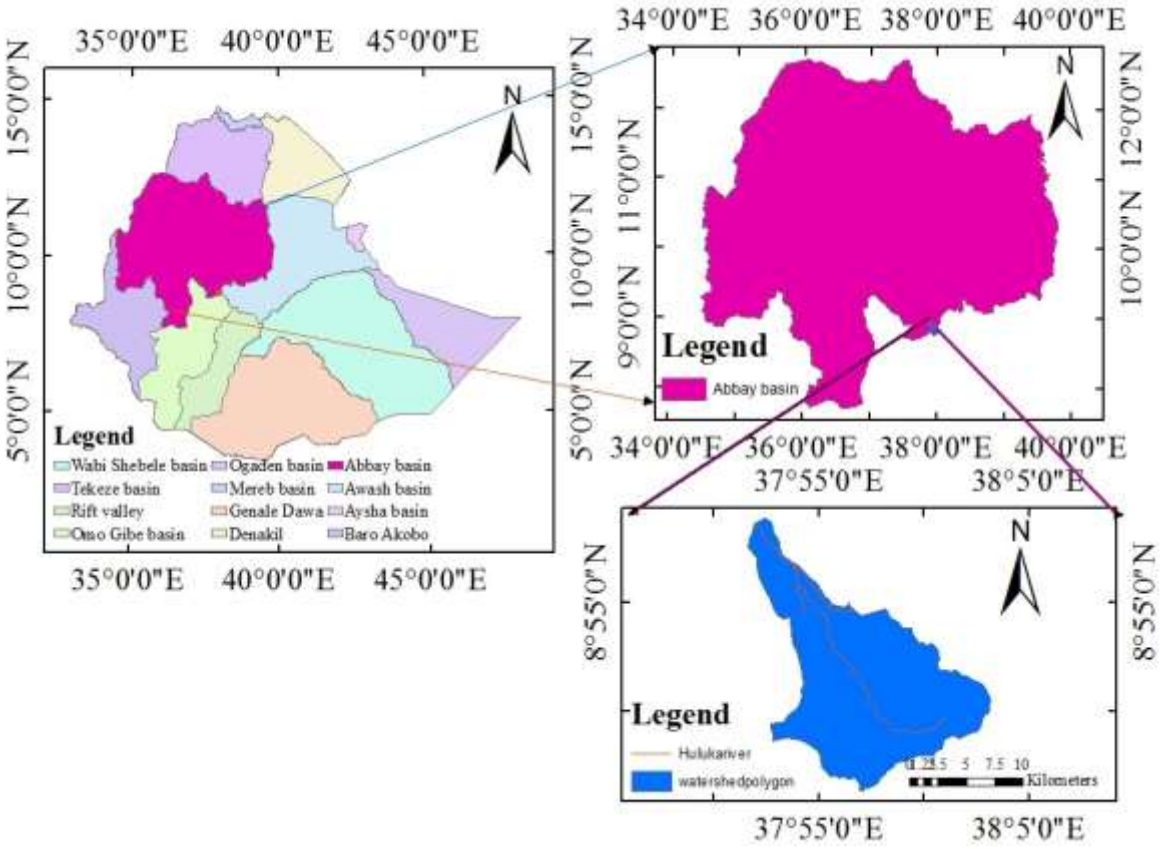

Figure 3 Description of study area

Theoretical framework

The conceptual work flow under taken throughout the study was given as in the figure4

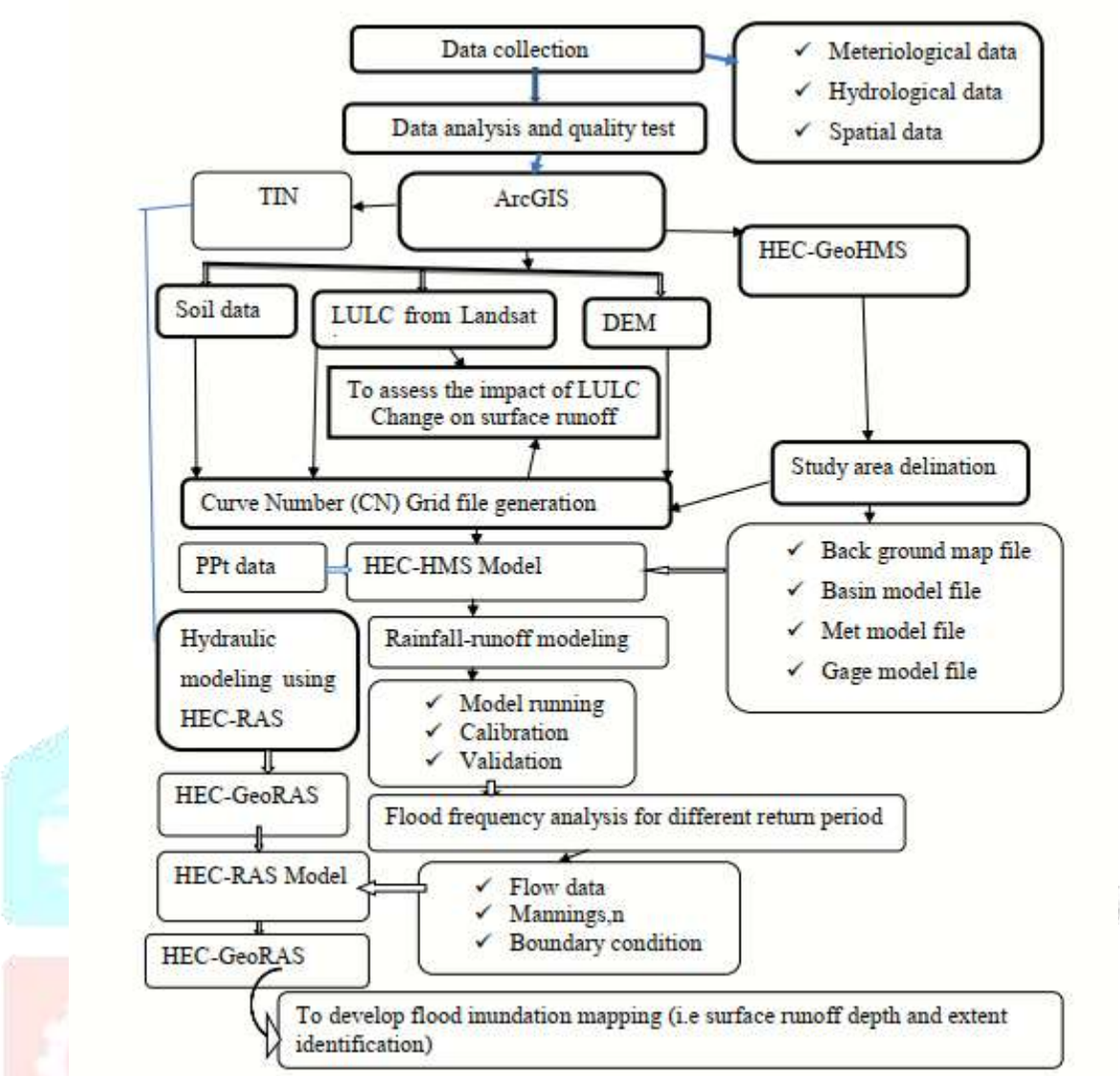

Figure 4 General schematic representation of work flow diagram for the study area

Digital Elevation Model Data Processing

Delineation of a watershed area using traditional method like processing topographic maps consumes much time and its accuracy is very low. But now a time this traditional method hasbeen replaced by automatic extraction from a Digital Elevation Model (DEM) due to the release of different type of high-resolution satellites to space at different time and the production of high-quality data (Nega, 2016). DEM data is used to describe topographic characteristics such as contour, slope, elevation difference, aspect and hill shade. DEM is the main dataset used for development of the basin model components and geometrical data in theHEC-HMS and HEC -RAS models respectively.

The DEM in the form of GCS_WGS_1984 raster format is changed in to the Universal Transverse Mercator (UTM) projection raster form by considering zone of the study area which Andinda, UTM Zone 37N by using Arc GIS 10.2 software package. The projected DEM clipped by using shape file of the study area. Fill sinks: If cells are available with higherelevation surrounding a cell, the water is surrounded in that cell and cannot flow. Therefore, this functions used to modify the elevation value to eliminate these problems by creating a depression less or hydro logically corrected DEM based on the input row DEM.

Flow directions: It is generated from the fill sinks grid and indicates the direction of the steepest descent to a neighbor cell and defined for each grid cell. the number in the legend represents directions; 1 = east, 2 = south east, 4 = south, 8 =south west, 16 = west, 32 = north west, 64 = north, 128 = north east that were listed on Appendex-A. Flow accumulation: Generated from the flow direction grid and defines the number of upstream cells draining intoany given cell in the grid. Stream definition: the cells that form the stream network are defined based on a threshold number of cells that drain into a given cell.

Stream segmentation: created by splitting the streams as defined in the stream definition grid at any junction. Catchment grid delineation: For every stream segment defined by the stream segmentation grid, the corresponding watershed is delineated and stored in a grid file. Catchment polygon processing: This polygon generated from the catchment grid to delineate the boundaries of each sub basin. Drainage line processing: Generated from stream segmentation grid are transformed into a vector stream layer by this function. Adjoint catchment processing: the upstream sub basins are aggregated at any stream confluence.

Before continue to the next step of hydrological modeling, data sets in the map document should be prepared and ready by the necessary data formats. Those datasets are inputs for HEC- GeoHMS for HEC-HMS basin model generation. Raster forms are: Projected DEM (considered as raw DEM), Fil (sink filled DEM), Fdr (flow direction grid), Fac (flow accumulation grid), Str (stream network grid), StrLnk (stream link grid), Cat (catchment grid),WshSlopePct (slope grid in %). Vector forms are: Catchment, Drainage Line, Adjoint Catchment.

Model set up

For rainfall runoff modeling, HEC-HMS requires Back ground map file of the study area, Basin model file, Gage file, met file, curve number grid, created impervious area and allthese can be generated by HEC-Geo HMS.

HEC-Geo HMS

By using HEC-Geo HMS eight data sets can be derived from DEM that collectively describe the drainage patterns of the watershed. This includes basin slope, river slope, river length, longest flow path, basin lag time, curve number grid, created impervious area and time of concentration.

HEC-Geo HMS operates on the DEM to derive sub-basin delineation and to prepare a numberof hydrologic inputs. HEC-HMS accepts the hydrologic input files as a starting boundary condition for hydrologic modeling system. HEC-Geo HMS consists of different menus that provide different functions specially, during preprocessing in Arc GIS work environment. These menus are: preprocessing, project setup, basin processing, basin characteristics, basin parameters, HMS and utility (figure 5).

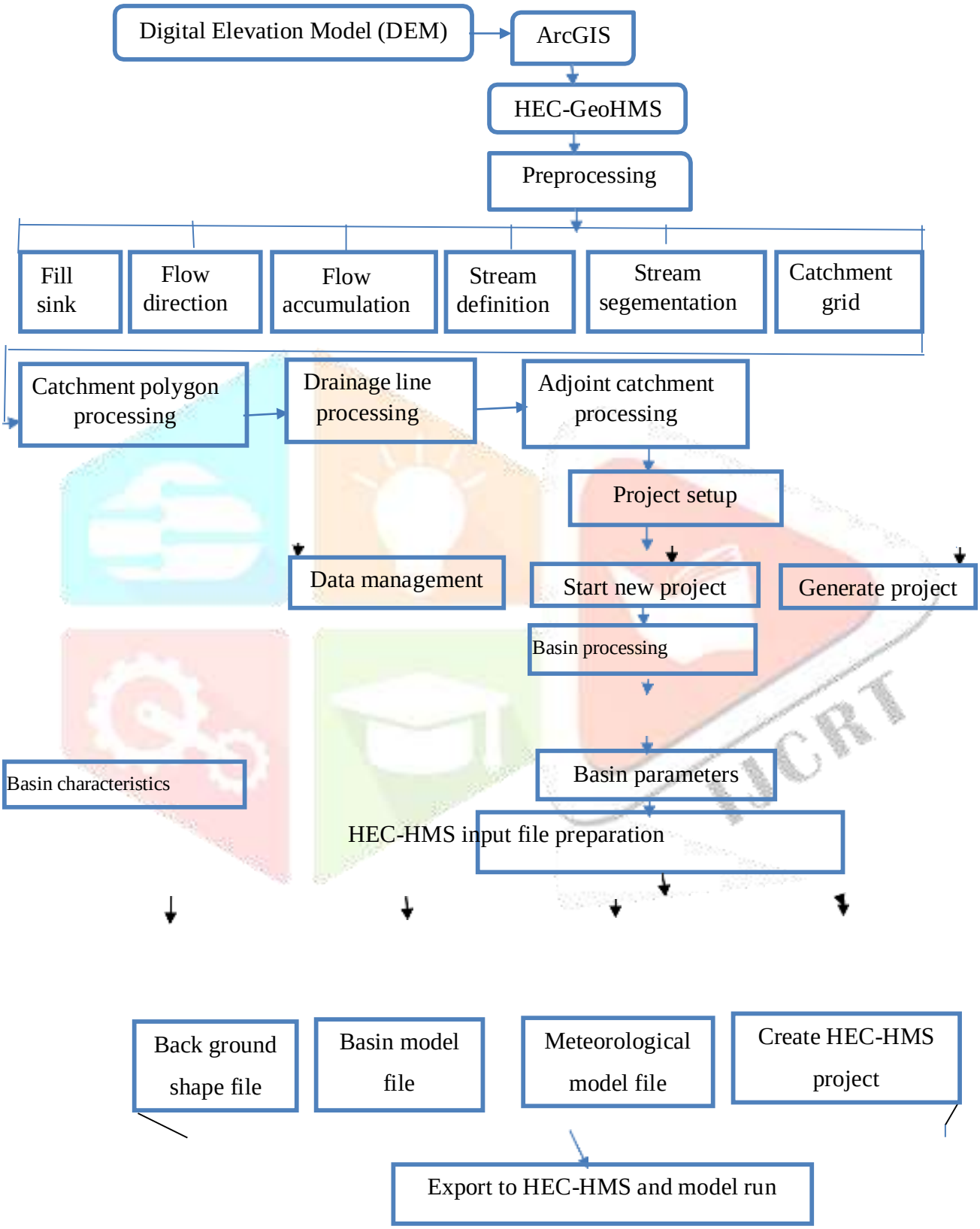

Figure 5 Summary of the model setup

Curve Number (CN) Grid Input Preparation

The runoff curve number is generated from the study area's LULC classified and hydrologic soil groups. Watershed land cover has a great importance in estimating the basin's curve number with the identification of soil textures and its permeability. Thus, according to the classification of Soil Conservation Service (SCS) method soil types of the watershed are grouped for each of the Huluka river watershed already created. This method has been widely applied to estimate storm runoff depth for every cover within a watershed based on runoff curve numbers (CN). Having a curve number grid gives the utility of extracting curve number for any area in the watershed without performing any calculations. The main input data of curve number generation are clipped DEM, Land use land cover classified and soil data.

Preparing land use data for CN grid

Landsat Data Processing

Determination of Runoff Curve Number (CN) requires land use classification and the potential of deriving land use maps from satellite images is one of the main objectives of this study due to the expansion of urbanization currently increased in Ambo town. Land use from large areas can be detected easily in a short time with low cost compared to the traditional methods.

The landsat data used is downloaded from the official website of United States Geological Survey (USGS). The landsat data of the watershed for 1997, 2005 and 2011 with a resolution of 30*30m is selected and used. The selection is based on the available daily rainfall, quality of image and resolution available.

Figure 6 Landsat7data downloaded from official website of US Geological Survey (USGS)

As shown from figure 6, to downloading the landsat data first KML shape file with a maximum of 30 points of the watershed is prepared and uploaded to the above site. The landsat data downloaded from the landsat archive in the form of Geotiff with different bands. Before utilizing the data, the following activities are done using Arc GIS 10.2 softwarepackage. Frist all the available bands of satellite image are combined by using composite band's function. The next step was combined landsat data in the form of GCS_WGS_1984 raster format is changed in to the Universal Transverse Mercator (UTM) projection raster form by considering zone of the study area which Adindan, UTM Zone 37N by using Arc GIS10.2 software package. The third step was projected landsat data is clipped by using the shapefile of Huluka river watershed prepared.

The fourth step were Individual bands composite in a Red, Green and Blue (RGB) combination in order to visualize the data in color. There are many different combinations thatcan be made but in this study case 3, 2, 1 RGB combination is selected**.** The selected color composite is as close to true color. At this stage the Landsat data is ready for land use classification. The land use classification was performing using a unsupervised classification method using create signature and maximum likelihood classification functions of ArcGIS. Land use/cover class is carried out by assigning a grid code for each class. Accordingly, four types of land use were identified in the study area, namely Water body, Urban area, Forest

area and Agricultural land. The classified LULC for selected different years were indicated on Appendex-J. The classified land use raster maps were vectorized and converted to land use shape file maps using raster to polygon function. At this stage the land use data can merge with soil data for curve number generation and extraction of area coverage for each class is possible.

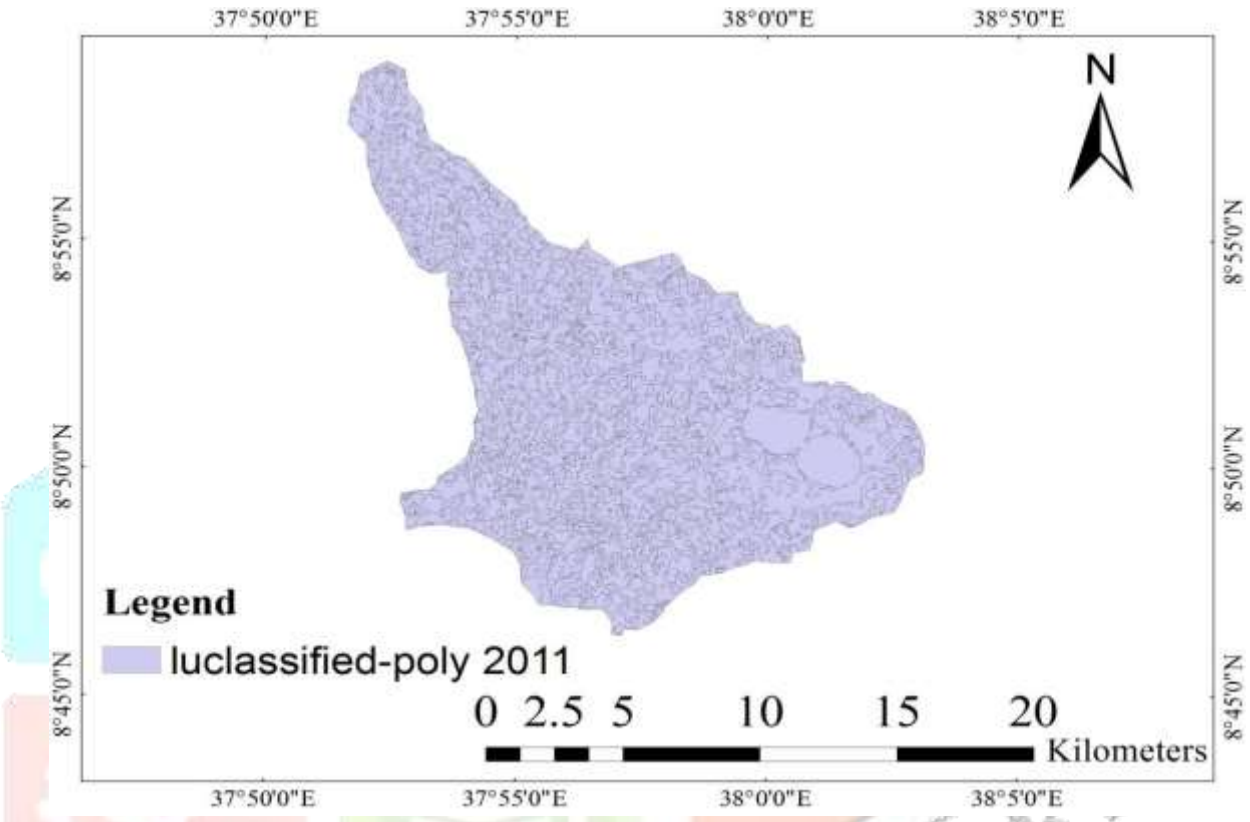

Figure 7 Processed land uses as shape file

Preparing Soil Data for CN Grid

Accordingly, the soil map of the study area found as shape file and all of these soil types found in the area categorized on three Hydrological Soil Groups (HSG), namely B, C and D. Hydrological Soil Groups types (table 4).

Table 4 Soil types and its Hydrological soil group types of the study area

Soil types	Hydrological Soil Group (HSGs) types
Haplic Luvisols	D
Calcic Vertisols	D
Haplic Nitisols	B
Chromic Luvisols	B
Haplic Alisols	C
Eutric Vertisols	D

Merging of Soil and Land Use Data

Both the land use class and soil class of the study area are prepared in shape file format whichare very important data for curve number (CN) generation. But, to utilize this data for CN generation the two shape files are merged by using union function of ArcGIS 10.2 software package. The union function uses the both land use and soil feature classes as input. The output of merged features contains attributes values from both inputs.

Creating CN Look-up Table

Curve number look up table is the most fundamental input table for CN grid generation and created by using create table function of Arc GIS 10.2 and assigned Hydrological Soil Group (HSG) for each land use type (table 5).

Table 5 Created CN look up table

LUvalue	Description	A	B	C	D
1	Water body	100	100	100	100
2	Agricultura area	68	78	86	89
3	Forest area	30	60	73	79
4	Urban area	61	75	85	88

The columns represented by A, B, C and D stores curve numbers for each of corresponding soil groups for each land use category and the values are determined by using SCS TR55 (1986) which is indicated in Appendex-L. The CN values range from 100 (for water bodies)

to approximately 30 for permeable soils with high infiltration rates. Accordingly, the minimumand maximum CN values of the study area are 60 and 100 respectively. Now all the necessaryinputs for hydrological modeling are prepared and ready based on the required standard.

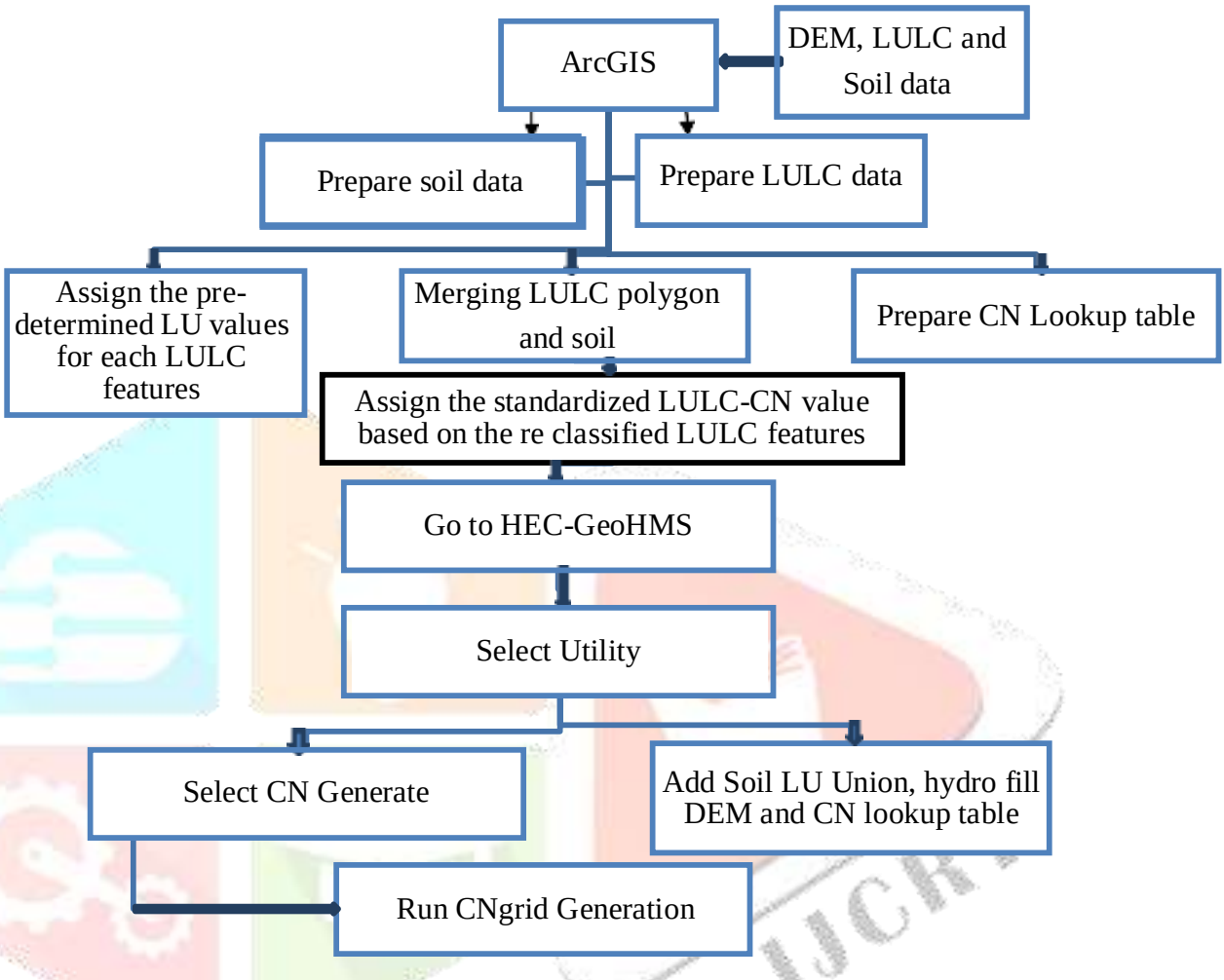

Figure 8 Schematic representation of CNgrid generation procedures

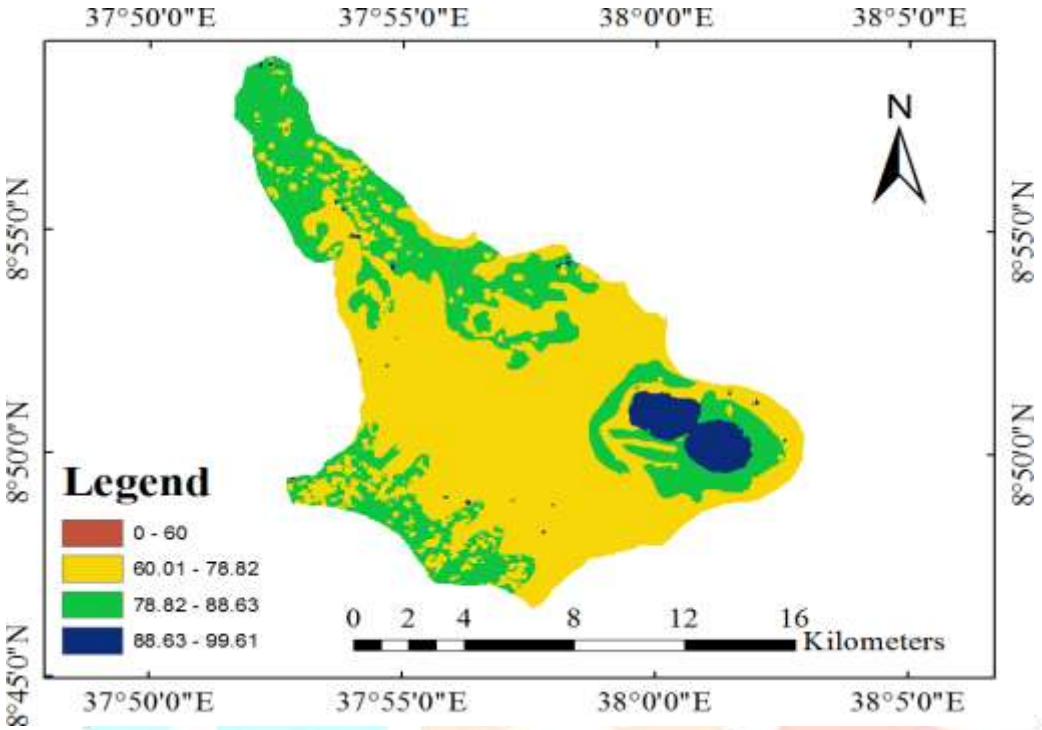

Figure 9 Generated Curve number of Huluka river watershed for 2011

Areal Precipitation

For analyses involving areas larger than a few square miles, it may be necessary to make estimates of average rainfall depths over watershed areas since a rain gauge records rainfall at a geographical point (Fetter, 2018). There are many methods available to determine the areal rainfall over the watershed from the rain gauge measurement: Arithmetic Mean, Thiessen Polygon, Isohyetal, Grid Point, Percent Normal and Hypsometric are available for estimating average precipitation over a drainage basin (Tegine, 2018).

Choice of methods requires judgment in consideration of quality and nature of the data, and the importance, use, and required precision of the result. A Thiessen polygon method is most widely used method compared to other (Aasa, 2019).

In HEC-HMS meteorological modeling can be under taken using the frequency storm, gridded precipitation, specified hyetograph method, inverse distance method and Gage weightmethod. In this study Gage weight method for meteorological modeling was selected as this method considered all the areal contributions of the stations under consideration. In this method, weights are given to all the measuring gauges on the basis of their areal coverage of

the watershed, thus eliminating the discrepancies in their spacing over the basins on table (3.8). In this procedure, areas and lines between adjacent stations were generated on a map of the study area by using Arc GIS 10.2 software with Arc tool box extension by selecting analysis tools under proximity create theissen polygons. The perpendicular bisector of these lines forms a pattern of polygons with one station in each polygon (figure 3.13). The area witheach station is taken represents the area of its polygon, and this area is used as a factor for weighting the station precipitation. The contribution of the rainfall from each gauging station is limited by its weighing factor. According to Thiessen, the average rainfall, R_{areal} over the area can be computed (equation 1) (Nharo, 2019)

$$R_{areal}=\sum_{i=1}^{n}\frac{RiAi}{At} \quad (1)$$

Where, Ri is the rainfall at station i, Ai is the polygon area of station i, At is total watershed area, and n is the number of stations. The area functions Ai/At are known as the Thiessen coefficients and once they are determined for a given stable station network, the areal rainfall can be computed for the set of rainfall measurements.

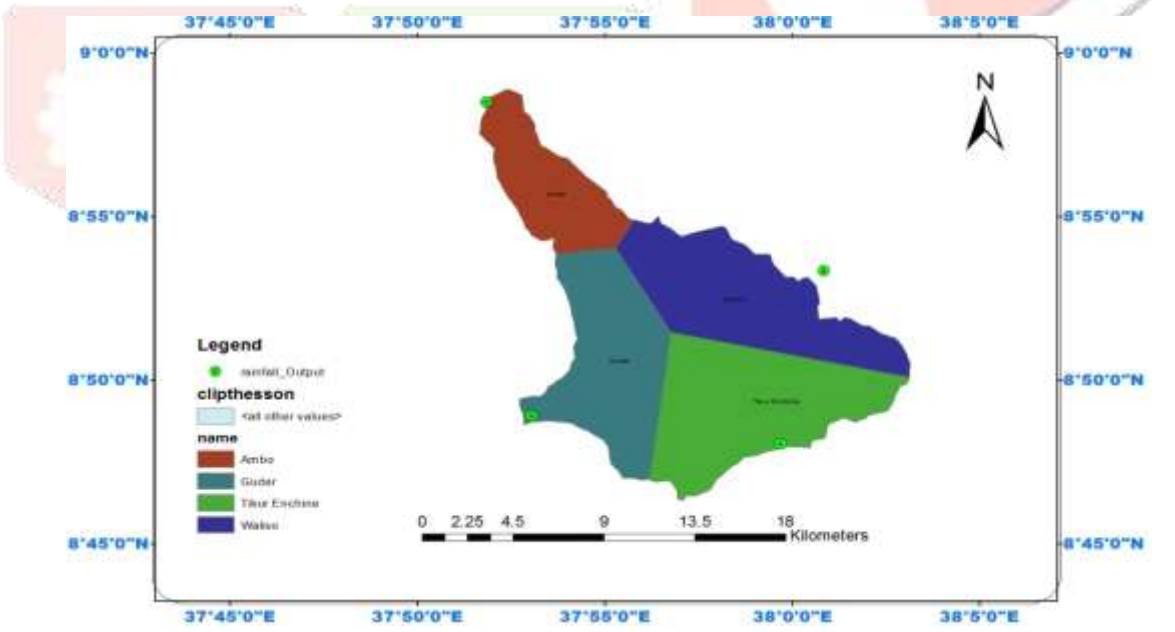

Figure 10 Theissen polygon for areal precipitation

Table 6 Stations areal weight of theissen polygon

S.no	Name of station	Area of polygon	Areal weight(ai/at)
1	Ambo	26.763	0.13
2	Guder	45.8	0.222
3	Dire Enchine	77.02	0.374
4	Waliso	57.5	0.279
Total		206.05	1.00

Creating Impervious Grid of study Area

Knowing percentage of impervious cover is very important in land use planning and management. It is a key factor for hydrological modeling especially in small urban watersheds. Percentage of impervious grid needed to map as a continuous variable and its value ranges from 0 to 100 percent. 0 indicates the entire area is pervious almost all of the rainfall in the area infiltrates in to subsurface of the area and 100 means all the available rainfall gives runoff and infiltration is almost 0 (Labbas, 2013).

Based on the land use classification of this study; there are 4 classifications namely, Water body, Urban area, Forest and Agriculture lands. Accordingly, percentage of impervious value for it assigned for each category and table. The assigned values are based on SCS TR55 (1986) and user's guide for the California impervious surface coefficients (Beck, 2017). Land uses may vary from watershed to watershed, but can be defined on a given range. The first step in impervious grid generation using HEC-GeoHMS is converting land use map (grid) into a polygon feature class and add percentage of impervious as on the attribute table of land use polygon feature class. Percent land use impervious is prepared in excel format and openedin Arc GIS. By using join function of Arc GIS the land use polygon feature class and the excel table are joined. Previously created impervious field on the land use polygon feature class was calculated based on the assigned impervious percent values of excel by using field calculator function.

The second step is generating impervious grid using HEC-GeoHMS feature to raster function use (Input features: land use polygon, field: land use impervious percentage area). This generated percentage of impervious grid is basic input for HEC-HMS project generation.

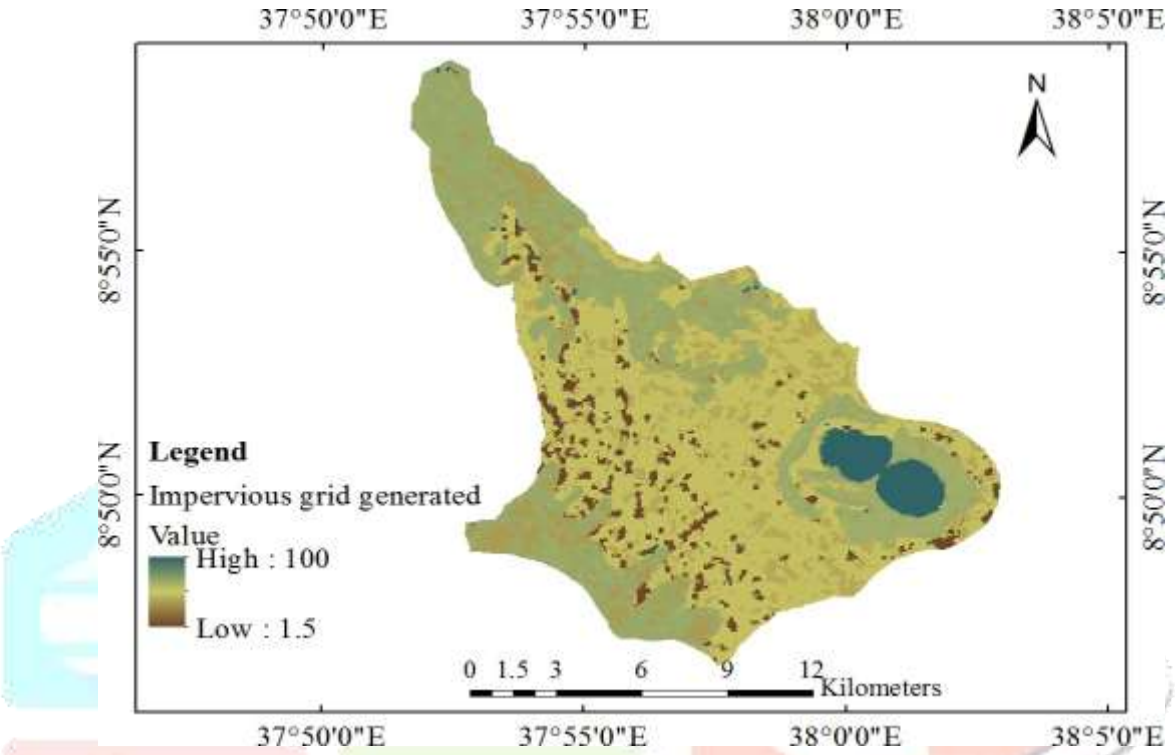

Figure 11 Generated impervious grid

To create an HMS project different tools of HEC- GeoHMS are used which are found on four main views namely; HMS model set up, basin characteristics, HMS input parameters and HMS menus.

HMS model setup

Data management window: The necessary data sets used for HMS project generation are added these are; row DEM, Sink filled DEM, flow direction grid, flow accumulation grid, stream network grid, stream link grid, catchment grid, adjoint catchment and drainage line. These data's are checked on the data management window of HEC- GeoHMS and assigned based on the corresponding map layers used to generate the project. Creating new HMS project: start new project; assign Huluka Watershed on project area and on the project point. Then project point and project area feature classes are created. Main outlet of the watershed assigned: the main outlet of the watershed is at Ambo town assigned by using add project

point tool of HEC- GeoHMS. Generate HMS project: before generating a project the data management window of HEC-GeoHMS is checked and HMS project is generated by creating a mesh (by delineating watershed created main outlet of the Huluka river watershed).

Extracting watershed characteristics

Extracting physical characteristics of sub-basins and streams into attribute tables is accomplished by using the basin characteristics menu of HEC- GeoHMS these are: River length: the length of each river segments is computed and stored by using the Huluka River name as input. River slope: this tool computes the slope of the river segments and stores by using raw DEM and created river. Basin slope: average slope of each the 4 sub-basins is computed using the slope grid and sub basin polygons.

Longest flow path: the longest flow path for each sub-basins of Huluka river watershed is created by using raw DEM, flow direction grid and sub basins as input. Basin centroid: apoint feature class is created and stored for the centroid of each sub-basin. Basin centroid elevation: the elevation for each centroid point is created by using raw DEM and basin centroid as inputs. Centroidal longest flow path: a polyline feature class is created by using this tool. The creation of this polyline shows the flow path for each centroid point along longest flow path of each sub basin.

HMS Inputs/Parameters

The hydrologic parameters menu of HEC - GeoHMS has tools to estimate and assign watershed and stream parameters. With this menu HMS processes selected, river auto name, basin auto name, sub-basin parameters and CN lag method are computed.

HMS project creation

By using tools found in the HMS menu input files for HEC-HMS are created. Activities accomplished using those HEC- GeoHMS menu are: HMS units assigned, data checking, HMS schematic, HMS toggling and legend, add coordinates, prepare data for model export, background shape file, basin model, meteorological model created and finally HMS project is created know the project is ready for HMS Process (figure 12).

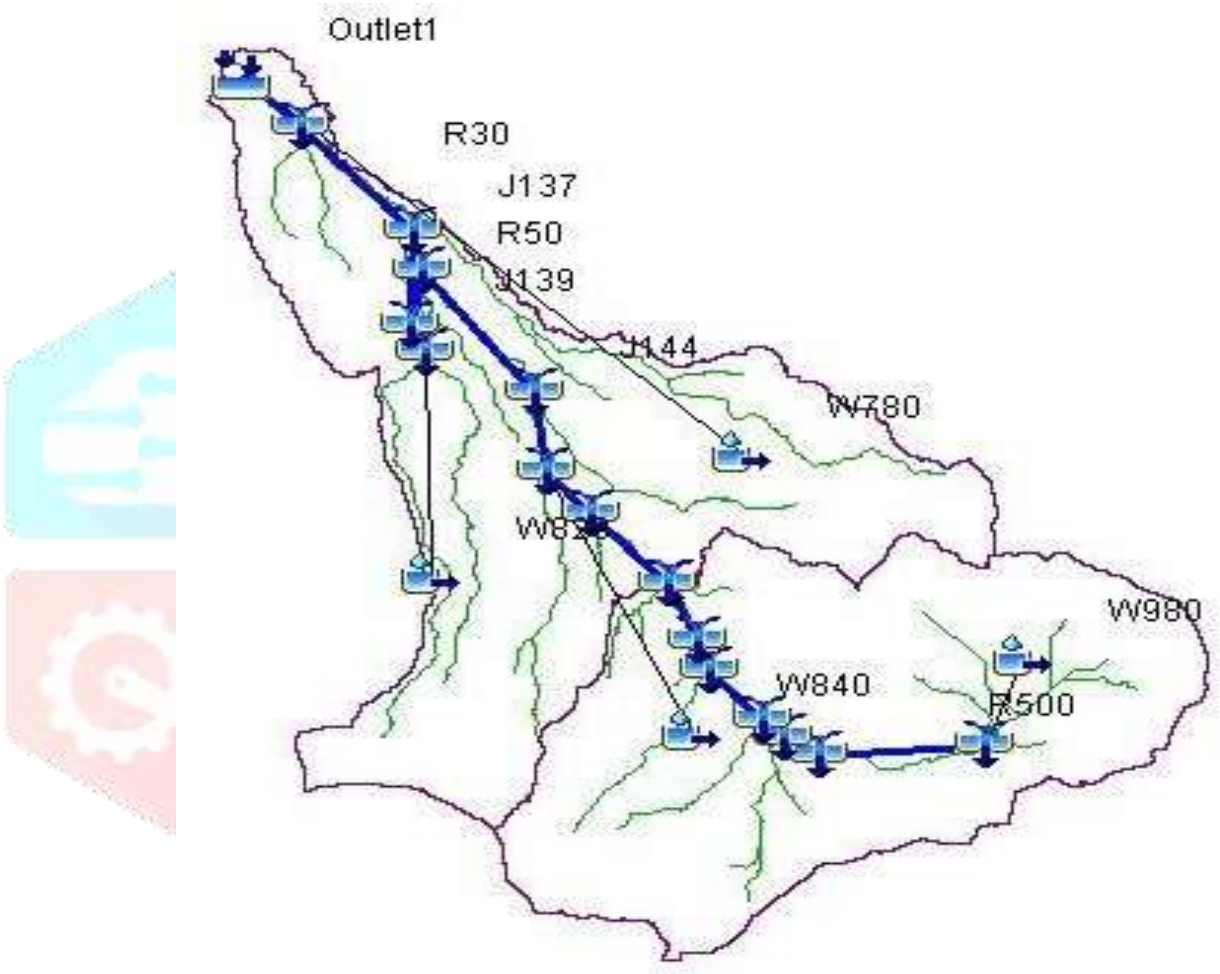

Figure 12 Created HEC-HMS setup

HEC-HMS Model Analysis

For simulating rainfall-runoff processes the HEC-HMS model has four major components. These are; basin model, meteorological model, control specification and time series. Totally the Huluka river watershed has 4 sub basins, 16 reaches and 16 junctions with upstream to downstream sequence. The control specification contains time related information (year,starting date and time, end date and time) for the simulation.

Rainfall (precipitation) loss modeling

SCS-CN was selected as a method for excess precipitation modeling. The method requires only three inputs. These are: Curve number, Initial abstraction and Percentage of impervious. As the curve number was already generated and embedded into the basin model file, the software automatically extracts and assigns the curve number value for each sub-basin (Pathan, 2019).

2

$$Pe = \frac{(P-Ia)2}{(P-Ia)+S}$$ ----------

Where: Pe = Accumulated precipitation excess at time t; P = Accumulated rainfall depth at time t; Ia = Initial abstraction and S = Potential maximum retention.

Ia and S are calculated (equations 3.2). The initial abstraction comprises all the losses that occur before surface runoff begins. According to the NRCS (1986), it includes water retained in surface depressions as well as water intercepted by vegetation, evaporation and infiltration. In the CN model, Ia is assumed to be correlated to maximum retention potential S.

Ia = 0.2S 3

The maximum retention S is further related to the soil and cover conditions of the analyzed watershed through the CN. Computing maximum retention potential (equation 4), the initial abstraction throughout each sub-basin was computed and manually assigned

$$S = \frac{25400}{CN} - 254$$ ----------4

Impervious surface area coverage of the study were analyzed depending up the the curve number value that can be generated from the land use land cover and hydrologic soil group types merged in well format (Dan-Jumbo, 2019).

Several factors, such as the percentage of impervious area and the means of conveying runoff from impervious areas to the drainage system should be considered in computing CN for urban areas. Among them Connected impervious areas and Unconnected impervious areas are the main considered

Transform Method

SCS-UH was chosen for transform method. The SCS-UH requires only basin lag time. As the HEC-Geo HMS can automatically extract the basin lag time from the inserted curve number grid, it is so easy to proceed with this method.

Flood routing method

The HEC-HMS contains different flood routing methods of which the Muskingum flood routing method was selected for Huluka river watershed. The Muskingum method is one of the most popular flood routing methods. Muskingum flood routing requires two parameters, namely: flood wave travel time (k) ranges from (0-100 hrs) and weighted coefficient of discharge (x) ranges from (0-0.5). The initial of Muskingum-K value lies between the specified ranges was calculated using (equation 3.6) and manually assigned for sub-basin and later calibrated. According to Haktanir and Ozmen (1997) the Muskingum flood routing method uses the following popular hydrologic flood routing equation.

$$\frac{ds}{dt} = I - Q \quad \text{----------5}$$

$$S = k[xI + (1 - x)Q] \quad \text{----------6}$$

Where; ds/dt is rate of change of storage per unit time, I is inflow, Q is outflow, S is Storage,x is weighted coefficient of discharge, k is wave travel length.

Wave travel time (k parameter) for each reach was calculated from equation (7) as the initialvalue. Running the model with this initial value, later the parameters were optimized.

$$K = \frac{v}{L} \quad \text{----------7}$$

$$V = \frac{Q}{A} \quad \text{----------8}$$

Where; k is flood wave travel length, v is permissible velocity, l is reaching length, Q is flooddischarge (m^3/s), A is cross sectional area.

Here the permissible velocity value should be in the range that neither causes erosion of thechannel nor letting deposition of sediment. According to (ERA drainage manual, 2013), this

permissible velocity is classified into numerous categories depending on the channel geometry. On the basis of this assumption, 1.5m/s permissible velocity was used (3.6) in orderto calculate the initial value of k. Based on this huluka river watershed has a total of 16 reaches and the correct values for Muskingum K and Muskingum X is assigned.

Sensitivity Analysis

Sensitivity analysis is a method to determine which parameters of the model have the greatest impact on the model results. There are three parameters (curve number, initial abstraction and lag-time) of the event model that were subject to the sensitivity analysis (Ahmadisharaf, 2019). The SCS curve number method, which is used to handle the infiltration loss in the sub-basins has three parameters such as curve number, initial abstraction and percent impervious area in the basin (Igulu, 2020). Percent impervious area is taken as 30% since there is urban settlements inside the sub-basin. Therefore, the parameters (curve number, initial abstraction and lag-time) of SCS curve number method were used for Calibration. The SCS unit hydrograph method which is used to model the transformation of precipitation excess into direct surface runoff, has lag time parameter. This parameter was also used for calibrated.

Model Performance Evaluation

Nash–Sutcliffe model efficiency coefficient (NSE):is used to assess the predictive power of hydrological models or used to analysis the correlation between simulated and observed hydrological data (Adla, 2019).It can be expressed as:

$$NSE = 1 - \frac{\sum(Q_{o(t)} - Q_{m(t)})^2}{\sum(Q_{ob(t)} - \overline{Q_{ob}})^2} \quad \text{----------9}$$

Where; Q_m= modeled flow, Q_o= observed flow, $\overline{Q}$ = mean of observed flow

It can range from $-\infty$ to 1. An efficiency of 1 (NSE = 1) corresponds to a perfect match of modeled discharge to the observed data. An efficiency of 0 (NSE = 0) indicates that the model predictions are as accurate as the mean of the observed data, where as an efficiency less than zero (NSE < 0) occurs when the observed mean is a better predictor than the model or, in other words, when the residual variance (described by the numerator in the expression above),is larger than the data variance (described by the denominator).

Essentially, the closer the model efficiency is to 1, the model is more accurate (Cakir, 2020).

Coefficient of Determination (R^2): The coefficient of determination (R^2) is a measure of the proportion of variance of a predicted outcome. With a value of 0 to 1, the coefficient of determination is calculated as the square of the correlation coefficient (R^2) between the sample and predicted data. The coefficient of determination shows how well a regression model fits the data. Its value represents the percentage of

variation that can be explained bythe regression equation (Piepho, 2019).

It can be expressed as:

$$R^2 = \frac{\sum(Q_{obs(t)} - \overline{Q}_{obs}) \sum(Q_{sim(t)} - \overline{Q}_{sim(t)})^2}{\sum(Q_{obs(t)} - \overline{Q}_{obs})^2 \sum(Q_{sim(t)} - \overline{Q}_{sim(t)})^2} \quad \text{------}$$

----------10

Where; R^2 is coefficient of determination, Q_{obs} is observed value at the i^{th} time interval,

$Q_{sim(t)}$ is simulated value at the i^{th} time interval, $\overline{Q}_{obs}$ is mean of observed discharges

$\overline{Q}_{sim(t)}$ is mean of simulated discharges value at i^{th} time interval.

A value of 1 means every point on the regression line fits the data; a value of 0.5 means only half of the variation is explained by the regression. A coefficient of determination (R^2) zero means that the dependent variable cannot be predicted from the independent variable. The coefficient of determination is also commonly used to show how accurately a regressionmodel can predict future outcomes (Myers, 2019).

Root Mean Squared Error (RMSE) of observations given by equation 11.

– – – – – – – – – – – – – – – – – – – –11

$$RMSE = \sum_{i=1}^{n} \left(\frac{(Q_i - S_i)^2}{Q_i - \bar{Q}} \right)$$

Where, Qi is observed stream flow data, Q is average observed stream flow data, Si issimulated stream flow data.

Flood Frequency Analysis

Flood frequency analysis is the most important statistical technique in understanding the nature and magnitude of peak discharge in a river or flood plain. Flood frequency analysis gives the probability model curve to the annual flood peaks which are recorded by the period observation and data of flood occurred in 15 years (1997-2011). This method is useful to predict recurrence interval and helps to cause no damage to the public and government properties. There are different types of methods for the estimation of Flood Frequency Analysis (FFA). Before the demarcation of flood inundation area of the flood plain, peak discharge analyzing is important to obtain Probability distribution. The terms return period and recurrence interval are used to denote the reciprocal of the annual probability of exceedance. Ethiopian Roads Authority (ERA) divided the country into eight Meteorological regions based on their rainfall pattern similarity (figure3.16) and develops intensity-duration frequency curves (IDF curve) for 24hr rainfall depth for each Meteorological region as a function of the 2, 5, 10, 25, 50 , 100, 200 and 500 years return period of the storm events.

Figure 13 Ethiopian Rainfall regions (ERA, 2013)

According to ERA classification, Huluka river watershed was found in rainfall region B1(RR-B1) and the 24 hour rainfall depth for each return period was taken (table 3.9) and (Figure 3.17) shows the intensity duration frequency curve (IDF curve) of Huluka river watershed adopted from Ethiopian IDF curve developed by Ethiopian road authority.

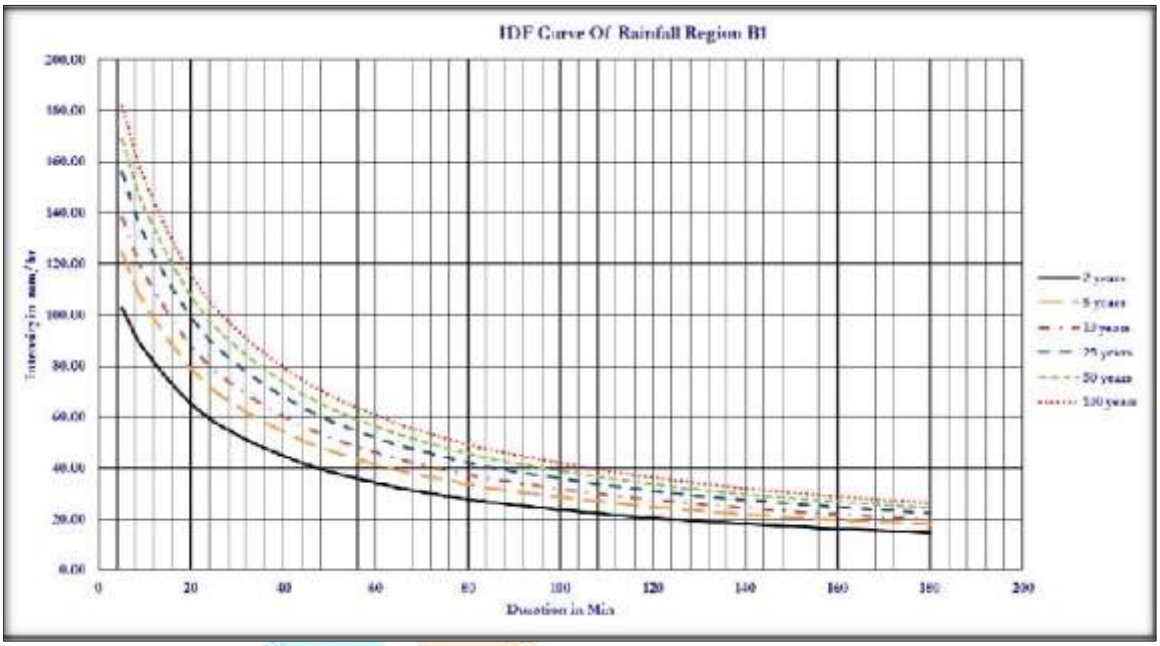

Figure 14 IDF curve for rainfall region B1

ERA has developed 24 hour rainfall depth for different rainfall regions of Ethiopia forcorresponding return periods. Using 24 hour rainfall depth of RR B1 provided on (table 3.9) that was specified for Huluka river watershed the rainfall depth of 1, 2, 3, 6 and 12 hour were developed using (equation 11) and used in HEC-HMS for flood inundation area estimation.

Table 7 24hr Rainfall Depth (mm) Vs Frequency (yr)

24 hr Rainfall Depth (mm) vs Frequency (yr)								
Return Period Years	2	5	10	25	50	100	200	500
RR-A1	50.30	66.02	76.28	89.13	98.63	108.06	117.48	130.00
RR-A2	51.92	65.52	74.45	85.70	94.07	102.45	110.91	122.27
RR-A3	47.54	59.61	67.66	77.92	85.62	93.34	101.13	111.58
RR-A4	50.39	63.83	72.28	82.55	89.97	97.20	104.32	113.63
RR-B1	58.87	71.26	79.29	89.35	96.84	104.37	112.02	122.41
RR-B2	55.26	69.95	79.68	92.03	101.29	110.61	120.07	132.87
RR-C	56.52	71.04	80.54	92.52	101.48	110.50	119.66	132.06
RR-D	56.23	76.84	90.37	107.46	120.23	133.05	146.00	163.44

Note: RR- Rainfall Region

For drainage areas in Ethiopia, to compute the rainfall intensity at any required time using the 24hr rainfall depth, which is known as a rainfall intensity-duration-frequency (IDF) relationship.

$$\frac{R_t}{R_{24}} = \frac{t(b+24)^n}{24(b+t)^n} \quad \text{----------12}$$

Where: R_{Rt}= Rainfall depth ratio R_t:R_{24}, R_t = Rainfall depth in a given duration't' R_{24}= 24hr Rainfall depth, b and n are constant coefficient in which b = 0.3 and n = (0.78 – 1.09) and t = Rainfall duration.

Simulation of Hydraulic Modelling: HEC-RAS

Data required for simulation of Hydraulic modelling (HEC-RAS) are:

Triangulated Irregular Network (TIN): Digital Terrain Model in the form of Triangulated Irregular Network (TIN) is required for the hydraulic analysis of river system. TIN must be ofhigh-resolution with continuous surface and should represent bottom of the river and adjacent flood plains as all the cross-sectional data was extracted from it. TIN of huluka river watershed were derived from respective DEM which is identified under (Appendex B). Flow data obtained from HEC-HMS software and LULC was required for the simulation of flood inundation assessement.

Hydraulic Model Development

A numerical model which is used to represent the hydraulic behavior of a water body is calleda hydraulic model. Hydraulic models may be broadly categorized into one dimensional(1-D), two-dimensional (2-D) and three-dimensional (3-D) schemes. 1-D mathematical models arethe most commonly used for flood inundation mapping and use the Saint Venant equations, and therefore rely on many high-resolution morphological parameters (cross sections). Hydraulic analysis of the river system was performed with the help of HEC-RAS along with HEC-GeoRAS, an extension in ArcGIS (Jaber, 2018).

The methodology used for performing simulation of hydraulic analysis can be dividing into three parts which are as follows:

Pre-processing: Developing geometry of river in ArcGIS Processing: Performing hydraulic computation in HEC-RAS

Post-processing: Processing RAS results in ArcGIS.

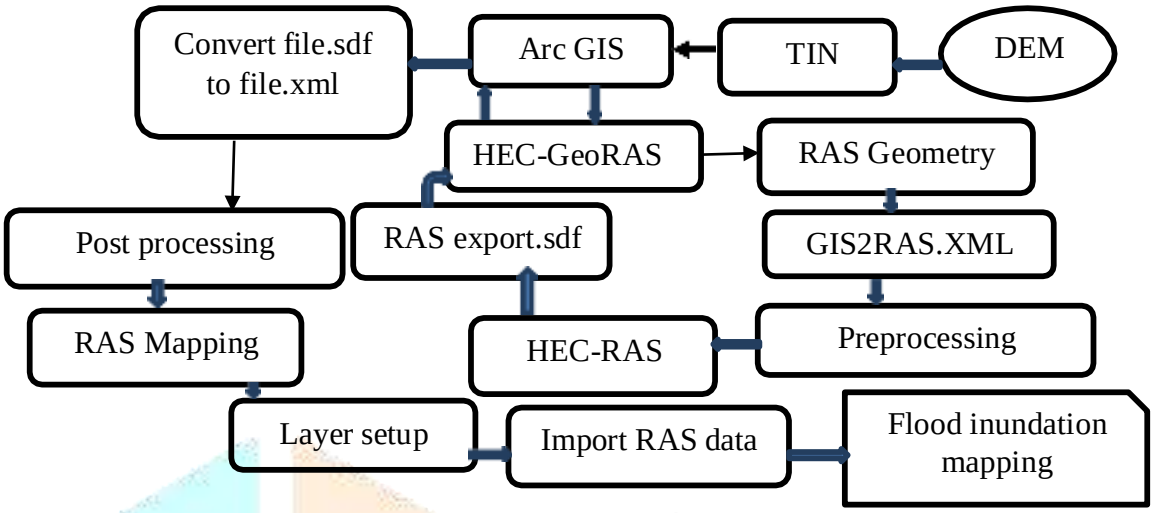

Figure 15 General work flow between HEC-Geo RAS and HEC-RAS for floodplain

RAS pre- processing

The RAS pre-processing is the task one's done in River Analysis system (RAS). Rivergeometry was done by HEC-Geo RAS software. The HEC-Geo RAS is a GIS extension witha set of procedures, tools and utilities for the preparation of river geometry (GURMU, 2018). HEC–Geo RAS software uses Digital Terrain Model (DTM) to create river geometry. Triangular irregular Network (TIN) for Huluka watershed was developed from DEM of the huluka watershed using the 3D spatial analysis extension. A TIN is a set of adjacent, nonoverlapping triangles, computed from irregularly spaced points with x, y coordinates and z-values (Zenner, 2000).

The TIN data structure is based on irregularly spaced point, line and polygon data interpreted as mass points and break lines. Thus, TIN allows efficient generation of surface models forthe analysis and display of terrain and other types of surfaces while preserving the continuous structure of features such as stream banks that are critical for hydrologic and hydraulic analyses (Burrough, 2015). Further, the river center line, River bank, flow path; XS cross- section, 3d river centerline, 3d river cross -section developed by HEC-Geo RAS. The river stream center line, bank lines, flow path center lines, and cross section lines has to be digitized from a previous river file and topographical datasets using HEC-Geo RAS interface.

The river reach (river segment between junctions), cross- section and other related data isstore in the geo-database file of HEC- Geo RAS.

Creating River Centre line: The River center line layer is very important, because it representsthe river network for HEC-RAS. The digitizing of stream centerline start with selecting the sketch tool from the Editor Toolbar and digitization proceed in the direction of a river flow (Akbari, 2014). The process begins from upstream end to the downstream end of the Huluka River watershed. After digitizing all of reaches, the user assigns the name of the river. This was accomplished by the selection of Assign River code / Reach Code menu item andassigning appropriate names.

Creating River bank: The interface extracts the geometric data in export RAS data in GIS2RAS.RASImport.sdf format. The bank lines layer is used to define river channel from overbank areas. The bank lines are created in similar way as the river centerline. The digitizing of bank lines starts from the upstream end, with the left bank (looking in downstream direction) being digitizing first.

Creating Flow paths:The flow path layer is a set of lines that follows the center of mass of the water flowing down the river, during the flood event (Julien, 2018). For Flood plains, the flowpath center lines are digitized to represent created water flow within the flood plain. Flowpath center lines are created in the upstream to downstream flow direction.

Creating cross-sections: Cross-sections are one of the most important inputs to HEC-RAS. Cross-section cut lines are used to extract the elevation data from the terrain and to create a ground profile across the flow (Patel, 2016). The intersection of cut line's with other RAS layers such as center line and flow path lines are used to compute HEC-RAS attributes suchas bank stations (locations that separate main channel from floods plain) and downstream reach length (distance between cross-section). The following important basic rules were followed during the process of drawing cross section cut lines (Michotte, 2017)

Cut lines are drawn perpendicular to a direction of flow, Cut lines are drawn directionally from left to right bank, looking downstream direction and Cut line's do not intersect each other. For Huluka watershed, there are about 99 cut lines was created. Thus, for each cut line's, the 2D feature class XS Cut lines are intersected with the TIN to create a feature class with 3D cross-section. Finally, Creating GIS import file for HEC-RAS so that it could import

the GIS data to create the geometry file. First, choosing layer set up window and under required surface choose TIN, under required layers select river layer, XS-Cut line's layer and XS-Cut line's 3D layer, under optional layers. choose banks, flow path, River 3D and optionaltables are not used in this study, show all null value.

Figure 16 River cross section extracted from TIN for Huluka river watershed

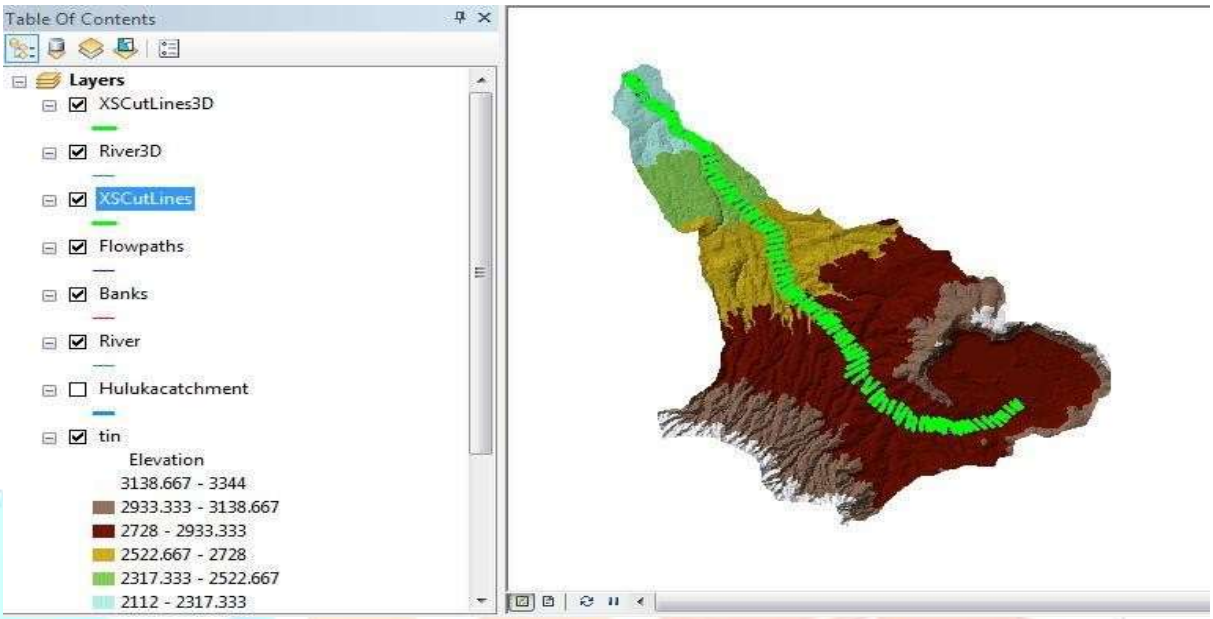

After creating of river cross section (figure 15), stream center line attributes (like topology, length/stations and elevation) and XS cut line attributes were added in order to compute river station at each cross-section. The channel length, left and right over bank length were shownin (Appendex-H). Executing river geometry cross-section using Arc GIS in conjunction with HEC Geo RAS, the constructed river geometry cross-section was exported to HEC-RAS in Arc GIS format (i.e.as 'GIS2RAS.sdf'). Exporting the river geometry cross-section to HEC- RAS it was displayed as a geometric data with all the river cross-section (figure 17).

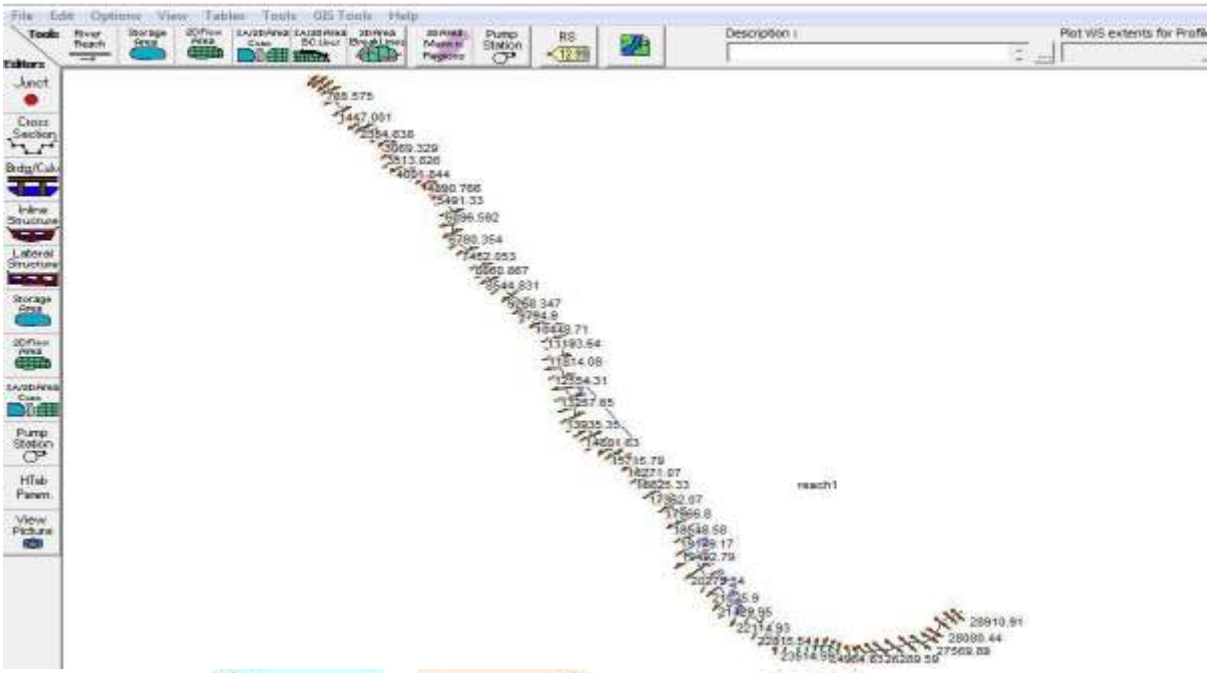

Figure 17 River station and river geometric cross-section exported

Having exporting the entire river cross-section from HEC-Geo RAS to HEC-RAS, it ispossible to see river stations, channel, left and right over bank length in table form tabulated under (Appendex-C). Also, the HEC-RAS can provide different outputs like total discharge of the channel, channel elevation, water surface elevation, critical water surface elevation, energy gradient elevation, energy gradient slope, channel velocity, flow area, top width and channel Froude number for each river station are identified. Then after exporting the river cross-section from Arc GIS through HEC-Geo RAS, geometric data like manning's roughness coefficient, flow data generally known as profile and boundary condition were added.

The manning's roughness coefficient n used for Huluka river watershed was taken from HEC-RAS reference manual considering the flood plain as the urban area and cultivated area as it was recommended in the manual in which n = 0.035 both for left and right over bank and n =
0.04 for channel. Flow data (profiles) was obtained from peak flood frequency analysissimulated in HEC-HMS for 10, 25, 50 and 100 year return period. Upstream critical depth anddownstream critical depth was selected as a boundary condition. A steady flow analysis with mixed flow regime was selected and the model was run. Having running the model, the 3D view of the multiple river cross section plots were presented as on (Appendex-D).

After running the HEC-RAS successfully, the GIS data such as water surface and water surface extent, velocity, river center lines and the entire river cross-section for all profiles were exported to GIS as 'RASexport.sdf' format were presented on (Appendex-E).

RAS post-processing

The delineation of floodplains was accomplished by integrating the RAS-GIS output file (RASexport.sdf) and the TIN layer on GIS. The next step was overlaying the terrain TIN withwater surface TIN. From this, inundation depths and floodplain boundaries are extracted.

RAS GIS output conversion: HEC- Geo RAS cannot recognize the direct output of RAS GIS file format and must be converted in to HEC-Geo RAS file format. By using 'Import RASSDF File' toolbar of HEC-Geo RAS, the RASexport.sdf file format was converted in to XML file format so that the Arc GIS can recognize it.

Layer setup: by using the layer setup window of HEC- Geo RAS, the type of analysis (in thiscase steady flow analysis), input (RAS GIS file, terrain TIN) and output data directory were identified.

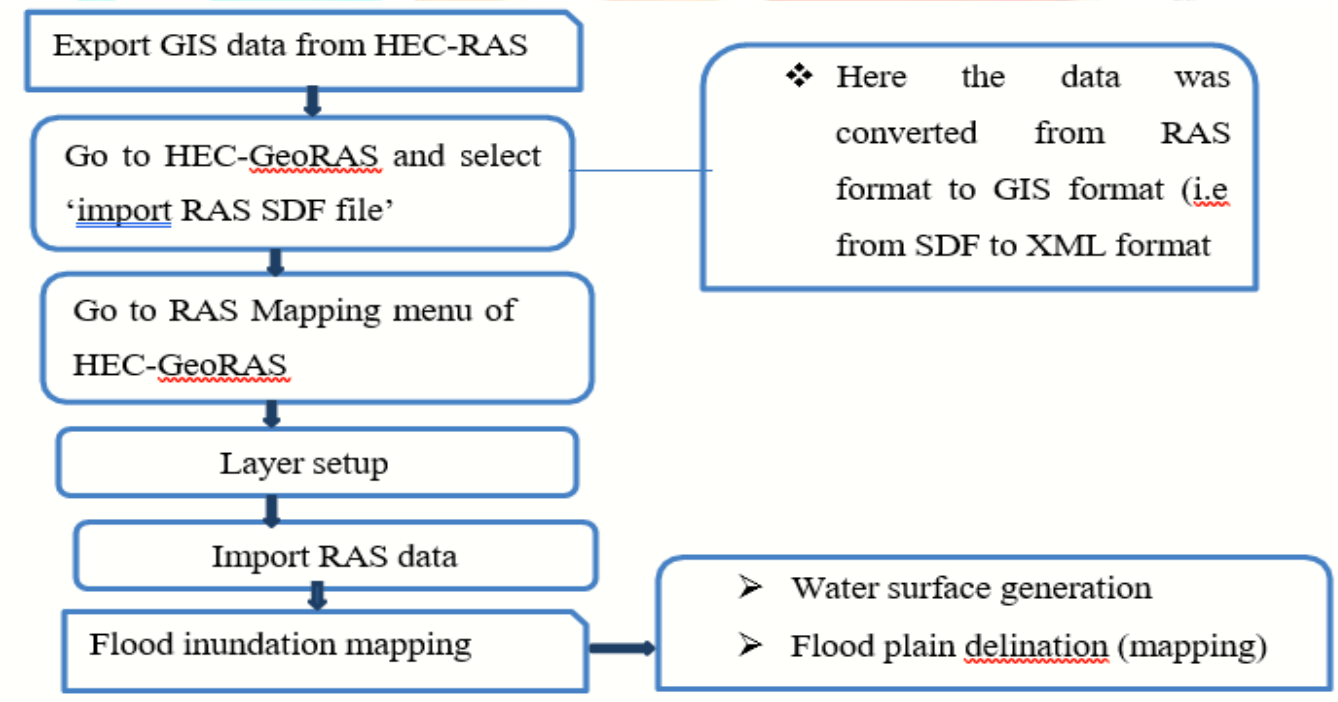

Figure 18 Flood inundation mapping work flow diagram

Generation of water surface TIN

The first step was to create a water surface TIN from the cross-section water surface elevations using HEC-Geo RAS. All Six water surface profiles like, bank points, velocities, river 2D, XS cutlines, bounding polygon

and TIN were selected from the window then for each selected water surface profile, a water surface TIN is created without consideration ofthe terrain model. The TIN was created using the Arc GIS triangulation method. This allowed for the creation of a surface using cut lines as hard break lines with constant elevation. The water surface TIN was generated using Arc GIS for flow profile used in HEC-RAS, indicated water surface TIN for 100 year return period of peak flood as in the (figure 3.22) and the water surface TIN for 10-, 25- and 50-year return period were presented on (Appendex-F).

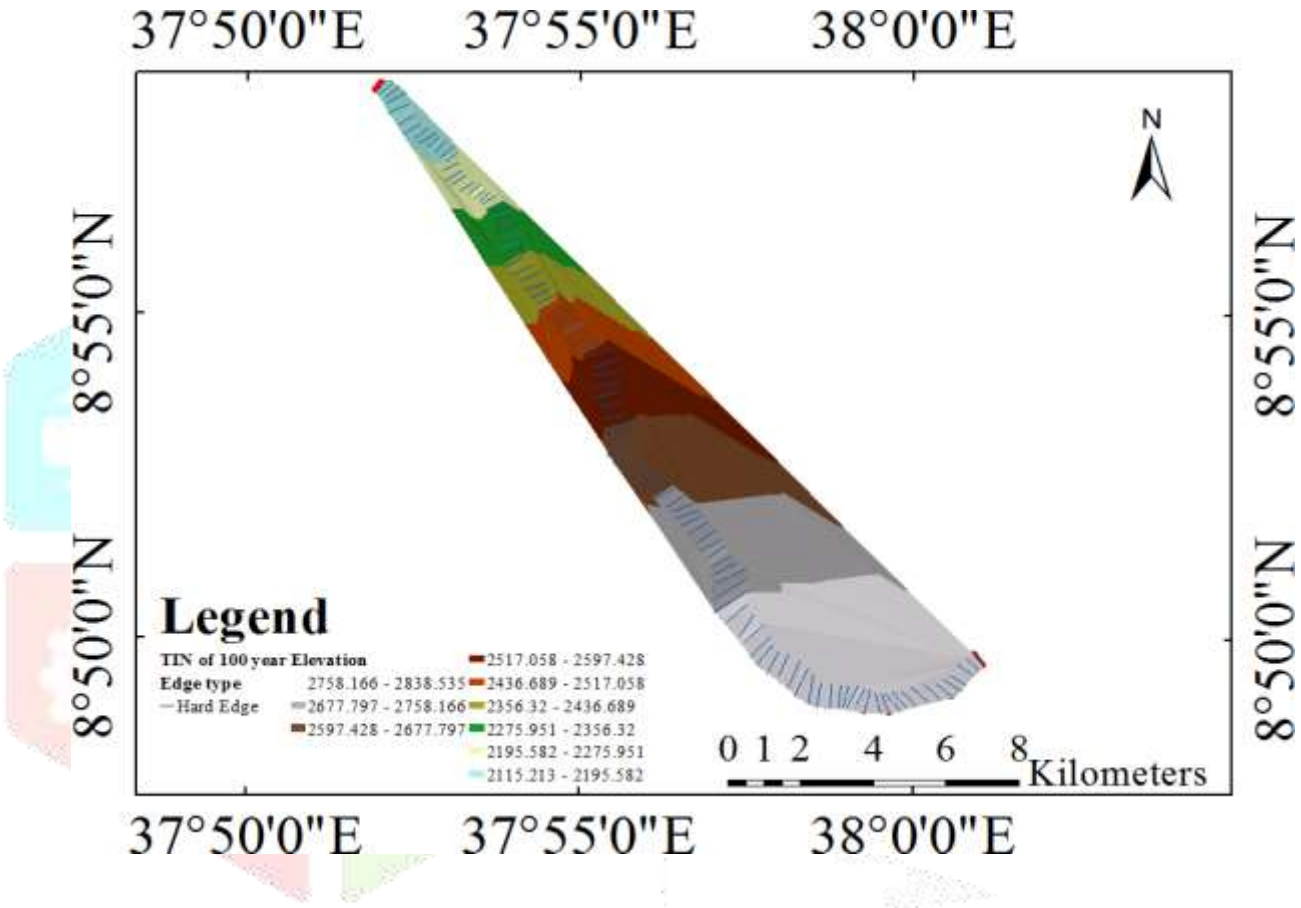

Figure 19 Water surface TIN for 100 year return period of peak flood

IV. RESULTS AND DISCUSSION

Model performancy check

Sensitivity Analysis

The Value of each parameter found in HEC-HMS must be specified to use the model for estimating run-off volume and routing hydrographs. Some of the model parameters cannot be estimated by observation or measurement of the watershed characteristics. Among the parameters used in HEC-HMS for rainfall runoff modeling of this study, flood wave travel time (Muskingum-K) and weighted coefficient of discharge (Muskingum-X) were the most sensitive parameters and the calibration was carried out considering these parameters. The objective function measures the goodness of fit between computed and observed flow at the

selected elements. (Table 8) were indicates the initial and optimized value of the parameters and objective function sensitivity value.

Table 8 HEC-HMS optimized parameters for Huluka river watershed

Elements	Parameters	Initial value	Optimized value	Objective function sensitivity
R10	Muskingum-K	0.6	1.303	-0.26
	Muskingum-X	0.2	0.19208	0.02
R120	Muskingum-K	0.6	0.60600	-0.01
	Muskingum-X	0.2	0.19208	0.00
R150	Muskingum-K	0.6	1.3500	0.00
	Muskingum-X	0.2	0.19208	0.00
W780	CN	80.034	52.289	0.00
W820	CN	77.122	77.122	0.00
W840	CN	77.228	46.337	0.02
W980	CN	85.747	86.55	0.00

A total of 15 years historical data from 1997 to 2011 was used. Out of this for calibration (1997- 2006) and validation (2007-2011) of HEC-HMS model.

Model Calibration

HEC-HMS calibration was performed for Huluka river watershed using rainfall and flow discharge at outlet on daily basis. The simulated flow from HEC-HMS was calibrated using the observed flow and optimization of the model parameters values were carried out within the recommended ranges. Nash-Sutcliffe efficiency (NSE) and coefficient of determination (R^2) result has a value of 0.744 and 0.8556 respectively, shows that there was a goodagreement between simulated and observed stream flow. These results are in the acceptable range. Among the different objective functions available in HEC-HMS, Mean absolute error and RMS error were used. Mean absolute error and RMS error during calibration on (Figure 20) were 1.6 m^3/s and 2.6 m^3/s respectively.

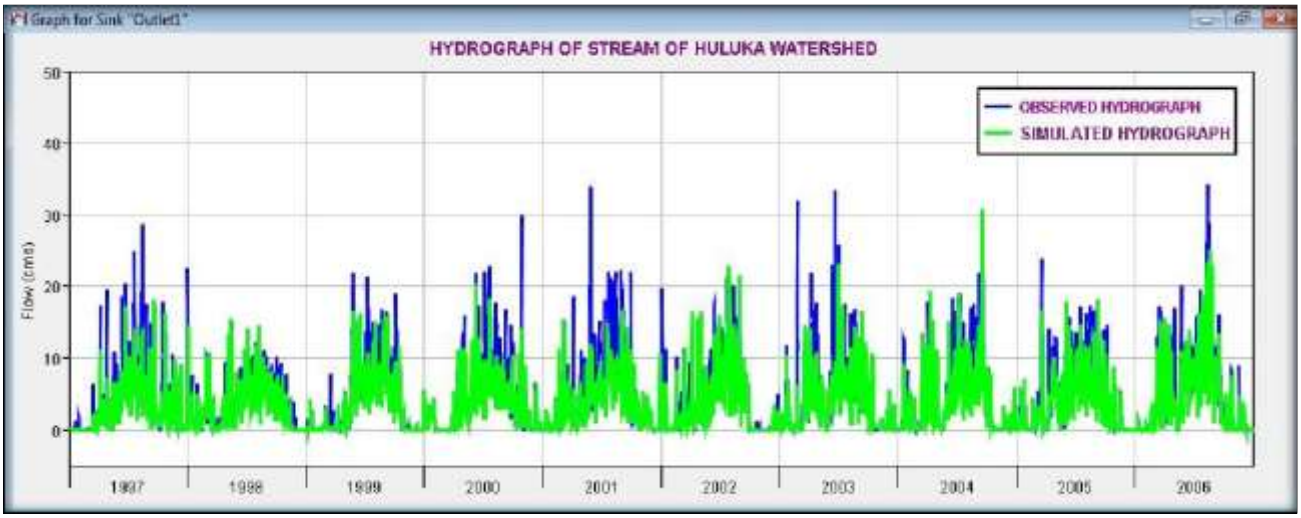

Figure 20 Daily hydrograph comparison between Simulated and Observed flow duringcalibration

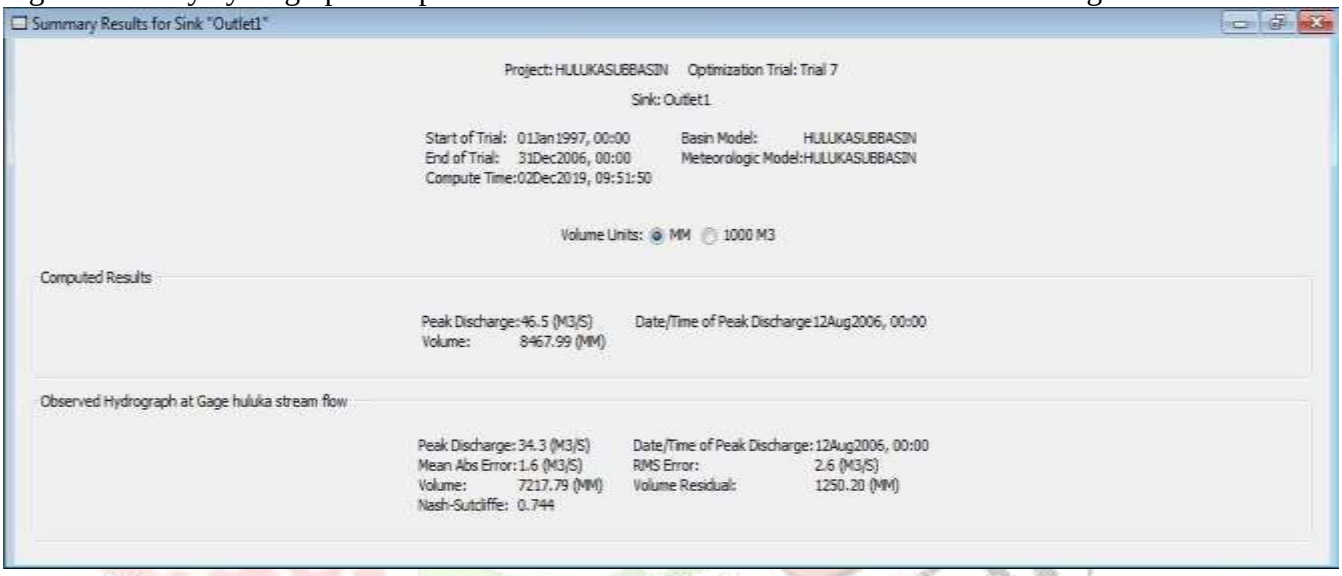

Figure 21 HEC-HMS Model calibration

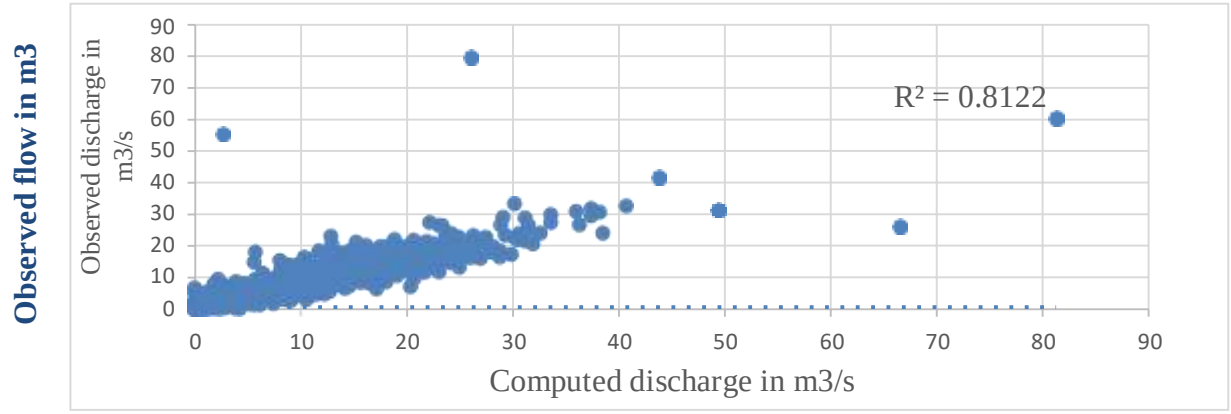

Figure 22 Scattering plot (R^2) of computed and observed flow during calibration results

Model Validation

After the calibration was completed and all model parameters were adjusted, a 5 years hydro- meteorological data (i.e. precipitation and observed flow) were entered and model validation was carried out to check whether the model with adjusted parameter was valid or not.

After processing the input data, the model was generated good results without any adjustment; especially, the sensitive parameters. The Nash Sutcliff efficiency and coefficient of determination during the model validation were 0.720 and 0.8122 respectively and graphically, Coefficient of determination during model validation were presented as figure 4.5and 4.6. Among the different objective functions available in HEC-

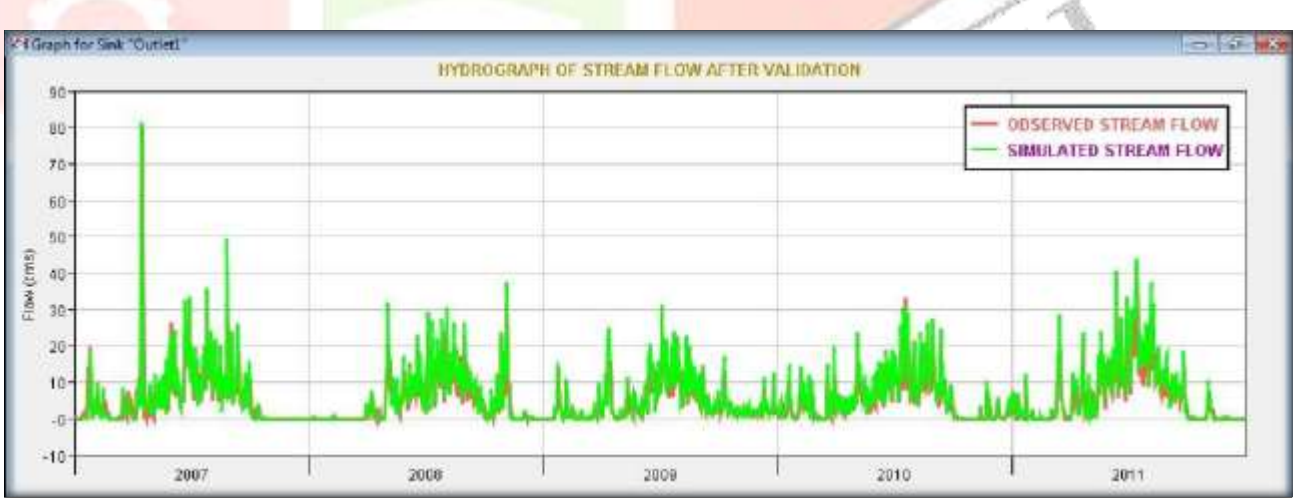

HMS, mean absolute errorand RMS error were used. Mean absolute error and RMS error during validation on (Figure 23) were 1.7 m^3/s and 3.4 m^3/s respectively.

Figure 23 Daily hydrograph comparison between Simulated and Observed flowduringvalidation

Figure 24 HEC-HMS Model efficiency results for validation

Rainfall-runoff modeling

Basin parameters

According to the soil classification and LULC of Huluka river watershed computed in Arc GIS 10.2 the basin parameters used were extracted and calculated in (table 9). The CN grid and the impervious grid incorporating LULC, soil type and hydro fill were analyzed on (figure 7 and 8 respectively).

Table 9 Basin parameters of Huluka river watershed

Sub-basin	Curve Numbers(CN)	Basin lag time(min)	Maximum retention potential (mm)	Intial abstractions(mm)
W780	80.034	378.174	63.365	12.673
W820	77.122	319.62	75.35	15.07
W840	77.228	416.37	74.9	14.98
W980	85.747	128.868	42.22	8.444

Land Use Change Effect on Hydrological Modeling Result

The land use of the study area is changing from time to time. Ambo town is found at the center of the watershed some portion of the agriculture land was converted in to Urban area due to current migrant of residents. Especially in recent years the change is dynamic. As shown on (Table 10) the percentage of Urban area increases from 5.2% in 1997 to 10.15% in 2011 whereas, agricultural land decreases from 58.58% to 56.31% within these years.

Table 10 Percentage of land use for 1997, 2005 and 2011

S no.	Land use /land cover type	Percentage of land use

		1997	2005	2011
1	Water body	0.73	0.68	0.56
2	Agricultural area	58.58	57.51	56.31
3	Forest area	35.49	33.31	32.98
4	Residential (Urbanization area)	5.2	8.5	10.15
	Totals	100	100	100

To evaluate the effect of the land use on surface runoff, equal amount of daily rainfall is selected. This helps to avoid the effect of rainfall variation on the generated peak discharge for all selected years. Accordingly, the generated peak discharge difference was found due to the land use change on the watershed.

The CN value is the cumulative effect of different soil types and LULC of the study area. The Curve Number value of the study area is increased from 1997 to 2011 as shown on (table 11).This result shows hydrological characteristics of the watershed are the major factors which alter the peak discharge of the study area using equal rain fall distribution. When the Curve Number (CN) increase the amount of peak discharge generated from Huluka River watershed also increases on (table 12).

Table 11 CN and impervious area for study area results by SCS TR55 table

Year	Composite Curve Number (CN)	Composite of Impervious area(%)	Peak discharges(m^3/s)
1997	70	20	36.5
2005	80	25	47.56
2011	85	30	61.04

The peak discharges found from HEC-HMS model at the main outlet of the study area for 1997, 2005 and 2011 are shown on (table 12)

Table 12 Huluka River watershed HEC- HMS model simulation result for different years of land use changes on surface runoff

Year	Peak discharges(m^3/s)
1997	36.5
2005	47.56
2011	61.04

Frequency Storm Method Analysis

The 1hr, 2hr, 3hr, 6hr, 12hr and 24hr duration rainfall depth for the corresponding return period was computed

using (equation 13 and table 7). As it can be seen from the table, every return period under consideration has maximum rainfall depth during the 24hr.

Table 13 Rainfall depth (mm) vs Return period (yr) for Huluka watershed

Rainfall intensity duration	Rainfall depth vs Return periods (mm)			
	10	25	50	100
1	51.05	57.53	62.35	67.20
2	59.89	67.49	73.15	78.84
3	64.10	72.23	78.29	84.38
6	70.04	78.92	85.54	92.19
12	74.93	84.44	91.52	98.63
24	79.29	89.35	96.84	104.37

The computed rainfall depth for each rainfall duration with corresponding to return period was used in HEC-HMS to generate peak discharge for each return period. Then the peak discharge simulated from HEC-HMS was compared with the result computed by different flood frequency distribution like General Extreme Value (GEV), Log normal and Log PearsonType 3. Those were selected based on the rank given for each statistical distribution methodby statistical software known as EASYFIT 5.6. After model setup was adjusted using different parameters and model validation was carried out using daily time series data a 1hr, 2hr, 3hr, 6hr, 12hr and 24hr rainfall depth provided on (table 14) was inserted into HEC- HMS for the computation of 10, 25, 50 and 100 year return period peak flood

Table 14 24 hr Rainfall depth and its peak flood for different return period simulated by HEC-HMS.

S/no	Return period (yr)	24 Rainfall depth (mm)	Peak flow (m^3/s)
1	10	79.29	38.2
2	25	89.35	47.2
3	50	96.84	54.2
4	100	104.37	61.4

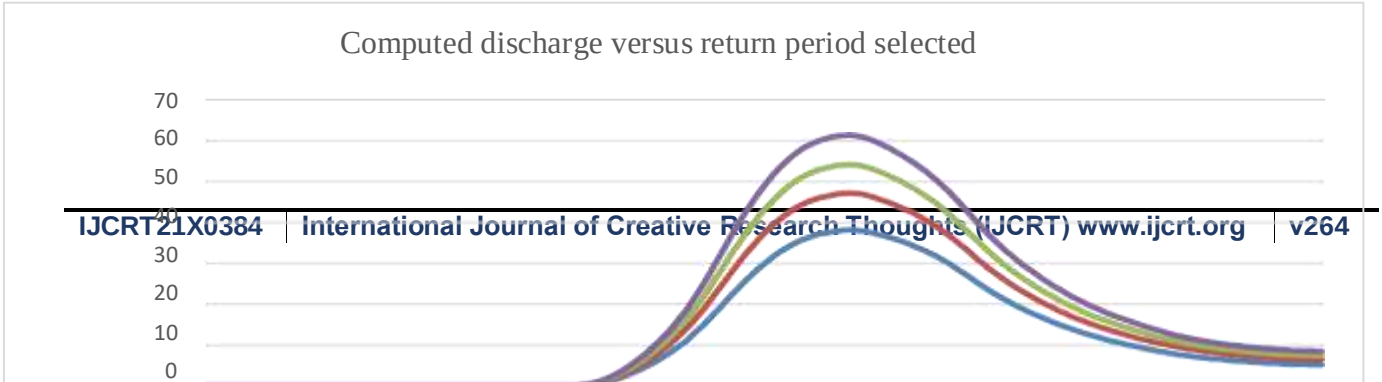

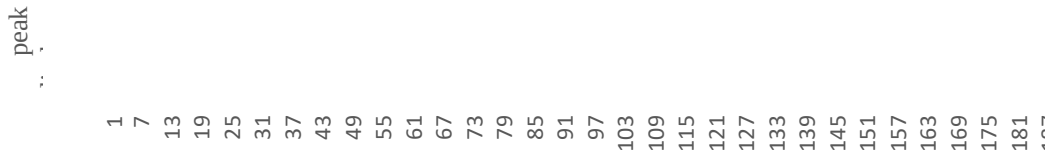

Figure 26 Peak discharge versus time for selected return period

The HEC-HMS result found is compared with different techniques of frequency analysis like General Extreme Value, Log normal and Log Pearson Type 3. These frequency analysis techniques are worldwide accepted methods and simple to use. For this purpose annual peak discharge record of Huluka river watershed from 1997-2011 is taken and the result is shown on (table 15).

Table 15 Flood frequency analysis and HEC-HMS results comparison

Return period(yr)	HEC-HMS(m^3/s)	GEV(m^3/s)	LOGNORMAL(3P)	LOG PEARSON III
10	38.2	37.7	46.37	47.119
25	47.2	47.7	53.732	58.059
50	54.2	56.6	59.084	66.059
100	61.4	65	68	76.541

Figure 27 Frequency analysis and HEC-HMS results comparison

Both (table 15 and figure 27) shows the GEV and Log Normal (3p) frequency analysis type values have a closer value than Log Pearson Type III to HEC-HMS. Based on physical observation and different studies the Ambo town is poor sewerage system creates highaccumulation of plastics and other materials on the river channel. This has high effect on the result found from the automatic recorder and creates less reliability on the historical river discharge data. Due to this, the result found from HEC-HMS assumed as a good representative.

Flood inundation mapping assessement

River geometry

River cross-section represents the river geometry like river center line, bank line, flow path line and XS Cut line along the flood plain. For Huluka river watershed 99 XS Cutlines were digitized in Arc GIS and HEC-

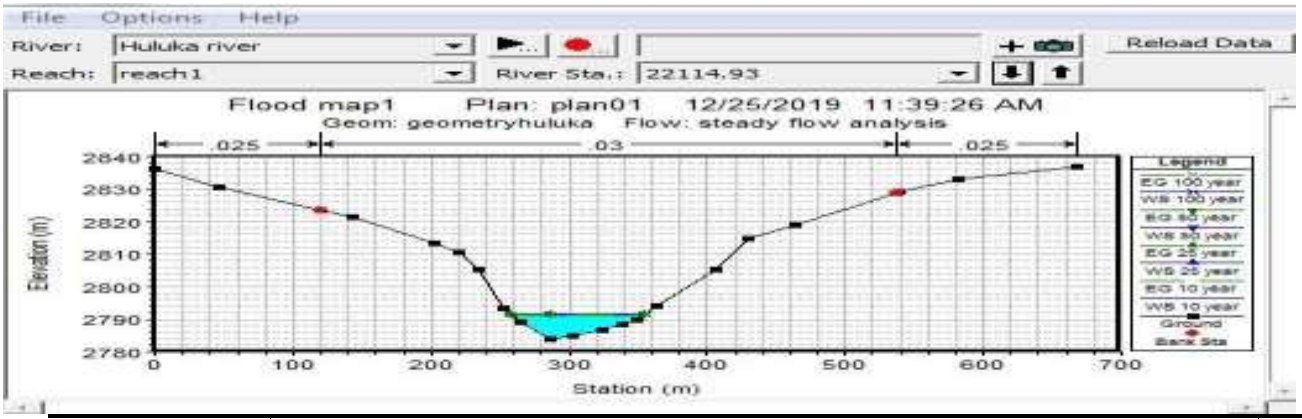

Geo RAS with the help of Arc GIS assigns the river stationsfor every XS Cut lines on (Appendex-I) and also calculated the channel length, left and right over bank length. On Appendex-I, the blue line indicated the river center line along the flood plain; the red points shown bank line points and yellow line represented the river XS Cut linesacross the river center line. Having a peak flood for different return periods from HEC-HMS, river geometry and river cross-section data extracted from digital terrain model as in the (Appendex-I), manning's roughness coefficient (n = 0.035 for right and left bank and n = 0.04for channel bed) taken from HEC-RAS manual in accordance with flood plain property and boundary condition (critical depth flow regime), the hydraulic modeling was developed for steady state 1-Dimensional flow condition. Having entering all the necessary data and runningthe RAS model for mixed flow regime, the river profile elevation along the flood plain was shown as on the figure 28.

Figure 28 River profile and water surface elevation along Huluka river flood plain

The main river channel profile for steady one dimensional flow modeled for mixed flowregime was given as in the figure 29.

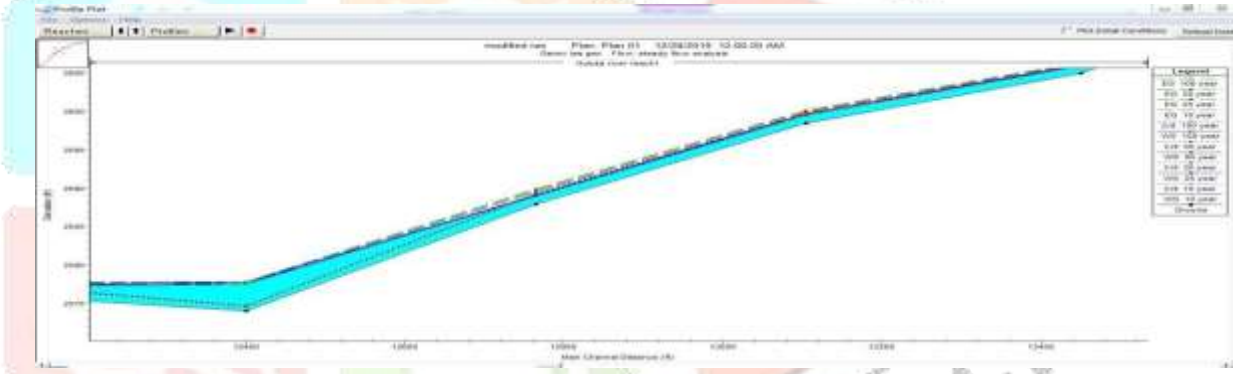

Figure 29 View of main channel profile

Flood inundation area

The GIS data exported from HEC-RAS in the RASexport.sdf file format was converted toxml file. so that it was easy to process in Arc GIS for the final flood inundation mapping. After converting the file to Arc GIS compatible using 'Import RAS SDF File' which is one of the HEC-GeoRAS menus, HEC-Geo RAS layer setup was adjusted and the RAS data was imported and then flood inundation mapping was take place. The result indicated that a 10,25, 50 and 100 year return period frequency storm inundates 97.58, 100.56, 103.34 and 105.54 ha respectively of the proposed flood plain with the minimum and maximum water depth of 0.002441- 17.7632, 0.00926 - 17.8779, 0.000488 - 17.95 and 0.000241-18.037 in meters respectively.

Maximum flood coverage resulted at 100 years return period frequency storm and it inundatesabout 105.54 ha with a minimum and maximum water depth of 0.000241 and 18.037 m respectively. The inundation area profile

was illustrated in the table 15 and Figure 30 indicates the flood inundation area of Huluka river flood plain for 10 and 25 years return period and Appendex-K shown the flood inundation mapping of the whole profiles.

Table 15 flood inundated area with respect to expected peak flood

S/No	Return period	24 Rainfall depth(mm)	Peak flow(m3/s)	Area (ha)
1	10	79.29	38.2	97.58
2	25	89.35	47.2	100.56
3	50	96.84	54.2	103.34
4	100	104.37	61.4	105.54

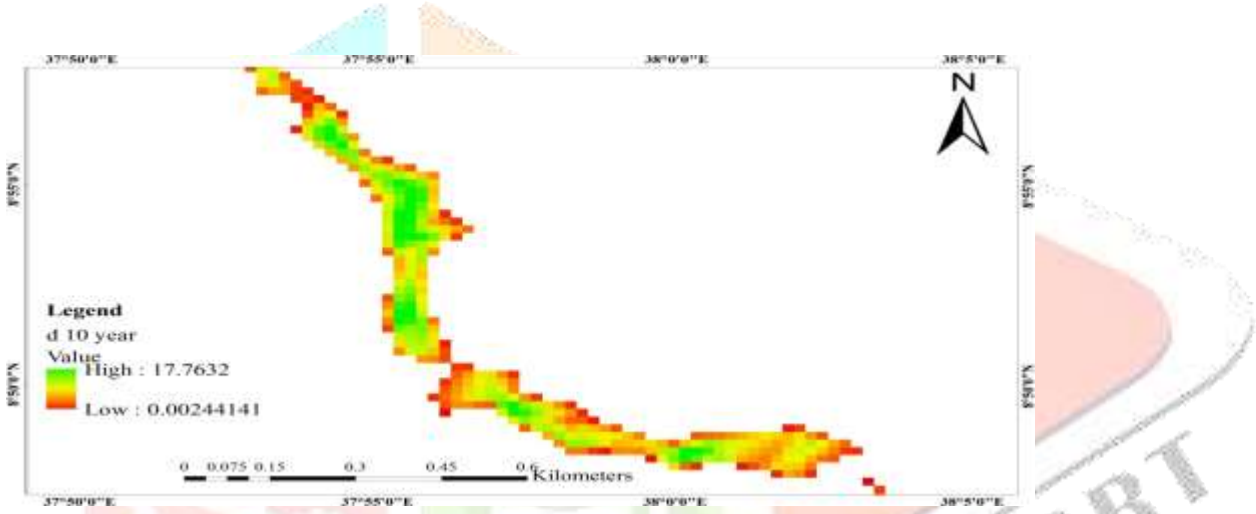

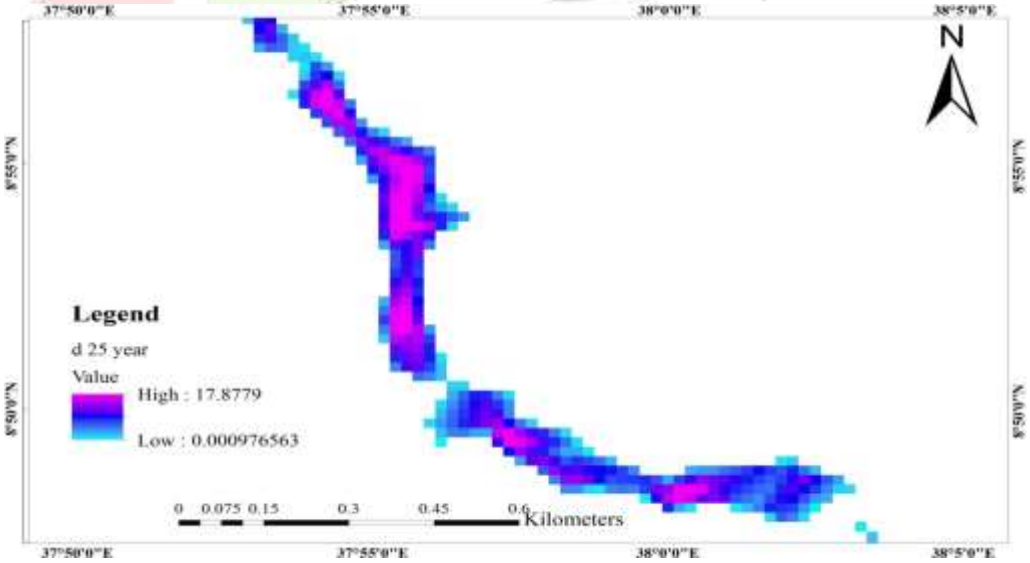

Figure 30 Huluka river floodplain for 10 and 25 year return period peak flow

APPENDEX

APPENDEX A: STUDY AREA DELINATION BY HEC-GeoHMS

Appendex A: Figures of study area delination by using HEC-GeoHMS

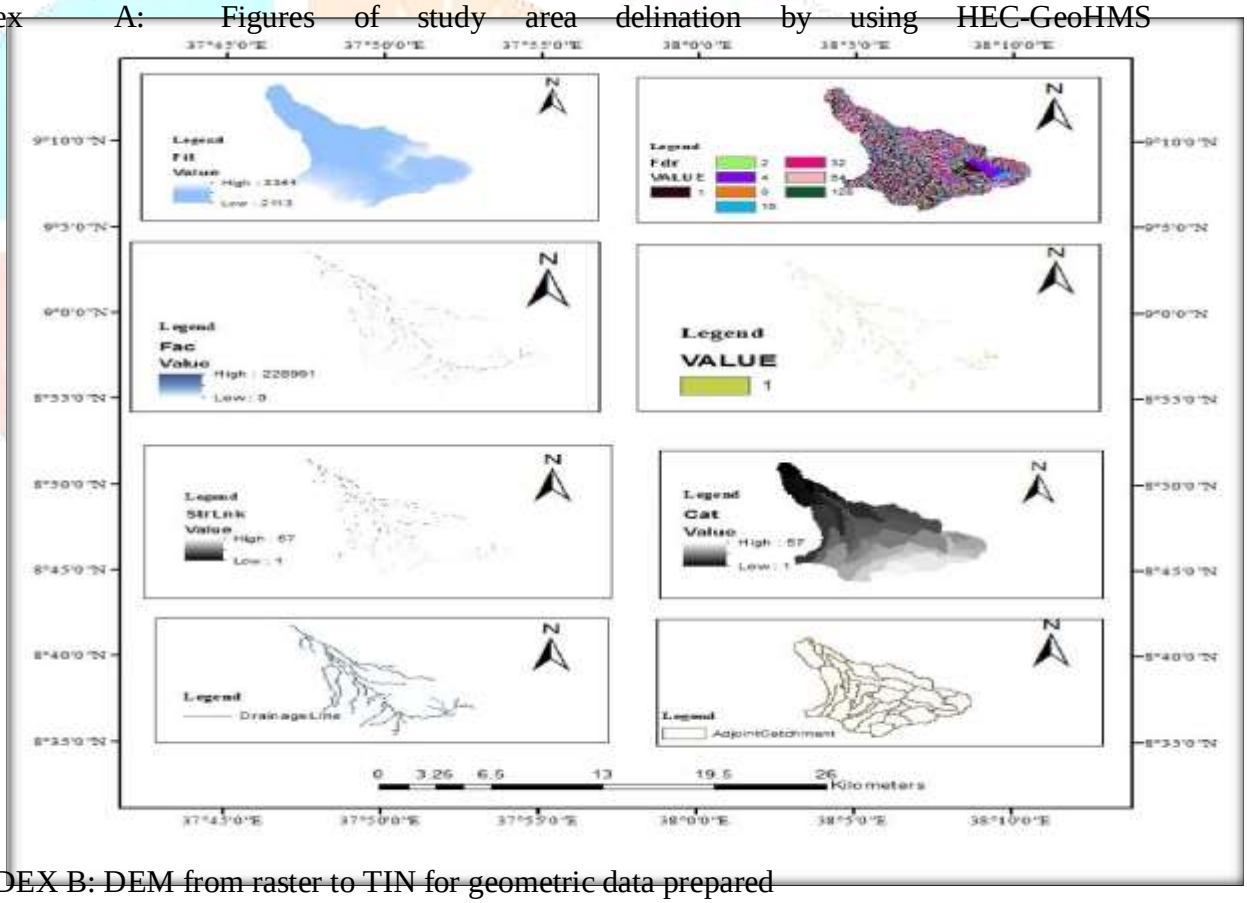

APPENDEX B: DEM from raster to TIN for geometric data prepared

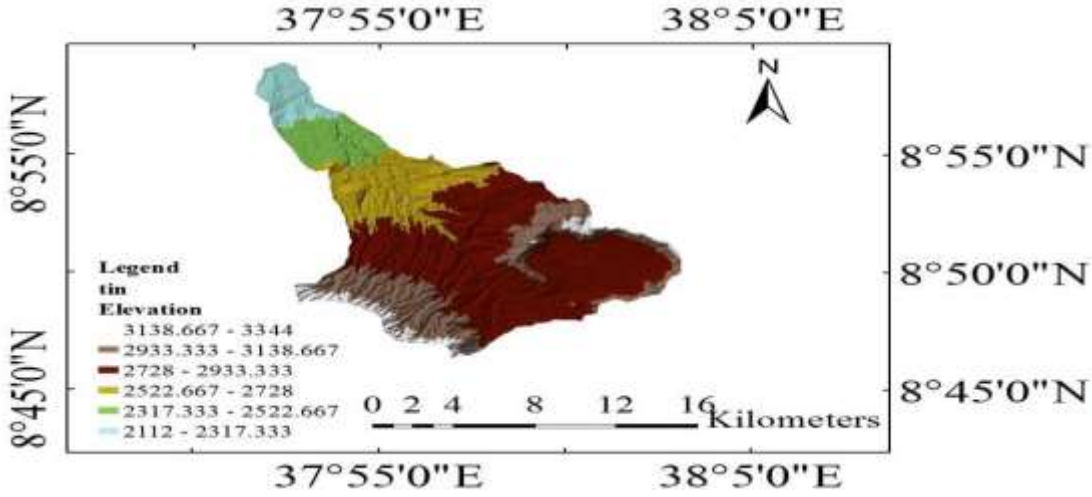
37°55'0"E
38°5'0"E
8°55'0"N
8°50'0"N
8°45'0"N
N
Legend
tin
Elevation
3138.667 - 3344
2933.333 - 3138.667
2728 - 2933.333
2522.667 - 2728
2317.333 - 2522.667
2112 - 2317.333
0 2 4 8 12 16
Kilometers

APPENDEX: C HEC-RAS Hydraulic computations

Profile Output Table - Standard Table 1

File Options Std. Tables Locations Help

HEC-RAS Plan: plan01 River: Huluka river Reach: reach1

Reach	River Sta	Profile	Q Total (m3/s)	Min Ch El (m)	W.S. Elev (m)	Crit W.S. (m)	E.G. Elev (m)	E.G. Slope (m/m)	Vel Chnl (m/s)	Flow Area (m2)	Top Width (m)	roude # Ch
reach1	28910.91	10 year	38.20	2833.00	2838.33	2833.18	2838.33	0.000000	0.04	939.43	190.52	0.01
reach1	28910.91	25 year	47.20	2833.00	2838.41	2833.21	2838.41	0.000000	0.04	956.12	190.98	0.01
reach1	28910.91	50 year	54.20	2833.00	2838.47	2833.23	2838.47	0.000000	0.05	967.84	191.30	0.01
reach1	28910.91	100 year	61.40	2833.00	2838.54	2833.25	2838.54	0.000000	0.06	979.53	191.62	0.01
reach1	28709.64	10 year	38.20	2837.18	2838.11	2838.11	2838.31	0.012412	1.96	19.45	50.39	1.01
reach1	28709.64	25 year	47.20	2837.18	2838.18	2838.18	2838.39	0.012150	2.05	22.99	54.85	1.01
reach1	28709.64	50 year	54.20	2837.18	2838.22	2838.22	2838.45	0.011758	2.12	25.58	56.79	1.01
reach1	28709.64	100 year	61.40	2837.18	2838.26	2838.26	2838.51	0.011723	2.22	27.70	57.36	1.02
reach1	28429.28	10 year	38.20	2829.76	2830.72	2831.07	2831.86	0.053660	4.72	8.09	16.81	2.17
reach1	28429.28	25 year	47.20	2829.76	2830.81	2831.19	2832.06	0.052932	4.95	9.53	18.24	2.19
reach1	28429.28	50 year	54.20	2829.76	2830.86	2831.27	2832.21	0.053688	5.15	10.52	19.16	2.22
reach1	28429.28	100 year	61.40	2829.76	2830.91	2831.35	2832.34	0.053066	5.29	11.60	20.13	2.23
reach1	28080.44	10 year	38.20	2824.06	2824.64	2824.64	2824.87	0.011615	2.15	17.78	38.41	1.01
reach1	28080.44	25 year	47.20	2824.06	2824.71	2824.72	2824.98	0.011197	2.27	20.79	40.21	1.01
reach1	28080.44	50 year	54.20	2824.06	2824.77	2824.77	2825.05	0.010833	2.34	23.11	41.54	1.00
reach1	28080.44	100 year	61.40	2824.06	2824.83	2824.83	2825.12	0.010556	2.42	25.41	42.82	1.00
reach1	27863.15	10 year	38.20	2821.00	2822.14	2821.49	2822.15	0.000364	0.52	73.26	98.71	0.19
reach1	27863.15	25 year	47.20	2821.00	2822.26	2821.55	2822.27	0.000361	0.55	85.51	105.07	0.20
reach1	27863.15	50 year	54.20	2821.00	2822.34	2821.59	2822.36	0.000359	0.57	94.65	109.57	0.20
reach1	27863.15	100 year	61.40	2821.00	2822.42	2821.63	2822.44	0.000359	0.59	103.56	113.85	0.20
reach1	27569.89	10 year	38.20	2820.50	2821.53	2821.53	2821.82	0.011014	2.36	16.19	29.16	1.01
reach1	27569.89	25 year	47.20	2820.50	2821.63	2821.63	2821.94	0.010646	2.46	19.17	31.54	1.01
reach1	27569.89	50 year	54.20	2820.50	2821.70	2821.70	2822.03	0.010400	2.53	21.41	33.23	1.01
reach1	27569.89	100 year	61.40	2820.50	2821.76	2821.76	2822.11	0.010237	2.60	23.62	34.80	1.01
reach1	27209.93	10 year	38.20	2818.47	2819.37	2819.13	2819.42	0.002465	0.99	38.60	83.44	0.46
reach1	27209.93	25 year	47.20	2818.47	2819.44	2819.19	2819.50	0.002507	1.06	44.61	88.30	0.48
reach1	27209.93	50 year	54.20	2818.47	2819.49	2819.23	2819.56	0.002502	1.10	49.27	91.91	0.48
reach1	27209.93	100 year	61.40	2818.47	2819.54	2819.27	2819.61	0.002526	1.14	53.70	95.20	0.49
reach1	26891.98	10 year	38.20	2817.00	2817.73	2817.73	2817.90	0.012808	1.82	20.94	62.19	1.00
reach1	26891.98	25 year	47.20	2817.00	2817.79	2817.79	2817.97	0.012396	1.90	24.84	67.76	1.00
reach1	26891.98	50 year	54.20	2817.00	2817.83	2817.83	2818.02	0.012478	1.97	27.49	71.29	1.01
reach1	26891.98	100 year	61.40	2817.00	2817.87	2817.87	2818.07	0.012264	2.02	30.39	74.96	1.01
reach1	26539.13	10 year	38.20	2812.00	2813.72	2813.13	2813.80	0.001531	1.25	30.65	32.57	0.41
reach1	26539.13	25 year	47.20	2812.00	2813.90	2813.25	2813.99	0.001521	1.27	37.10	38.08	0.41
reach1	26539.13	50 year	54.20	2812.00	2814.03	2813.33	2814.11	0.001493	1.29	42.09	41.84	0.41
reach1	26539.13	100 year	61.40	2812.00	2814.14	2813.41	2814.23	0.001457	1.30	47.19	45.37	0.41
reach1	26289.59	10 year	38.20	2811.11	2813.35		2813.44	0.001334	1.34	28.57	24.37	0.39
reach1	26289.59	25 year	47.20	2811.11	2813.50		2813.61	0.001453	1.46	32.41	25.92	0.42
reach1	26289.59	50 year	54.20	2811.11	2813.61		2813.73	0.001534	1.54	35.22	27.00	0.43
reach1	26289.59	100 year	61.40	2811.11	2813.71		2813.84	0.001605	1.62	38.01	28.03	0.44
reach1	26084.62	10 year	38.20	2811.51	2812.52	2812.52	2812.83	0.010708	2.45	15.62	26.01	1.01
reach1	26084.62	25 year	47.20	2811.51	2812.62	2812.62	2812.96	0.010350	2.59	18.20	27.02	1.01
reach1	26084.62	50 year	54.20	2811.51	2812.69	2812.69	2813.06	0.010079	2.69	20.16	27.77	1.01
reach1	26084.62	100 year	61.40	2811.51	2812.76	2812.76	2813.15	0.009925	2.78	22.05	28.47	1.01
reach1	25848.27	10 year	38.20	2808.36	2809.21	2809.28	2809.54	0.018694	2.56	14.90	35.26	1.26
reach1	25848.27	25 year	47.20	2808.36	2809.26	2809.36	2809.66	0.019859	2.77	17.05	37.64	1.31
reach1	25848.27	50 year	54.20	2808.36	2809.30	2809.41	2809.74	0.020704	2.94	18.44	38.39	1.35
reach1	25848.27	100 year	61.40	2808.36	2809.34	2809.47	2809.83	0.021300	3.09	19.86	39.15	1.39
reach1	25592.74	10 year	38.20	2802.35	2809.08	2803.83	2809.08	0.000003	0.15	260.24	69.67	0.02
reach1	25592.74	25 year	47.20	2802.35	2809.24	2803.97	2809.24	0.000005	0.17	271.50	70.39	0.03
reach1	25592.74	50 year	54.20	2802.35	2809.35	2804.06	2809.35	0.000006	0.19	279.40	70.89	0.03
reach1	25592.74	100 year	61.40	2802.35	2809.46	2804.15	2809.46	0.000007	0.21	286.98	71.36	0.03
reach1	25188.59	10 year	38.20	2806.72	2808.97		2809.06	0.001488	1.37	27.80	24.73	0.41
reach1	25188.59	25 year	47.20	2806.72	2809.11		2809.22	0.001654	1.51	31.32	26.25	0.44
reach1	25188.59	50 year	54.20	2806.72	2809.20		2809.33	0.001775	1.60	33.83	27.28	0.46
reach1	25188.59	100 year	61.40	2806.72	2809.29		2809.44	0.001882	1.69	36.33	28.25	0.48

Reach	River Sta	Profile	Q Total (m3/s)	Min Ch El (m)	W.S. Elev (m)	Crit W.S. (m)	E.G. Elev (m)	E.G. Slope (m/m)	Vel Chnl (m/s)	Flow Area (m2)	Top Width (m)	Froude # Ch
reach1	16271.07	50 year	54.20	2677.51	2681.31	2679.10	2681.34	0.000192	0.78	69.93	31.10	0.17
reach1	16271.07	100 year	61.40	2677.51	2681.44	2679.20	2681.47	0.000212	0.83	74.03	31.95	0.17
reach1	13930.37	10 year	38.20	2679.14	2680.42	2680.42	2680.81	0.009573	2.74	13.96	18.36	1.00
reach1	13930.37	25 year	47.20	2679.14	2680.55	2680.55	2680.98	0.009644	2.88	16.38	19.58	1.01
reach1	13930.37	50 year	54.20	2679.14	2680.64	2680.64	2681.10	0.009427	2.97	18.23	20.42	1.01
reach1	13930.37	100 year	61.40	2679.14	2680.73	2680.73	2681.21	0.009384	3.07	19.98	21.22	1.01
reach1	15715.79	10 year	38.20	2671.39	2671.76	2672.18	2674.47	0.351548	7.29	5.24	23.37	4.91
reach1	15715.79	25 year	47.20	2671.39	2671.86	2672.28	2674.92	0.334668	7.69	6.14	24.31	4.89
reach1	15715.79	50 year	54.20	2671.39	2671.83	2672.32	2674.95	0.307181	7.82	6.93	25.11	4.75
reach1	15715.79	100 year	61.40	2671.39	2671.87	2672.38	2675.04	0.279918	7.89	7.78	25.94	4.60
reach1	15450.97	10 year	38.20	2666.00	2667.23	2667.23	2667.54	0.010451	2.46	15.53	25.18	1.00
reach1	15450.97	25 year	47.20	2666.00	2667.34	2667.34	2667.68	0.010440	2.59	18.21	27.27	1.01
reach1	15450.97	50 year	54.20	2666.00	2667.42	2667.42	2667.77	0.010047	2.65	20.49	28.92	1.00
reach1	15450.97	100 year	61.40	2666.00	2667.49	2667.49	2667.86	0.010025	2.73	22.52	30.32	1.01
reach1	15309.41	10 year	38.20	2662.80	2663.50	2663.51	2663.76	0.011638	2.26	16.87	33.67	1.02
reach1	15309.41	25 year	47.20	2662.80	2663.57	2663.59	2663.88	0.011793	2.45	19.30	34.66	1.05
reach1	15309.41	50 year	54.20	2662.80	2663.62	2663.65	2663.96	0.012436	2.61	20.78	35.24	1.08
reach1	15309.41	100 year	61.40	2662.80	2663.67	2663.71	2664.05	0.012564	2.73	22.49	35.90	1.10
reach1	14801.63	10 year	38.20	2655.32	2656.34	2656.54	2657.23	0.048500	4.40	8.68	18.55	2.06
reach1	14801.63	25 year	47.20	2655.32	2656.52	2656.66	2657.42	0.045666	4.63	10.20	19.36	2.03
reach1	14801.63	50 year	54.20	2655.32	2656.40	2656.74	2657.51	0.041163	4.67	11.61	20.08	1.96
reach1	14801.63	100 year	61.40	2655.32	2656.48	2656.82	2657.63	0.039684	4.80	12.80	20.66	1.95
reach1	14568.96	10 year	38.20	2646.03	2647.23	2647.58	2648.23	0.031526	4.42	8.63	13.11	1.74
reach1	14568.96	25 year	47.20	2646.03	2647.33	2647.70	2648.46	0.032779	4.71	10.02	14.26	1.79
reach1	14568.96	50 year	54.20	2646.03	2647.39	2647.81	2648.66	0.033060	4.99	10.86	14.92	1.87
reach1	14568.96	100 year	61.40	2646.03	2647.46	2647.90	2648.82	0.033925	5.18	11.85	15.65	1.90
reach1	14250.23	10 year	38.20	2633.35	2634.58	2634.97	2635.91	0.048841	5.17	7.39	13.33	2.13
reach1	14250.23	25 year	47.20	2633.35	2634.66	2635.11	2636.11	0.048936	5.32	8.87	13.51	2.10
reach1	14250.23	50 year	54.20	2633.35	2634.79	2635.22	2636.24	0.043772	5.41	10.01	14.39	2.07
reach1	14250.23	100 year	61.40	2633.35	2634.82	2635.31	2636.37	0.042213	5.51	11.15	15.14	2.05
reach1	13935.35	10 year	38.20	2617.18	2617.72	2618.11	2619.18	0.057042	3.31	7.50	18.97	2.02
reach1	13935.35	25 year	47.20	2617.18	2617.78	2618.21	2619.49	0.062456	3.68	8.53	20.24	2.15
reach1	13935.35	50 year	54.20	2617.18	2617.81	2618.29	2619.75	0.067547	3.96	9.21	21.04	2.25
reach1	13935.35	100 year	61.40	2617.18	2617.86	2618.35	2619.88	0.066326	4.12	10.20	22.14	2.26
reach1	13600.5	10 year	38.20	2604.91	2605.92	2606.09	2606.48	0.025019	3.33	11.48	22.82	1.50
reach1	13600.5	25 year	47.20	2604.91	2606.00	2606.19	2606.62	0.024592	3.49	13.54	24.78	1.51
reach1	13600.5	50 year	54.20	2604.91	2606.07	2606.27	2606.71	0.023581	3.55	15.26	26.31	1.49
reach1	13600.5	100 year	61.40	2604.91	2606.13	2606.33	2606.81	0.023509	3.66	16.78	27.58	1.50
reach1	13257.65	10 year	38.20	2598.43	2599.67	2599.77	2600.20	0.013787	3.24	11.80	15.43	1.18
reach1	13257.65	25 year	47.20	2598.43	2599.79	2599.91	2600.39	0.013788	3.43	13.74	16.42	1.20
reach1	13257.65	50 year	54.20	2598.43	2599.87	2600.01	2600.53	0.014060	3.59	15.08	17.07	1.22
reach1	13257.65	100 year	61.40	2598.43	2599.95	2600.11	2600.66	0.013975	3.71	16.54	17.76	1.23
reach1	12919.07	10 year	38.20	2587.88	2588.92	2589.42	2590.75	0.078875	5.99	6.38	12.24	2.65
reach1	12919.07	25 year	47.20	2587.88	2589.01	2589.58	2591.01	0.078816	6.25	7.55	13.32	2.65
reach1	12919.07	50 year	54.20	2587.88	2589.09	2589.68	2591.15	0.073519	6.36	8.53	14.15	2.62
reach1	12919.07	100 year	61.40	2587.88	2589.15	2589.77	2591.33	0.072754	6.54	9.38	14.85	2.63
reach1	12554.31	10 year	38.20	2574.00	2577.88	2574.75	2577.88	0.000007	0.17	225.23	83.23	0.03
reach1	12554.31	25 year	47.20	2574.00	2578.04	2574.83	2578.04	0.000009	0.20	238.88	84.45	0.04
reach1	12554.31	50 year	54.20	2574.00	2578.15	2574.88	2578.16	0.000010	0.22	248.59	85.30	0.04
reach1	12554.31	100 year	61.40	2574.00	2578.26	2574.94	2578.27	0.000012	0.24	257.95	86.12	0.04
reach1	12247.64	10 year	38.20	2576.04	2577.47	2577.47	2577.83	0.010186	2.67	14.32	20.02	1.01
reach1	12247.64	25 year	47.20	2576.04	2577.60	2577.60	2577.99	0.009877	2.78	16.97	21.79	1.01
reach1	12247.64	50 year	54.20	2576.04	2577.69	2577.69	2578.10	0.009636	2.85	19.00	23.06	1.00
reach1	12247.64	100 year	61.40	2576.04	2577.77	2577.77	2578.21	0.009592	2.94	20.90	24.19	1.01
reach1	11814.08	10 year	38.20	2556.49	2557.04	2557.68	2563.31	0.621654	11.09	3.44	12.49	6.75
reach1	11814.08	25 year	47.20	2556.49	2557.09	2557.77	2563.85	0.595710	11.51	4.10	13.63	6.70
reach1	11814.08	50 year	54.20	2556.49	2557.12	2557.83	2564.59	0.621065	12.10	4.48	14.25	6.89
reach1	11814.08	100 year	61.40	2556.49	2557.17	2557.89	2564.24	0.531138	11.77	5.22	15.38	6.46
reach1	11503.85	10 year	38.20	2552.67	2553.47	2553.47	2553.70	0.011843	2.13	17.96	39.90	1.01
reach1	11503.85	25 year	47.20	2552.67	2553.54	2553.54	2553.80	0.011132	2.25	20.95	40.74	1.00

reach1	11503.85	50 year	54.20	2552.67	2553.59	2553.59	2553.87	0.010789	2.35	23.11	41.34	1.00
reach1	11503.85	100 year	61.40	2552.67	2553.64	2553.64	2553.95	0.010628	2.44	25.15	41.89	1.01
reach1	11193.64	10 year	38.20	2538.44	2539.51	2540.29	2543.86	0.187630	9.25	4.13	7.76	4.05
reach1	11193.64	25 year	47.20	2538.44	2539.60	2540.46	2544.40	0.185662	9.71	4.86	8.42	4.08
reach1	11193.64	50 year	54.20	2538.44	2539.66	2540.57	2544.72	0.181012	9.96	5.44	8.91	4.07
reach1	11193.64	100 year	61.40	2538.44	2539.73	2540.68	2544.90	0.171369	10.06	6.10	9.43	3.99
reach1	10858.33	10 year	38.20	2532.91	2534.45	2534.45	2534.83	0.010085	2.73	14.01	18.81	1.01
reach1	10858.33	25 year	47.20	2532.91	2534.59	2534.59	2535.00	0.009668	2.82	16.73	20.68	1.00
reach1	10858.33	50 year	54.20	2532.91	2534.68	2534.68	2535.11	0.009494	2.90	18.72	21.95	1.00
reach1	10858.33	100 year	61.40	2532.91	2534.77	2534.77	2535.22	0.009417	2.97	20.64	23.11	1.00
reach1	10448.71	10 year	38.20	2504.55	2504.89	2505.51	2520.61	2.939846	17.56	2.18	12.75	13.58
reach1	10448.71	25 year	47.20	2504.55	2504.93	2505.59	2520.16	2.447481	17.28	2.73	14.29	12.63
reach1	10448.71	50 year	54.20	2504.55	2504.97	2505.65	2518.98	1.996371	16.58	3.27	15.64	11.58
reach1	10448.71	100 year	61.40	2504.55	2504.97	2505.71	2523.15	2.601257	18.89	3.25	15.59	13.21
reach1	10117.76	10 year	38.20	2495.48	2497.20	2497.37	2497.92	0.018186	3.76	10.16	11.63	1.29
reach1	10117.76	25 year	47.20	2495.45	2497.35	2497.54	2498.14	0.015874	3.94	11.99	12.65	1.29
reach1	10117.76	50 year	54.20	2495.45	2497.46	2497.67	2498.28	0.015136	4.00	13.54	13.44	1.27
reach1	10117.76	100 year	61.40	2495.45	2497.51	2497.78	2498.47	0.017082	4.32	14.21	13.77	1.36
reach1	9794.9	10 year	38.20	2489.85	2490.91	2491.09	2491.90	0.024662	3.41	11.21	21.22	1.50
reach1	9794.9	25 year	47.20	2489.85	2490.99	2491.20	2491.86	0.023756	3.65	12.93	22.78	1.55
reach1	9794.9	50 year	54.20	2489.85	2491.03	2491.28	2491.80	0.027738	3.89	13.95	23.67	1.62
reach1	9794.9	100 year	61.40	2489.85	2491.12	2491.35	2491.86	0.024388	3.82	16.07	25.41	1.53
reach1	9562.237	10 year	38.20	2462.91	2463.76	2464.78	2474.55	0.623511	14.55	2.63	6.15	7.11
reach1	9562.237	25 year	47.20	2462.91	2463.86	2464.94	2474.57	0.536483	14.50	3.26	6.85	6.72
reach1	9562.237	50 year	54.20	2462.91	2463.94	2465.06	2474.23	0.463450	14.20	3.82	7.42	6.32
reach1	9562.237	100 year	61.40	2462.91	2463.97	2465.17	2475.74	0.510071	15.19	4.04	7.63	6.67
reach1	9268.347	10 year	38.20	2458.80	2460.45	2460.51	2460.94	0.011559	3.10	12.31	14.90	1.09
reach1	9268.347	25 year	47.20	2458.80	2460.59	2460.66	2461.14	0.011641	3.28	14.39	16.11	1.11
reach1	9268.347	50 year	54.20	2458.80	2460.69	2460.76	2461.27	0.011451	3.37	16.06	17.02	1.11
reach1	9268.347	100 year	61.40	2458.80	2460.75	2460.87	2461.41	0.012524	3.60	17.05	17.54	1.17
reach1	8927.437	10 year	38.20	2453.67	2455.42	2455.63	2456.18	0.017057	3.86	9.89	11.30	1.32
reach1	8927.437	25 year	47.20	2453.67	2455.57	2455.79	2456.41	0.016678	4.04	11.69	12.28	1.32
reach1	8927.437	50 year	54.20	2453.67	2455.67	2455.92	2456.57	0.016735	4.19	12.95	12.93	1.34
reach1	8927.437	100 year	61.40	2453.67	2455.81	2456.03	2456.69	0.015236	4.17	14.73	13.79	1.29
reach1	8544.831	10 year	38.20	2423.91	2424.58	2425.46	2435.99	0.888247	14.96	2.55	7.63	8.25
reach1	8544.831	25 year	47.20	2423.91	2425.60	2425.60	2436.05	0.009756	2.95	15.98	18.36	1.01
reach1	8544.831	50 year	54.20	2423.91	2424.71	2425.71	2436.25	0.714775	15.05	3.60	9.06	7.62
reach1	8544.831	100 year	61.40	2423.91	2424.74	2425.80	2437.35	0.740391	15.73	3.90	9.43	7.81
reach1	8304.63	10 year	38.20	2414.52	2416.20	2416.49	2417.13	0.021915	4.25	8.98	10.67	1.48
reach1	8304.63	25 year	47.20	2414.52	2415.81	2416.68	2419.85	0.136325	8.90	5.30	8.20	3.54
reach1	8304.63	50 year	54.20	2414.52	2416.43	2416.78	2417.55	0.022485	4.69	11.56	12.11	1.53
reach1	8304.63	100 year	61.40	2414.52	2416.51	2416.90	2417.74	0.023411	4.91	12.50	12.59	1.57
reach1	8060.867	10 year	38.20	2411.27	2413.06	2413.07	2413.56	0.009867	3.14	12.18	12.62	1.02
reach1	8060.867	25 year	47.20	2411.27	2413.24	2413.24	2413.78	0.009225	3.23	14.60	13.75	1.00
reach1	8060.867	50 year	54.20	2411.27	2413.33	2413.36	2413.93	0.009822	3.43	15.81	14.28	1.04
reach1	8060.867	100 year	61.40	2411.27	2413.44	2413.47	2414.07	0.009652	3.52	17.46	14.97	1.04
reach1	7723.669	10 year	38.20	2400.30	2401.27	2402.09	2405.06	0.129573	8.63	4.43	6.85	3.43
reach1	7723.669	25 year	47.20	2400.30	2401.37	2402.28	2405.65	0.130261	9.16	5.16	7.31	3.48
reach1	7723.669	50 year	54.20	2400.30	2401.48	2402.45	2405.66	0.114006	9.05	5.99	7.80	3.30
reach1	7723.669	100 year	61.40	2400.30	2401.56	2402.59	2405.94	0.111029	9.27	6.63	8.15	3.28
reach1	7452.053	10 year	38.20	2384.95	2385.75	2385.94	2386.37	0.037969	3.50	10.90	27.41	1.77
reach1	7452.053	25 year	47.20	2384.95	2385.80	2386.02	2386.53	0.040191	3.77	12.51	29.36	1.85
reach1	7452.053	50 year	54.20	2384.95	2385.84	2386.09	2386.66	0.043225	4.02	13.48	30.37	1.93
reach1	7452.053	100 year	61.40	2384.95	2385.87	2386.14	2386.78	0.043536	4.21	14.58	30.82	1.95
reach1	7116.062	10 year	38.20	2357.38	2358.52	2359.32	2362.61	0.164589	8.97	4.26	7.50	3.80
reach1	7116.062	25 year	47.20	2357.38	2358.63	2359.49	2362.85	0.148400	9.09	5.19	8.28	3.67
reach1	7116.062	50 year	54.20	2357.38	2358.73	2359.61	2362.87	0.131944	9.01	6.02	8.92	3.50
reach1	7116.062	100 year	61.40	2357.38	2358.80	2359.72	2363.11	0.128250	9.19	6.68	9.39	3.48
reach1	6780.354	10 year	38.20	2350.05	2350.88	2350.90	2351.18	0.012484	2.44	15.65	29.32	1.07
reach1	6780.354	25 year	47.20	2350.05	2350.95	2350.98	2351.31	0.012997	2.67	17.66	29.71	1.11

reach1	6780.354	50 year	54.20	2350.05	2350.99	2351.05	2351.40	0.013411	2.84	19.08	29.98	1.14
reach1	6780.354	100 year	61.40	2350.05	2351.04	2351.11	2351.50	0.013736	3.00	20.49	30.25	1.16
reach1	6480.047	10 year	38.20	2323.00	2323.53	2324.36	2337.85	1.489416	16.76	2.28	8.55	10.37
reach1	6480.047	25 year	47.20	2323.00	2324.47	2324.47	2324.85	0.010038	2.71	17.42	23.65	1.01
reach1	6480.047	50 year	54.20	2323.00	2324.56	2324.56	2324.95	0.009705	2.77	19.57	25.06	1.00
reach1	6480.047	100 year	61.40	2323.00	2324.64	2324.64	2325.05	0.009544	2.84	21.62	26.34	1.00
reach1	6096.592	10 year	38.20	2302.93	2303.85	2303.98	2304.33	0.025267	3.05	12.51	28.45	1.47
reach1	6096.592	25 year	47.20	2302.93	2304.07	2304.07	2304.39	0.010403	2.49	18.96	30.03	1.00
reach1	6096.592	50 year	54.20	2302.93	2304.13	2304.13	2304.48	0.010142	2.60	20.88	30.49	1.00
reach1	6096.592	100 year	61.40	2302.93	2303.50	2304.19	2312.31	0.830785	13.14	4.67	16.36	7.85
reach1	5742.829	10 year	38.20	2293.00	2294.30	2294.59	2295.18	0.026345	4.17	9.16	13.22	1.60
reach1	5742.829	25 year	47.20	2293.00	2294.12	2294.73	2296.40	0.075050	6.68	7.07	11.04	2.66
reach1	5742.829	50 year	54.20	2293.00	2294.20	2294.83	2296.60	0.075966	6.86	7.90	11.95	2.69
reach1	5742.829	100 year	61.40	2293.00	2294.81	2294.93	2295.43	0.012926	3.47	17.70	19.78	1.17
reach1	5491.33	10 year	38.20	2280.46	2281.23	2281.65	2283.01	0.113835	5.92	6.46	16.85	3.05
reach1	5491.33	25 year	47.20	2280.46	2281.46	2281.75	2282.41	0.040751	4.32	10.93	21.16	1.92
reach1	5491.33	50 year	54.20	2280.46	2281.51	2281.83	2282.55	0.040631	4.51	12.02	21.77	1.94
reach1	5491.33	100 year	61.40	2280.46	2281.22	2281.91	2286.03	0.311432	9.72	6.32	16.67	5.04
reach1	5278.947	10 year	38.20	2274.08	2275.33	2275.42	2275.77	0.014836	2.95	12.94	20.73	1.19
reach1	5278.947	25 year	47.20	2274.08	2275.33	2275.54	2276.00	0.022493	3.64	12.98	20.75	1.47
reach1	5278.947	50 year	54.20	2274.08	2275.39	2275.62	2276.12	0.022618	3.77	14.36	21.83	1.49
reach1	5278.947	100 year	61.40	2274.08	2275.57	2275.69	2276.14	0.015023	3.34	18.39	24.70	1.24
reach1	5038.309	10 year	38.20	2267.78	2268.81	2269.13	2269.89	0.046124	4.58	8.33	16.12	2.04
reach1	5038.309	25 year	47.20	2267.78	2269.02	2269.23	2269.69	0.030894	3.62	13.04	26.69	1.65
reach1	5038.309	50 year	54.20	2267.78	2269.07	2269.30	2269.80	0.030789	3.79	14.32	27.32	1.67
reach1	5038.309	100 year	61.40	2267.78	2269.03	2269.36	2270.11	0.048496	4.59	13.37	26.85	2.08
reach1	4890.766	10 year	38.20	2258.54	2258.86	2259.12	2259.88	0.108381	4.47	8.55	32.83	2.80
reach1	4890.766	25 year	47.20	2258.54	2258.86	2259.20	2260.49	0.178532	5.66	8.35	32.75	3.58
reach1	4890.766	50 year	54.20	2258.54	2258.88	2259.25	2260.67	0.174783	5.92	9.16	33.05	3.59
reach1	4890.766	100 year	61.40	2258.54	2258.97	2259.31	2260.31	0.095531	5.13	11.97	34.04	2.76
reach1	4730.395	10 year	38.20	2249.72	2251.18	2251.49	2252.15	0.027050	4.36	8.76	12.01	1.63
reach1	4730.395	25 year	47.20	2249.72	2251.35	2251.64	2252.30	0.022950	4.32	10.92	13.41	1.53
reach1	4730.395	50 year	54.20	2249.72	2251.43	2251.76	2252.46	0.023129	4.49	12.08	14.10	1.55
reach1	4730.395	100 year	61.40	2249.72	2251.45	2251.86	2252.71	0.028021	4.97	12.35	14.25	1.71
reach1	4548.986	10 year	38.20	2222.00	2223.56	2223.56	2223.95	0.009877	2.77	13.77	17.71	1.00
reach1	4548.986	25 year	47.20	2222.00	2223.69	2223.69	2224.12	0.009675	2.90	16.27	19.24	1.01
reach1	4548.986	50 year	54.20	2222.00	2223.79	2223.79	2224.24	0.009394	2.97	18.24	20.38	1.00
reach1	4548.986	100 year	61.40	2222.00	2223.88	2223.88	2224.36	0.009198	3.04	20.19	21.44	1.00
reach1	4270.501	10 year	38.20	2218.64	2219.81	2219.94	2220.31	0.018295	3.14	12.17	20.77	1.31
reach1	4270.501	25 year	47.20	2218.64	2219.90	2220.06	2220.47	0.018974	3.36	14.06	22.33	1.35
reach1	4270.501	50 year	54.20	2218.64	2219.96	2220.14	2220.59	0.019760	3.53	15.37	23.34	1.39
reach1	4270.501	100 year	61.40	2218.64	2220.01	2220.22	2220.70	0.020401	3.68	16.70	24.41	1.42
reach1	4001.844	10 year	38.20	2207.77	2208.80	2209.33	2210.85	0.088967	6.34	6.03	11.67	2.81
reach1	4001.844	25 year	47.20	2207.77	2208.91	2209.47	2211.04	0.081496	6.46	7.30	12.84	2.74
reach1	4001.844	50 year	54.20	2207.77	2208.99	2209.56	2211.14	0.075545	6.50	8.33	13.72	2.66
reach1	4001.844	100 year	61.40	2207.77	2209.06	2209.66	2211.25	0.071133	6.56	9.36	14.54	2.61
reach1	3782.173	10 year	38.20	2207.81	2208.53	2208.53	2208.80	0.011113	2.31	16.53	30.90	1.01
reach1	3782.173	25 year	47.20	2207.81	2208.62	2208.62	2208.92	0.010735	2.45	19.30	32.28	1.01
reach1	3782.173	50 year	54.20	2207.81	2208.69	2208.69	2209.01	0.010310	2.52	21.50	33.34	1.00
reach1	3782.173	100 year	61.40	2207.81	2208.75	2208.75	2209.09	0.010178	2.61	23.52	34.28	1.01
reach1	3513.826	10 year	38.20	2199.94	2200.73	2201.12	2202.20	0.089530	5.37	7.11	17.93	2.72
reach1	3513.826	25 year	47.20	2199.94	2200.80	2201.22	2202.45	0.090886	5.69	8.29	19.35	2.78
reach1	3513.826	50 year	54.20	2199.94	2200.84	2201.30	2202.65	0.094016	5.97	9.08	20.25	2.85
reach1	3513.826	100 year	61.40	2199.94	2200.88	2201.37	2202.80	0.093183	6.14	10.00	21.26	2.86
reach1	3261.167	10 year	38.20	2196.00	2197.33	2197.33	2197.67	0.010278	2.56	14.90	22.37	1.00
reach1	3261.167	25 year	47.20	2196.00	2197.45	2197.45	2197.81	0.010170	2.69	17.53	24.27	1.01
reach1	3261.167	50 year	54.20	2196.00	2197.53	2197.53	2197.92	0.009901	2.76	19.64	25.69	1.01
reach1	3261.167	100 year	61.40	2196.00	2197.61	2197.61	2198.02	0.009779	2.83	21.66	26.98	1.01
reach1	3069.329	10 year	38.20	2189.50	2190.39	2190.93	2192.72	0.121609	6.75	5.66	12.67	3.22
reach1	3069.329	25 year	47.20	2189.50	2190.48	2191.05	2192.95	0.114950	6.96	6.78	13.86	3.18

reach1	3069.329	50 year	54.20	2189.50	2190.53	2191.14	2193.15	0.113177	7.17	7.56	14.64	3.18
reach1	3069.329	100 year	61.40	2189.50	2190.59	2191.22	2193.32	0.109869	7.31	8.40	15.43	3.16
reach1	2768.386	10 year	38.20	2185.87	2187.16	2187.16	2187.50	0.010423	2.57	14.86	22.45	1.01
reach1	2768.386	25 year	47.20	2185.87	2187.28	2187.28	2187.64	0.010151	2.68	17.64	24.63	1.01
reach1	2768.386	50 year	54.20	2185.87	2187.36	2187.36	2187.74	0.009876	2.74	19.81	26.20	1.00
reach1	2768.386	100 year	61.40	2185.87	2187.44	2187.44	2187.84	0.009813	2.81	21.84	27.58	1.01
reach1	2544.211	10 year	38.20	2178.79	2179.10	2179.41	2180.81	0.277289	5.79	6.60	34.85	4.25
reach1	2544.211	25 year	47.20	2178.79	2179.13	2179.48	2181.10	0.269526	6.21	7.60	35.30	4.28
reach1	2544.211	50 year	54.20	2178.79	2179.15	2179.53	2181.33	0.268467	6.53	8.29	35.62	4.32
reach1	2544.211	100 year	61.40	2178.79	2179.17	2179.58	2181.53	0.264333	6.81	9.01	35.94	4.34
reach1	2354.638	10 year	38.20	2175.76	2178.61	2177.29	2178.64	0.000358	0.79	48.30	33.92	0.21
reach1	2354.638	25 year	47.20	2175.76	2178.76	2177.42	2178.80	0.000413	0.88	53.66	35.76	0.23
reach1	2354.638	50 year	54.20	2175.76	2178.87	2177.52	2178.91	0.000453	0.94	57.50	37.02	0.24
reach1	2354.638	100 year	61.40	2175.76	2178.96	2177.61	2179.02	0.000494	1.00	61.13	38.17	0.25
reach1	2054.857	10 year	38.20	2176.95	2178.03	2178.03	2178.31	0.011054	2.32	16.45	30.40	1.01
reach1	2054.857	25 year	47.20	2176.95	2178.13	2178.13	2178.43	0.010878	2.43	19.39	33.01	1.01
reach1	2054.857	50 year	54.20	2176.95	2178.19	2178.19	2178.51	0.010658	2.50	21.68	34.90	1.01
reach1	2054.857	100 year	61.40	2176.95	2178.28	2178.28	2178.59	0.010456	2.45	25.05	40.96	1.00
reach1	1794.641	10 year	38.20	2170.00	2170.98	2171.38	2172.38	0.065412	5.25	7.28	14.92	2.40
reach1	1794.641	25 year	47.20	2170.00	2171.05	2171.50	2172.66	0.067978	5.62	8.40	16.04	2.48
reach1	1794.641	50 year	54.20	2170.00	2171.12	2171.59	2172.77	0.064555	5.70	9.50	17.06	2.44
reach1	1794.641	100 year	61.40	2170.00	2171.17	2171.67	2172.93	0.064363	5.88	10.45	17.88	2.45
reach1	1447.001	10 year	38.20	2162.00	2163.20	2163.25	2163.56	0.012608	2.66	14.38	23.94	1.09
reach1	1447.001	25 year	47.20	2162.00	2163.30	2163.36	2163.70	0.012575	2.80	16.87	25.93	1.11
reach1	1447.001	50 year	54.20	2162.00	2163.37	2163.43	2163.80	0.012896	2.92	18.54	27.18	1.13
reach1	1447.001	100 year	61.40	2162.00	2163.43	2163.50	2163.89	0.013004	3.03	20.30	28.43	1.14
reach1	1073.795	10 year	38.20	2143.62	2144.39	2145.12	2149.78	0.344906	10.28	3.72	9.65	5.29
reach1	1073.795	25 year	47.20	2143.62	2144.47	2145.25	2150.10	0.317834	10.51	4.49	10.61	5.16
reach1	1073.795	50 year	54.20	2143.62	2144.53	2145.35	2150.14	0.288683	10.49	5.17	11.38	4.97
reach1	1073.795	100 year	61.40	2143.62	2144.58	2145.43	2150.29	0.271333	10.58	5.81	12.06	4.87
reach1	550.3049	10 year	38.20	2132.97	2134.39	2134.39	2134.76	0.010199	2.67	14.33	20.12	1.01
reach1	550.3049	25 year	47.20	2132.97	2134.52	2134.52	2134.91	0.009971	2.79	16.93	21.87	1.01
reach1	550.3049	50 year	54.20	2132.97	2134.61	2134.61	2135.03	0.009745	2.86	18.95	23.14	1.01
reach1	550.3049	100 year	61.40	2132.97	2134.69	2134.69	2135.13	0.009628	2.94	20.90	24.30	1.01
reach1	377.8101	10 year	38.20	2124.90	2125.24	2125.87	2129.41	0.281070	9.04	4.23	11.45	4.75
reach1	377.8101	25 year	47.20	2124.90	2125.31	2125.99	2129.70	0.261369	9.27	5.09	12.57	4.65
reach1	377.8101	50 year	54.20	2124.90	2125.36	2126.08	2129.92	0.250829	9.45	5.73	13.34	4.61
reach1	377.8101	100 year	61.40	2124.90	2125.41	2126.16	2130.09	0.239333	9.58	6.41	14.10	4.54
reach1	163.0885	10 year	38.20	2113.97	2115.02	2115.21	2115.62	0.024729	3.41	11.20	21.25	1.50
reach1	163.0885	25 year	47.20	2113.97	2115.11	2115.31	2115.78	0.025517	3.64	12.98	22.87	1.54
reach1	163.0885	50 year	54.20	2113.97	2115.16	2115.39	2115.90	0.026046	3.79	14.28	23.99	1.57
reach1	163.0885	100 year	61.40	2113.97	2115.21	2115.47	2116.01	0.026567	3.94	15.57	25.05	1.60

APPENDEX D 3D view of multiple river cross sections

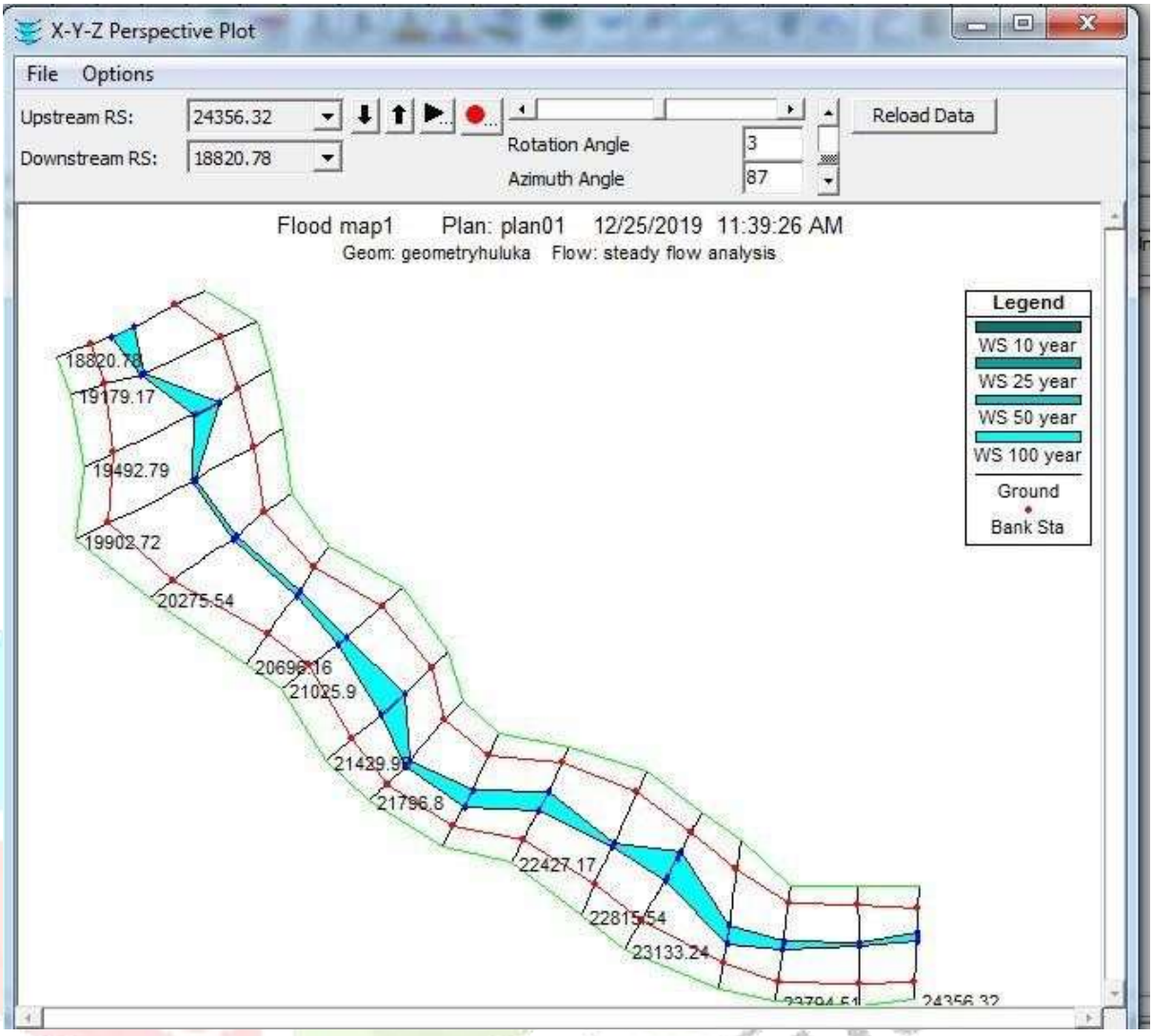

APPENDEX-E GIS data exported from HEC-RAS to Arc GIS

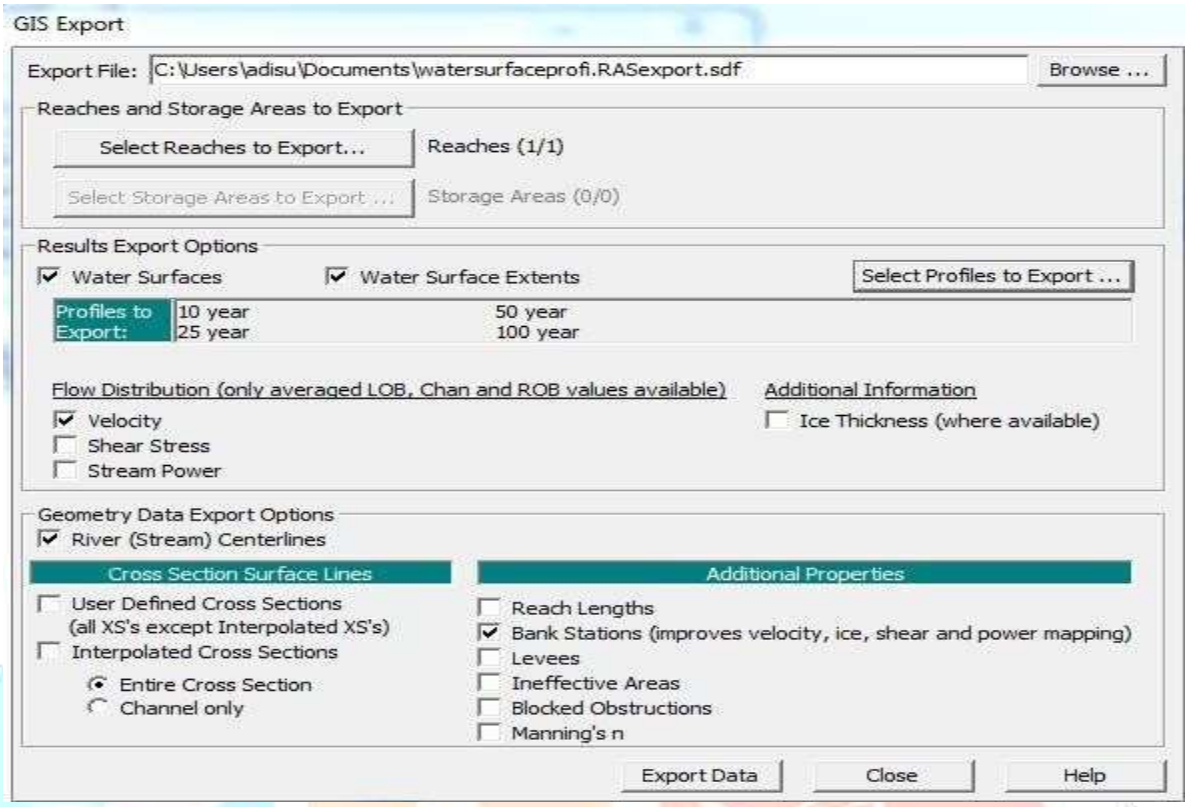

APPENDEX F Water surface TIN profiles for 10, 25 and 50

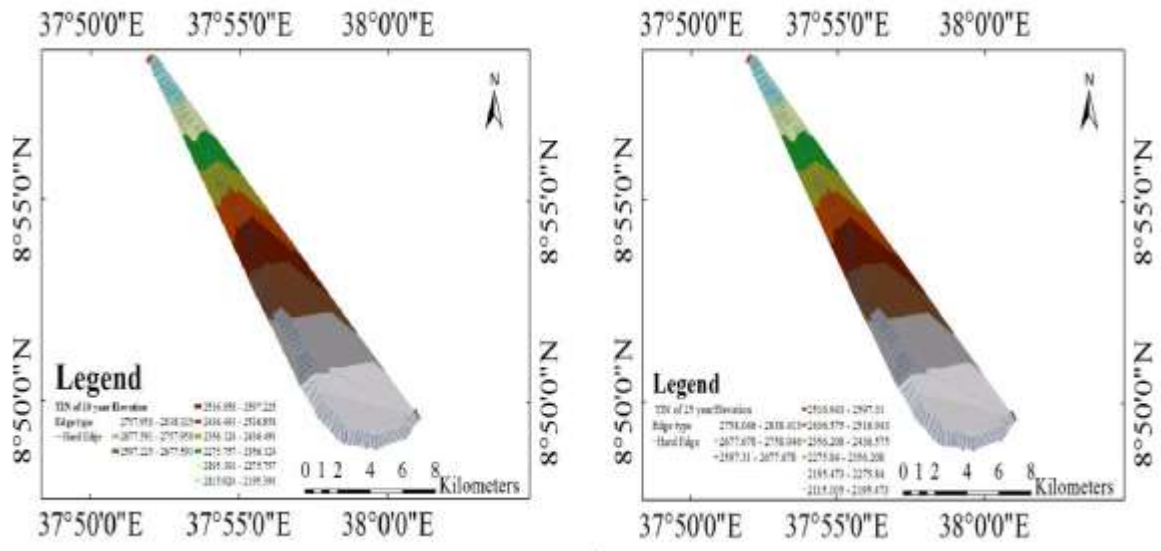

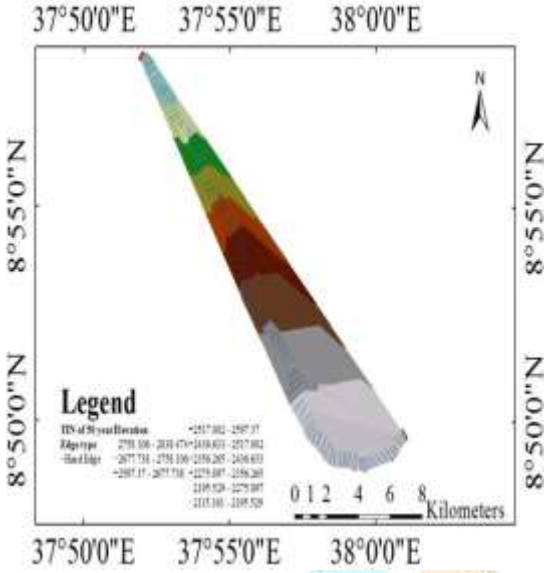

APPENDEX G: Rating curve

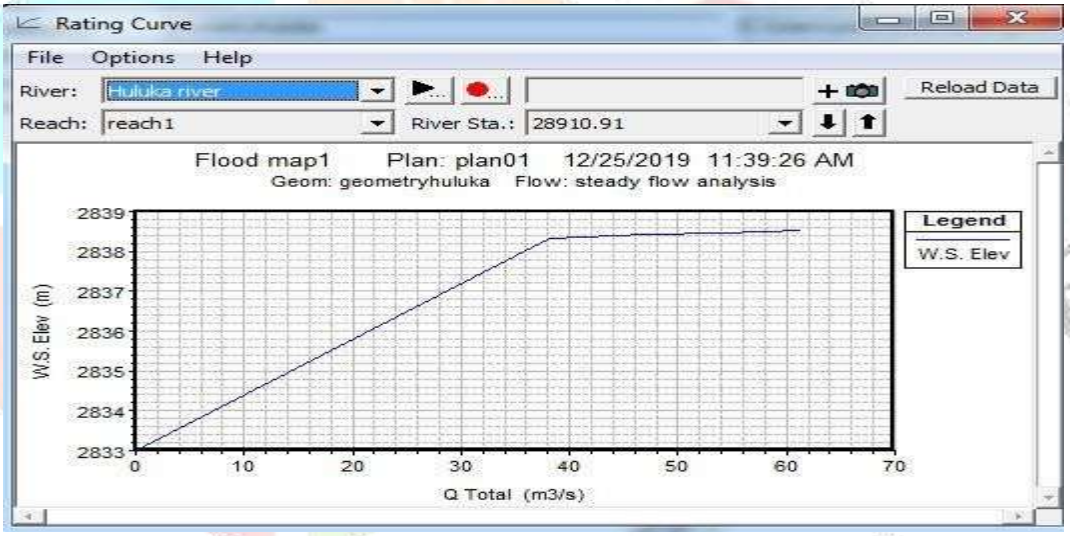

APPENDEX: H Table of River station with Left over bank, Channel and Right over banklength

Edit Downstream Reach Lengths

River: Huluka river | Edit Interpolated XS's

Reach: (All Reaches)

Selected Area Edit Options

Add Constant ... | Multiply Factor ... | Set Values ... | Replace ...

	Reach	River Station	LOB	Channel	ROB
1	reach1	28910.91	209.59	201.39	217.79
2	reach1	28709.64	269.13	280.63	299.14
3	reach1	28429.28	308.46	349.49	384.32
4	reach1	28080.44	224.75	216.65	212.99
5	reach1	27863.15	272.69	293.69	315.81
6	reach1	27569.89	396.19	361.24	283.67
7	reach1	27209.93	342.35	317.41	370.26
8	reach1	26891.98	348.84	353.54	320.11
9	reach1	26539.13	262.4	249.62	209.44
10	reach1	26289.59	192.08	203.66	207.68
11	reach1	26084.62	287.04	236.59	124.32
12	reach1	25848.27	260.73	256.99	195.85
13	reach1	25592.74	453.52	402.66	195.23
14	reach1	25188.59	318.8	223.7	149.94
15	reach1	24964.83	189.92	214.8	211.09
16	reach1	24749.72	135.85	200.24	247.32
17	reach1	24549.58	141.37	193.39	229.11
18	reach1	24356.32	236.91	246.31	255.14
19	reach1	24110.04	354.43	315.32	297.93
20	reach1	23794.51	250.56	280.48	285.8
21	reach1	23514.59	446.93	379.55	263.64
22	reach1	23133.24	298.02	317.11	320.35
23	reach1	22815.54	435.4	388.64	355.56
24	reach1	22427.17	305.47	312.92	317.05
25	reach1	22114.93	391.21	319.97	287.13
26	reach1	21796.8	301.74	366.28	285.25
27	reach1	21429.95	478.01	402.97	396.89
28	reach1	21025.9	229.35	329.05	379.65
29	reach1	20696.16	532.78	421.08	372.52
30	reach1	20275.54	437.38	372.12	392.91
31	reach1	19902.72	413.02	410.04	336.01
32	reach1	19492.79	410.43	314.22	496.96
33	reach1	19179.17	256.21	364.99	287.07
34	reach1	18820.78	287.11	273.78	295.8
35	reach1	18548.58	302.69	332.09	337.83

APPENDEX-I River station and cross section network exported from Arc GIS to HEC-RAS

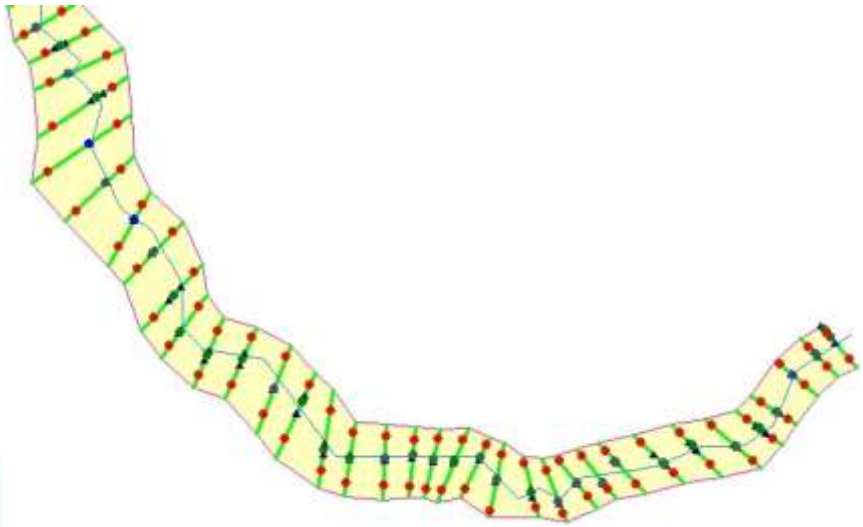

APPENDEX-J Land use /land cover classified for different selected years for 1997, 2005 and2011

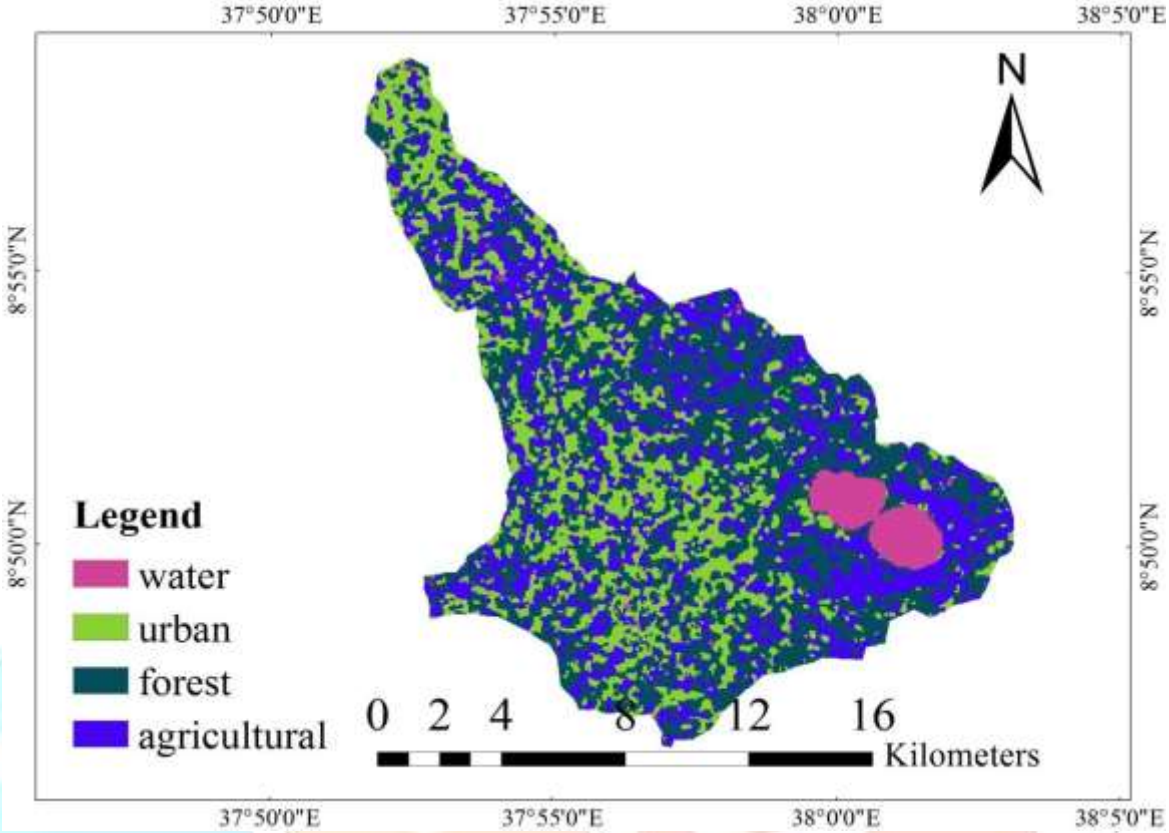

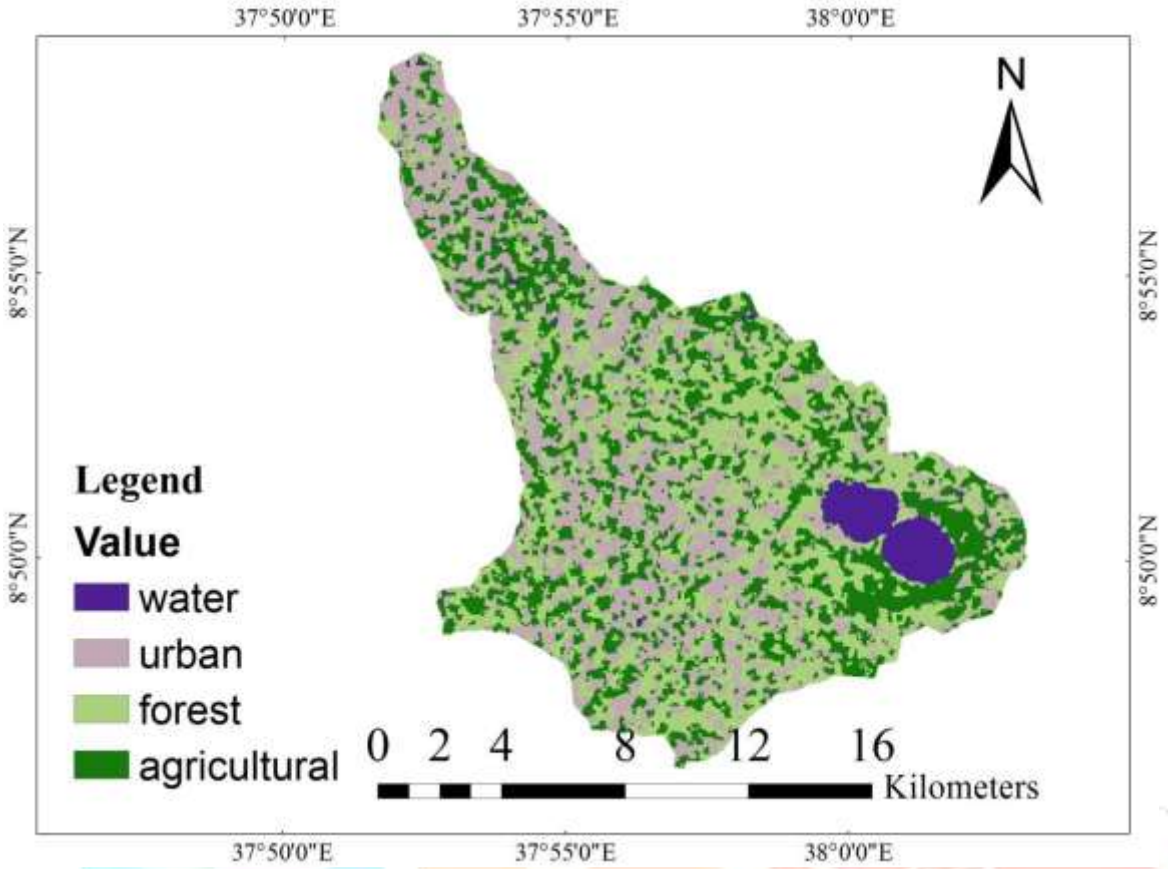
37°50'0"E
37°55'0"E
38°0'0"E
8°55'0"N
8°50'0"N
N
Legend
Value
water
urban
forest
agricultural
0 2 4 8 12 16
Kilometers

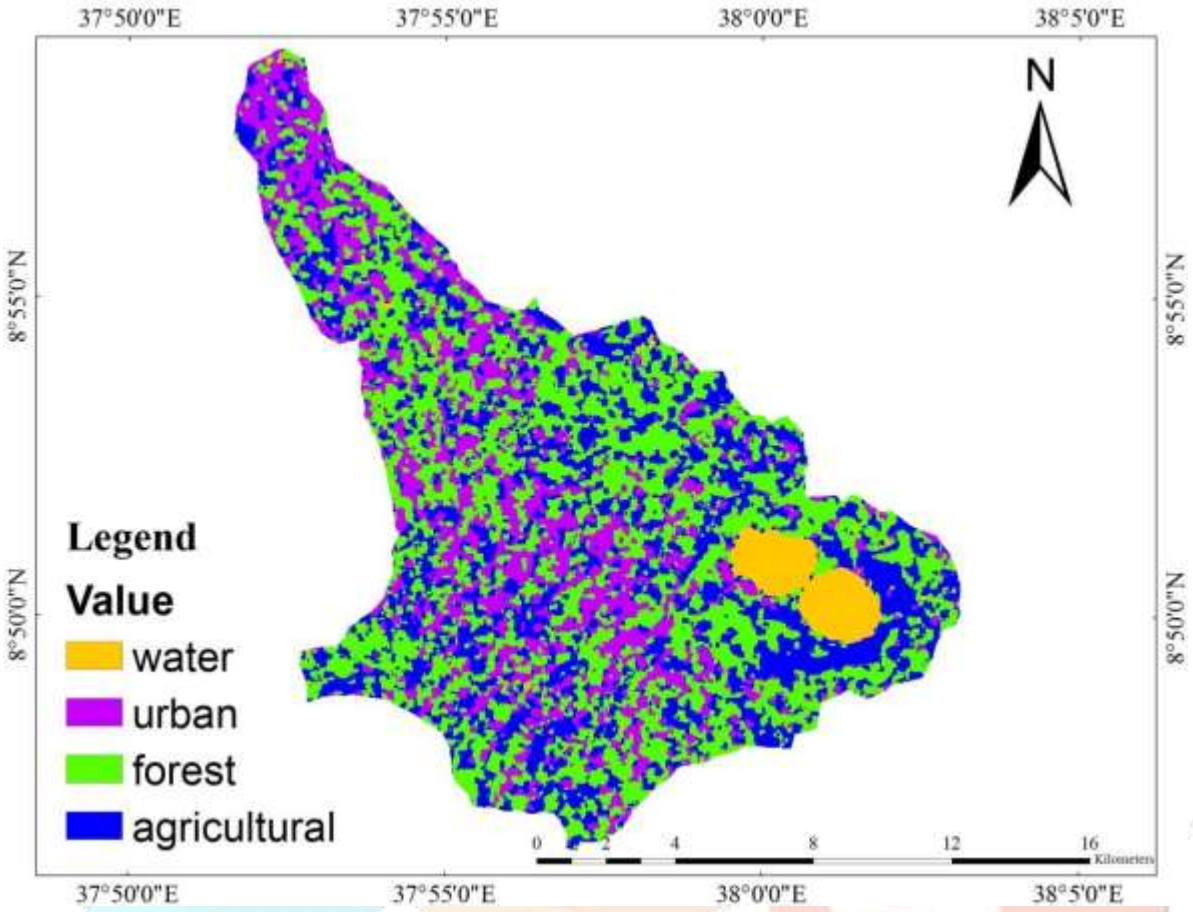
37°50'0"E
37°55'0"E
38°0'0"E
38°5'0"E
8°55'0"N
8°50'0"N
N
Legend
Value
water
urban
forest
agricultural
0
2
4
8
12
16
Kilometers

Appendex-K Floodplain area for 50 and 100 year return period of Huluka river watershed

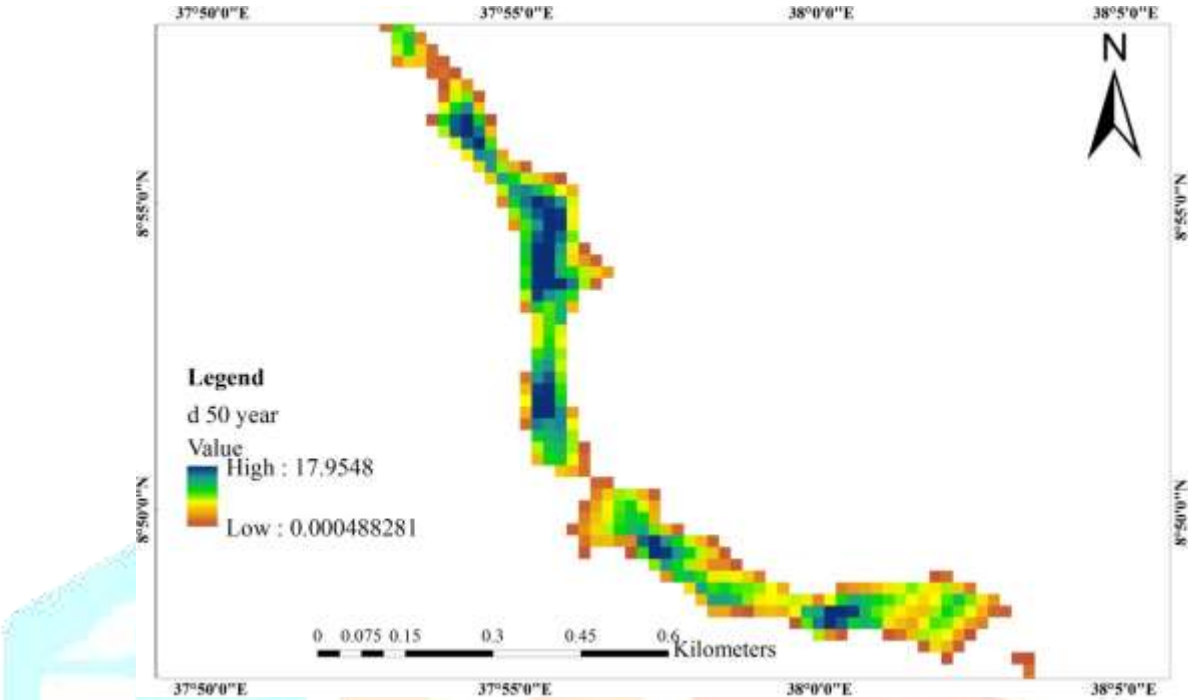

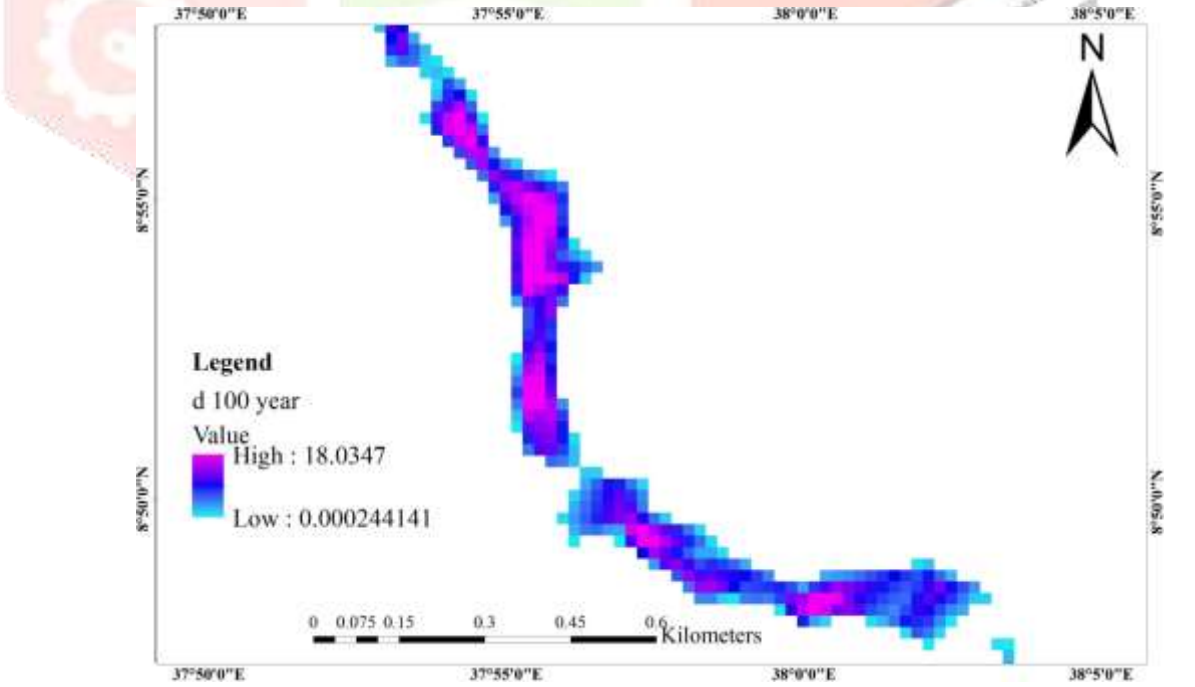

Appendex-L Soil, land use classification and percentage of impervious area determination bySCS TR55 Data's

Cover description		Curve numbers for hydrologic soil group			
Cover type and hydrologic condition	Average percent impervious area [2]	A	B	C	D
Fully developed urban areas (vegetation established)					
Open space (lawns, parks, golf courses, cemeteries, etc.) [3]:					
Poor condition (grass cover < 50%)		68	79	86	89
Fair condition (grass cover 50% to 75%)		49	69	79	84
Good condition (grass cover > 75%)		39	61	74	80
Impervious areas:					
Paved parking lots, roofs, driveways, etc. (excluding right-of-way)		98	98	98	98
Streets and roads:					
Paved; curbs and storm sewers (excluding right-of-way)		98	98	98	98
Paved; open ditches (including right-of-way)		83	89	92	93
Gravel (including right-of-way)		76	85	89	91
Dirt (including right-of-way)		72	82	87	89
Western desert urban areas:					
Natural desert landscaping (pervious areas only) [4]		63	77	85	88
Artificial desert landscaping (impervious weed barrier, desert shrub with 1- to 2-inch sand or gravel mulch and basin borders)		96	96	96	96
Urban districts:					
Commercial and business	85	89	92	94	95
Industrial	72	81	88	91	93
Residential districts by average lot size:					
1/8 acre or less (town houses)	65	77	85	90	92
1/4 acre	38	61	75	83	87
1/3 acre	30	57	72	81	86
1/2 acre	25	54	70	80	85
1 acre	20	51	68	79	84
2 acres	12	46	65	77	82
Developing urban areas					
Newly graded areas (pervious areas only, no vegetation) [5]		77	86	91	94

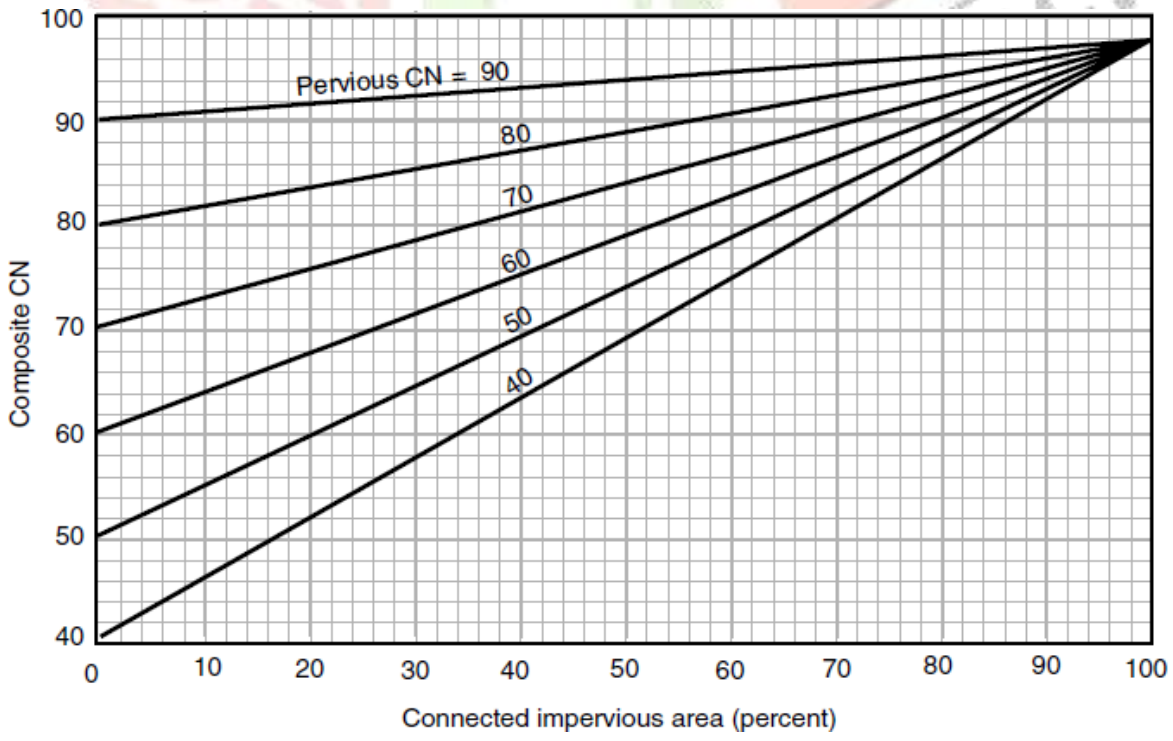

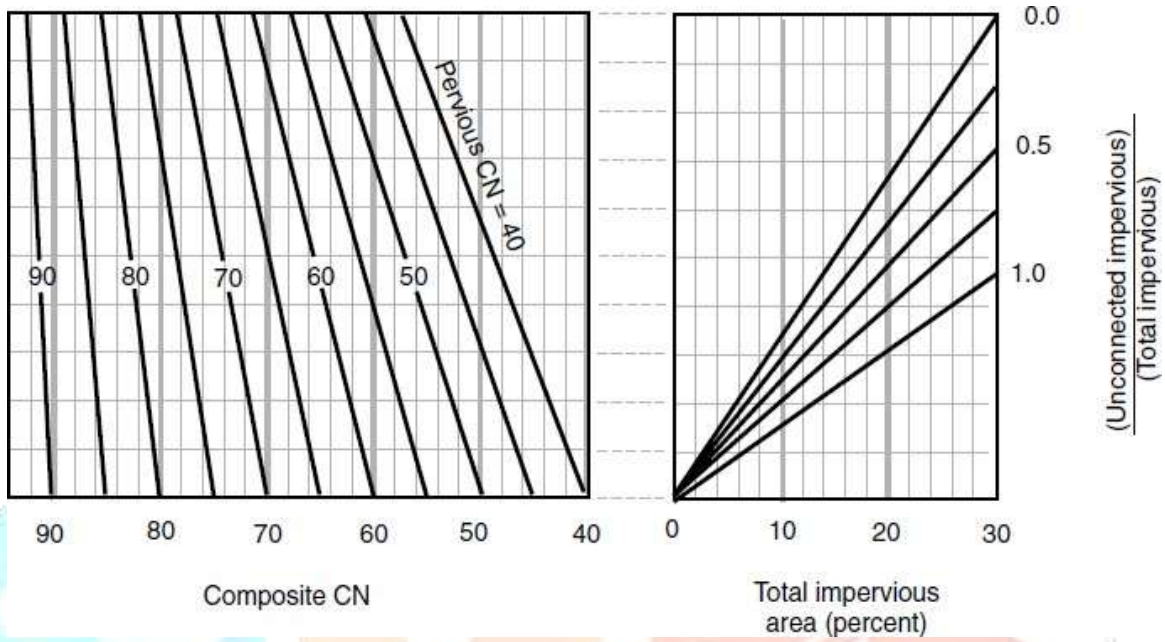

Acknowledgment

First of all, honor to almighty God who made it possible, to begin and finished this thesis successfully.

My appreciation also goes to my advisor Tamene Adugna (PhD.) and co-advisor Walabuma Oli (MSc.) giving general constructive comment and suggestion to implement this thesis.

I like also to say Ethiopian Road Authority to give this enjoyable chance with cooperative to Jimma University.

Moreover, I wish to express my deepest gratitude my family and all of my friends for providing financial supporting and strength motivation to success in my study. In addition, all friends and professional collogues thanks your collaboration and motivation.

Finally, my deepest gratitude and humble thanks go my immediate parents for their never-ending support, encouragement and motivation.

References

Aasa, A. S. E. K. P. R. J. Š. J. a. P. T., 2019. Spatial interpolation of mobile positioning data for population statistics. In 15th International Conference on Location-Based Services,p. p. 171.

Adla, S. T. S. a. D. M., 2019. Can We Calibrate a Daily Time-Step Hydrological Model UsingMonthly Time-Step Discharge Data?. Water, pp. 11(9), p.1750.

Ahmadisharaf, E. C. R. Z. H. H. M. a. M. Y., 2019. Calibration and validation of watershed models and advances in uncertainty analysis in TMDL studies. Journal of Hydrologic Engineering, pp. 24(7), p.03119001.

Akbari, A. M. G. F. M. a. H., 2014. M.S. Impact of Landuse Change on River Floodplain Using Public Domain Hydraulic Model. Modern Applied Science, pp. 8(5), p.80.

Anon., 1998. Agriculture Organization for the United Nations, and Agriculture Organization. World reference base for soil resources. Vol. 3. ., , s.l.: Food & Agriculture Org.

Arsiso, B. K., 2017. Trends in climate and urbanization and their impacts on surface water supply in the city of Addis Ababa, Ethiopia. Doctoral dissertation.

Barbero-Sierra, C. M. M. a. R.-P. M., 2013. The case of urban sprawl in Spain as an active and irreversible driving force for desertification. Journal of Arid Environments, 90, pp.pp.95-102.

Beck, N. C. G. K. L. a. M. M., 2017. An urban runoff model designed to inform stormwater management decisions. Journal of environmental management, pp. pp.257-269.

Benchimol, E. S. L. G. A. H. K. M. D. P. I. S. H. v. E. E. L. S. a. R. W. C., 2015. The REporting of studies Conducted using Observational Routinely-collected health Data. RECORD Working Committee.

Berhanu, B., M. & Yilma, S., 2012. GIS-based Hydrological. Department of Earth and Environment.

Berner, E. K. & Robert, B. A., 2012. Global environment: water, air, and geochemical cycles.. Princeton University Press.

Beven, K. a. G. P., 2013. Macropores and water flow in soils revisited. Water Resources Research, pp. 49(6), pp.3071-3092.

BEYENE, M. N., 2016. Urbanization and Its Effect on Surface Runoff. p. 6 .

Bilotta , G., Brazier , R. & Haygarth , P., 2007 . The impacts of grazing animals on the qualityof soils, vegetation, and surface waters in intensively managed grasslands.. Advances in agronomy. , 1(94), pp. 237-80.

Boorman, . D. B., John , M. . H. & Lilly, A., 1995. Hydrology of soil types: a hydrologically- based classification of the soils of United Kingdom.. Institute of Hydrology, .

Burrough, P. M. R. M. R. a. L. C., 2015. Principles of geographical information systems. Oxford university press.

Buytaert, W. a. D. B. B., 2012. Water for cities: The impact of climate change and demographic growth in the tropical Andes. Water Resources Research, p. 48(8).

Cakir, R. R. M. S. S. P.-A. J. G. Y. R. L. M. M. N. E. S.-C. M. L.-C. J. a. G. P. J., 2020. Hydrological Alteration Index as an Indicator of the Calibration Complexity of Water Quantity and Quality Modeling in the Context of Global Change. Water, pp. 12(1), p.115.

Cosby , B., Hornberger , G., Clapp , R. & Ginn, . T., 1984 . A statistical exploration of the relationships of soil moisture characteristics to the physical properties of soils.. Water resources research. , Volume 20(6), pp. 682-90.

Dan-Jumbo, N. a. M. M., 2019. Relative Effect of Location Alternatives on Urban Hydrology.The Case of Greater Port-Harcourt Watershed, Niger Delta. Hydrology, pp. ,6(3), p.82.

Datoo, A., 2019. Legal Data for Banking: Business Optimisation and Regulatory Compliance. s.l.:s.n.

Davis, A. a. M. R., 2005. Stormwater Hydrology. Stormwater Management for SmartGrowth, pp. pp.63-104.

Di Baldassarre, G. a. C. P., 2011. A hydraulic study on the applicability of flood ratingcurves. Hydrology Research, pp. 42(1), pp.10-19.

Fetter, C., 2018. Applied hydrogeology. Waveland Press.

Gant, . R. L., Guy , M. R. & Shahab , F., 2011. "Land-use change in the ‘edgelands’: Policiesand pressures in London's rural–urban fringe.". Land use policy 28.1 .

Gary W., B. C.-H., 2016. Hydraulic analysis system user's manual. manual.

Gashaw, W. & Dagnachew , L., 2011. Flood hazard and risk assessment using GIS andremote sensing in Fogera Woreda, Northwest Ethiopia.". Nile River Basin. Springer, Dordrecht , pp. 179-206.

Good, S. N. D. a. B. G., 2015. Hydrologic connectivity constrains partitioning of global terrestrial water fluxes. Science, 349(6244), pp. pp.175-177.

Guarino, . L., Jarvis , A., Hijmans , R. & Maxted, . N., 2002. 36 Geographic Information Systems (GIS) and the Conservation and Use of Plant Genetic Resources. Managing plant genetic diversity..

Gulliver, J. S., 2015. Determination of Effective Impervious Area in UrbanWatersheds,Department of Civil. Environmental and Geo- Engineering University of Minnesota.

Gumindoga, W. R. D. N. I. a. D. T., 2017. Ungauged runoff simulation in Upper Manyame Catchment, Zimbabwe: Application of the HEC-HMS model. Physics and Chemistry of the Earth, Parts A/B/C, pp. 100, pp.371-382.

Guohua, F., 2018. Flood control to urban agglomerations. Internationa journals on flood control, p. 123.

GURMU, A., 2018. FLOOD MODELING AND MAPPING OF LOWER OMO GIBE RIVER BASIN. Doctoral dissertation, ADDIS ABABA SCIENCE AND TECHNOLOGY UNIVERSITY.

Han, J., 2010. Stream flow Analysis Using ArcGIS and HEC-GeoHMS. Texas A&M University. Zachry Department of Civil Engineering..

Hasani, H., 2013. Determination of Flood Plain Zoning in Zarigol River Using the Hydraulic Model of HECRAS. International Research Journal of Applied and Basic Sciences, 5(3), pp. pp.399-403.

Hoornweg, ,. L. T. G. C., 2011. Cities and greenhouse gas emissions: moving forward. Environment and Urbanization, pp. 23(1), pp.207-227.

Hungr, O., Morgan, G. C., Van Dine, D. F. & Lister, 1987. Debris flow defenses in British Columbia. Debris Flows/Avalanches: Process, Recognition, and Mitigation.. Geological Society of America Reviews in Engineering Geology, 7., pp. 201-222..

Igulu, B. a. M. E., 2020. The impact of an urbanizing tropical watershed to the surface runoff. Global J. Environ. Sci. Manage, pp. 6, p.2.

Jaber, A. E.-N. a. M., 2018. Floodplain Analysis using ArcGIS, HEC-GeoRAS and HEC- RAS in Attarat Um Al-Ghudran Oil Shale Concession Area, Jordan. Journal of Civil & Environmental.

James H., D., 2013. Geospatial hydrologic model extension. manual.

Jameson, A., 2019 . On the Importance of Statistical Homogeneity to the Scaling of Rain. Journal of Atmospheric and Oceanic Technology, pp. 36(6), pp.1063-1078.

Jantz, C. A., Scott, . G. J. & Mary , K. S., 2004. "Using the SLEUTH urban growth model to simulate the impacts of future policy scenarios on urban land use in the Baltimore- Washington metropolitan area.". Environment and Planning B: Planning and Design 31 , Volume 2, pp. 251-271..

Jha, A. L. J. B. R. B. N. L. A. P. N. B. A. P. D. D. J. a. B. R., 2011. Five feet high and rising: cities and flooding in the 21st century. The World Bank.

Julien, P., 2018. River mechanics. Cambridge University Press.

Kabangure, H., 2016. Gerald Munyoro. Doctoral dissertation, Chinhoyi University of Technology.

Kaffas, K. a. H. V., 2014. Application of a continuous rainfall-runoff model to the basin of Kosynthos river using the hydrologic software HEC-HMS. Glob. NEST, pp. 16(188203), p.16.

Kim, N. W. Y. L. J. L. J. a. J. J., 2011. Hydrological impacts of urban imperviousness in White Rock Creek watershed. Transactions of the ASABE, pp. 54(5),pp.1759-1771.

Kirkby, . R. J., 2018. Urbanization in China: town and country in a developing economy 1949-2000 AD. Routledge.

Kotir, . J. H., 2011. Climate change and variability in Sub-Saharan Africa: a review of currentand future trends and impacts on agriculture and food security.. Environment, Development and Sustainability, pp. 13(3), pp.587-605.

Labbas, M. B. F. B. I. K. S. J. C. K. S. M. K. J. T. D. C. a. V. E. 2., 2013. Multi-scale approach to assess the impacts of land use evolution and rainwater managementpractices on the hydrology of periurban catchments.. Application to the Yzeron catchment (150 km 2).

Lastoria, B., 2008. Hydrological processes on the land surface: A survey of modellingapproaches.Università di Trento. Dipartimento di ingegneria civile e ambientale,.

Ligtenberg, J., 2017. Runoff changes due to urbanization. p. 3 .

Li, Y., 2009. "Impacts of urbanization on surface runoff of the Dardenne Creek watershed, St. Charles County, Missouri.". Physical Geography 30.6, pp. 556-573.

Lloyd, E., 2019. Spatial Decision Support Systems Use in Peacekeeping and Stability Operations Analysis: Spatial Analysis for US Army Civil Affairs Civil Information Management (Doctoral dissertation).

Maguire, D., 2008. ArcGIS: general purpose GIS software system. Encyclopedia of GIS, pp. pp.25-31.

Mark, O. et al., 2004. "Potential and limitations of 1D modelling of urban flooding.". Journal of hydrology 299, Volume 3-4 , pp. 284-299.

Mathew J., F. J., 2012. Hydrologic Engineering Center's Geospatial River Analysis System. Manual.

McColl, K. et al., 2017. The global distribution and dynamics of surface soil moisture. NatureGeoscience, p. 100.

McDonald, W., 2010. Applications of GIS Using ArcGIS, HEC - GeoHMS and HEC-HMS. Model Ticky Creek Watershed, Texas A&M University, Zachry Department of Civil.

Michotte, A., 2017. The perception of causality. Routledge.

Mihiretie, Y., 2017. Assessment of Environmental Impact of Quarrying Activities in Eastern Addis Ababa. Implications on Urbanization (Doctoral dissertation, Addis Ababa University).

Monteith, J. a. U. M., 2013. Principles of environmental physics: plants, animals, and the atmosphere. Academic Press.

Myers, J., 2019. Modeling continuous variables. Multiple regression.

Nega, M., 2016. Urbanization and Its Effect on Surface Runoff (A Case Study on Great AkakiRiver, Addis Ababa, Ethiopia). Doctoral dissertation, Addis Ababa University.

Nharo, T. M. H. a. G. W., 2019. Mapping floods in the middle Zambezi Basin using earth observation and hydrological modeling techniques. Physics and Chemistry of theEarth, Parts A/B/C, pp. 114,p.102787.

Olson, G., 2012. Soils and the environment: A guide to soil surveys and their applications.. Springer Science & Business Media.

Panigrahya., P. K. G. a. S., 2008. Agriculture, Forest and Environment Group, Space Applications Centre, ISRO, Geo-spatial Modeling of Runoff of Large Land Mass, Analysis,.

Patel, C. a. G. P., 2016. Floodplain Delineation Using HECRAS Model—A Case Study of Surat City. Open Journal of Modern Hydrology, pp. 6(01), p.34.

Pathan, H. a. J. G., 2019 . Estimation of Runoff Using SCS-CN Method and Arcgis for KarjanReservoir Basin. International Journal of Applied Engineering Research, pp. 14(12), pp.2945-2951.

Pawan, 2016. Urbanization and Its Causes and Effects.. IJRSI International Journal of Research and Scientific Innovation Volume III, p. 110.

Peters, N. E., 1994. Biogeochemistry of Small Catchments. A tool for Environmental.

Piepho, H., 2019. A coefficient of determination (R2) for generalized linear mixed models. Biometrical Journal, pp. 61(4), pp.860-872.

Prakash, C. S. B., 2017. Land-Use Land-Cover Change and Its Impact on Surface Runoff. International Journal of Advanced Remote Sensing and GIS , p. 2104 .

Raes, D. W. P. a. G. F., 2006. RAINBOW - a software package for analyzing data and testing the homogeneity of historical data sets. Proceedings of the 4th International Workshopon 'Sustainable management of marginal drylands'.

Ramakrishnan, D., Bandyopadhyay, A. & Kusuma, , . K., 2009. SCS-CN and GIS-based approach for identifying potential water harvesting sites in the Kali Watershed, Mahi River Basin, India.. Journal of Earth System Science, 118(4), , pp. 355-368.

Ramirez, J. A., 2000. Prediction and Modeling of Flood Hydrology and Hydraulics, Inland FloodHazards: Human, Riparian and Aquatic Communities: Cambridge University Press.

Schaeffer, R. et al., 2012. "Energy sector vulnerability to climate change: a review.". Energy 38, Volume 1, pp. 1-12.

Shabir, O., 2013. A summary case report on the health impacts and response to the Pakistan floods of 2010, s.l.: PLoS currents 5.

ShahiriParsa, A. N. M. H. M. a. R. M., 2016. Floodplain zoning simulation by using HEC- RAS and CCHE2D models in the Sungai Maka river. Air, Soil and Water Research, 9,pp. pp.ASWR-S36089.

Sharffenberg, W., 2016. Hydrologic Engineering Center Hydrologic Modeling System. User'sManual.

Taube, N., 2019 . Understanding and linking anthropogenic and natural riverine disturbances to in-stream nutrient dynamics in an urbanized river reach.

Tausch , A., 2019. Migration from the Muslim World to the West. Jewish Political Studies Review, pp. 30(1/2), pp.65-225.

Tegine, E., 2018. FLOODPLAIN MAPPING AND MODELING FOR GERAY RIVER. Doctoral dissertation, ADDIS ABABA SCIENCE AND TECHNOLOGY UNIVERSITY.

Tshewang, J., 2017. Rainfall-runoff simulation model based on water balance concept for basinwide water resource assessment. water resource assessment.

UNDESA, 2015 Revision. Population Division World Urbanization Prospects.

UNEP, U., U. -H. & E., 2003. Scientific Report on the GroundwaterVulnerability Mapping of,the Addis Ababa Water Supply Aquifers, 2003, Addis Ababa, Ethiopia., s.l.: s.n.

Wang, X. Z. J. S. S. G. E. W. Y. G. J. a. H. R., 2016. Adaptation to climate change impacts onwater demand. Mitigation and Adaptation Strategies for Global Change, pp. 21(1), pp.81-99.

Weng, Q., 2001. Modeling Urban Growth Effects on Surface Runoff. Department of Geography, Geology, and Anthropology, Indiana State ,USA.

Zellou, B. a. R. H., 2017. Assessment of reduced-complexity landscape evolution model suitability to adequately simulate flood events in complex flow conditions. Natural hazards, pp. 86(1), pp.1-29.

Zenner, ,. H. D., 2000. A new method for modeling the heterogeneity of forest structure.. Forest ecology and management, pp. 129(1-3), pp.75-87.

Zhang, X. Q., 2016. The trends, promises and challenges of urbanisation in the world. HabitatInternational, pp. 54, pp.241-252.

Zhou, F., Youpeng Xu, Y. C.-Y. X., Gao, Y. & Du, J., 2013. Hydrological response to urbanization at different spatio-temporal scales simulated by coupling of CLUE-S and the SWAT model in the Yangtze River Delta region.". Journal of Hydrology 485, pp. 113-125.